Simulated exploration of improvements to microfluidic cell sorting using sheath flow and inertial ordering methods

Josh Zembles, Sara Wagers, Caleb Heerts, and Hunter Hefti

Department of Biomedical Engineering
University of Wisconsin-Madison
Skala Lab, Morgridge Institute for Research

Through the use of optics techniques, cells can be excited, identified, and sorted based on their activation state, an improvement on traditional cell sorting techniques which are difficult and time consuming. The aim of this work was to design a microfluidic device that will allow for this process to be performed within a single device in order to speed up and improve the accuracy of these research techniques. CAD models were developed for two designs utilizing sheath flow and inertial ordering. By using Solidworks fluid modeling simulations and parametric studies, we demonstrated that the designs will effectively focus the cells within a confined range. Investigation of pressures throughout the range of the pump capabilities revealed ideal parameters for use of the system.

1. Introduction

1.1. Initial Motivation and Research

Cell sorting is the process of separating cells based on expressed characteristics. This can be helpful in a variety of applications such as separating different cell types by the expression of a protein or by their activation state. Cell sorting is traditionally performed using size identification or by tagging the cells with labels such as small molecules or RNA sequences. Tagging or sorting by size can be difficult or time consuming and can potentially affect the structure and function of the cell [1]. To combat this, the Skala lab is researching the use of optics to analyze cells using label-free techniques which would result in the activation, identification, and sorting of certain cells all within a single device. This could increase rates of identification, analysis, and research regarding cells as well as aid in the search for cures of diseases such as cancer or immunological deficiencies. They have shown that optical excitation, detection, and signal processing can achieve high accuracy to classify quiescent and activated T-cells. The next step in their research requires the design of a microfluidic device to flow the cells at speeds that allow hundreds of milliseconds of integration time on the detector to improve the testing system and allow the Skala lab to conduct this research more effectively. The current devices on the market often use sheath flow to move and analyze cells. This involves a sheath fluid such as deionized water or phosphate buffered saline (PBS) flowing at a high velocity on both sides of a slower moving cell sample solution. The velocity of the sheath fluid will speed up

the cell sample as well as focus it in the middle (much like a sword in a sheath) as it travels [2]. The biggest issue with devices using sheath flow is that the cells would move past the light detector too quickly for the cells to be analyzed. Additionally, once the sheath fluid is slowed down, cells do not maintain their Y and Z axis location which makes it increasingly difficult to both excite and image the cells.

In order to design a device that will allow cells to flow past the laser and be able to integrate into their system, the Skala Lab has laid out specific parameters that the device needs to maintain. As outlined in the Product Design Specifications (see Appendix I), the cells need to pass through the laser one at a time while keeping the diameter of the stream containing cells at a maximum of 20-50 microns. The flow speed of the cells would optimally approach 1 mm/s to allow sufficient integration time for the light sensor to read emission signals from each cell. In order for the lenses to focus the laser on the cells, the distance between the bottom of the device and the stream of cells needs to be about 150 microns. The device should be able to fit on a microscope stage and be compatible with their pump system.

1.2. Traditional sheath fluid designs and the Funnel

Fluorescent Lifetime Imaging provides a non-invasive and label-free evaluation of the cellular metabolism of each cell. Fluorescence occurs when an emission lightwave excites molecules within or attached to cells and emits a lower energy wavelength that can be detected by sensors [4]. This method is used in many applications including Flow Cytometry. Typical flow cytometry chips are designed with the intent to usher cells towards an objective. The most typical method for driving the sample is through the use of sheath fluid which, in a typical flow cell, arrives from side channels and converges upon the cellular inlet to carry the sample forward. Sheath fluid designs are frequently used in a two dimensional placement where fluid arrives from one or two directions [8]. While remaining a staple of the experiment, the two dimensional sheath fluid flow has the potential to introduce turbulent flow at the point where convergence occurs. Alternatives to the two dimensional design commonly include three dimensional alterations. Funnel designs involve the utilization of a cone-shaped sheath fluid inlet which allows for complete encapsulation of the incoming cell sample. In these cases, a core diameter is formed in which the cells are centered in all directions within the channel which is guided by laminar flow in the form of the sheath fluid.

1.3. Inertial ordering and the Snake

Multiple sources which informed the design process mentioned a property known as inertial lift. When laminar flow is made to pass through a channel or pipe that does not generate uniformly parallel streamlines, flow will seek out a path of least resistance. In many occasions, the shape of the piping and the presence of a certain amount of curvature allow for the formation of Dean vortices, which promote a type of fluid flow that influences the manner in which particulate is able to move within the fluid. This displays itself as an outlet streamline which is uniformly pushed towards the center of the channel. Such a concept was first introduced in 2007

in which symmetrical designs resulted in two separate cell flows when streamlines were forced towards the sides of the channel via centripetal forces. Implementation of an asymmetric design results in a single streamline of cells [9]. The Snake design was expanded, and the concept of inertial ordering was added to a set of potential improvements for cell sorting [2]. Most designs concentrate on cell ordering prior to the addition of sheath fluid. One such design even incorporated an asymmetric squiggle pattern in an effort to create order from the sample directly [10]. But it was hypothesized that adding the sheath fluid prior to entry into the inertial ordering system would allow cells to avoid potential turbulence and order the fluid prior to observation by the laser.

2. Methods

2.1. Crafting the Funnel Design

The Funnel design was heavily influenced by the multitude of traditional sheath fluid designs that came before it. Building this design in SolidWorks allowed for simulation and testing of various parameters. These simulations were intended to ensure the design should be able to center the cells and to learn how changing velocities would impact the behavior of the fluids. In short, the design consisted of using a 0.18 mm diameter flat tip needle to introduce the cell solution while a sheath flow surrounded the needle until the end. The sides of the device begin to enclose the fluid into a smaller 0.4 mm diameter channel that carries the cells over the laser for reading. As the fluid moves through the Funnel part of the design, the velocity will increase as the diameter decreases. The sheath fluid should confine the cells into the center as the sheath flow is on all sides of the cell flow. The final velocity of the fluid within the channel depends on the speed and the volume of fluid entering the system at the two inlets.

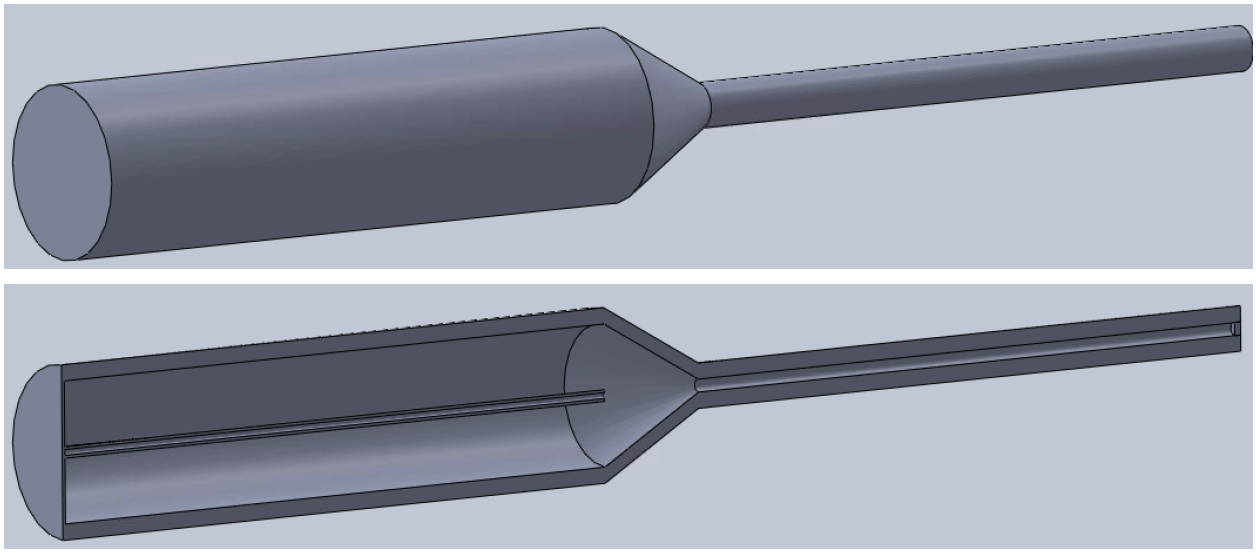

Figure 1. An angled view of the Funnel design. A cross sectional view of the design shows the needle that contains the cell solution flow and the sheath flow volume that surrounds the needle.

Flow simulations were conducted once the SolidWorks model was completed. The fluid flow of the needle that contained the cells was examined in order to look at how well the sheath flow was confining the core flow as it traveled into the channel. A particle study was conducted as well to examine the behavior of particles that represented cells in the core flow. Another simulation that was conducted looked at the fluid velocity within the channel, an important parameter because the cells ought to be traveling between 1-5 mm/s for the laser to efficiently read each individual cell as it passes through. The channel fluid velocity was measured with varying inlet velocity speeds to gain an understanding of the circumstances that would allow for the optimal flow for the laser to read.

2.2. Modelling Inertial Ordering with and without sheath fluid

Due to the complicated nature of inertial ordering, multiple iterations of the Snake were needed to test the validity of the concept while making room for various design alterations and potential errors with the simulation software. While tools such as OnShape or COMSOL were considered to help with the modeling and fluid simulation processes, SolidWorks was ultimately decided upon as it makes for good comparisons to the Funnel.

For the initial testing phase regarding the potential use of sheath fluid, a design was generated based on previous research that involved a small amount of inertial ordering followed by the immediate introduction of sheath fluid [10]. This channel would undergo a fluid simulation and a subsequent particle simulation before qualitative analysis would reveal if enough of an improvement had been achieved to begin quantitative data collection. The resulting design can be viewed in Figure 2. The concept was, once some inertial ordering had taken place, sheath fluid would further center the cells, potentially in another plane, and direct the focus more precisely towards the target.

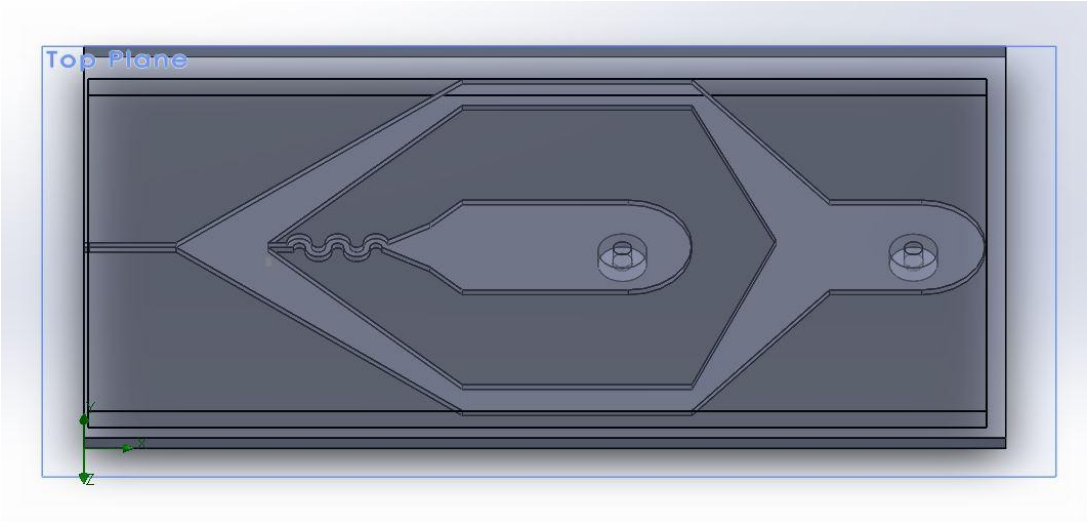

Figure 2. An angled view from above of the sheath fluid design. One inlet allows for particles to pass through an small inertial ordering system while another allows entry for sheath fluid.

Snake models were all constructed within the bounds of SolidWorks extrusion techniques, in which an initial sketch was made to function as a base while several more sketches served to simulate the effect of applying soft lithography techniques and symmetrically mirroring and placing the top planes together. Once a model was completed, a fluid simulation and particle injection would be applied. This typically consisted of setting up two or three boundary conditions and running a test for volume flow rate. At the outlet of the device, a static pressure was set; this would ensure that the pressure of the water inside the device would gradually force the fluid to move towards the hypothetical exit. The inlet was set to have a velocity between 0.05m/s and 1m/s depending on the scale of the particular device that was being tested. If sheath fluid was being added, this defaulted to a volume flow rate of $10m^3/s$. Upon completion of a flow simulation, a quantitative analysis of the flow trajectories could be made immediately. This was followed by the insertion of a particle injection, a type of particle simulation in which a quantity of particles is made to enter at a specified entry point and reacts to the flow that surrounds it. Such a simulation was accomplished using 10μm diameter polyethylene particles; results were observed in a similar fashion.

2.3. Dean drag force

The client's initial instructions for this design were for the channel to ultimately have a width of approximately 50μm while the cells were estimated to be 10μm in diameter. To analyze the effectiveness of these parameters, a few equations which were used by former researchers in the initial development of this technique had to come into play [9]. The first equation, the Reynolds number, is used to define the much more relevant and important parameter, the Dean number. The Reynolds number is a dimensionless ratio of inertial forces to viscous forces. Inertial forces are typically represented by density, flow speed, and a length scale. In the case of the Snake, two separate Reynolds numbers are required for a proper analysis. The Channel Reynolds number is altered by the addition of U_m (the maximum channel velocity), v (the kinematic viscosity of the fluid), and D_h (the diameter of the channel). For an altered form of the equation that uses mean velocity instead, the Channel number is ⅔ of the original Reynolds number.

$$R_c = \frac{U_m D_h}{\nu} \qquad R_p = R_c \frac{a^2}{D_h^2} = \frac{U_m a^2}{\nu D_h}.$$

Equations 1 and 2. Channel and Particle Reynolds Number

The Particle Reynolds number is more a measure of the way the particle behaves within the channel. This can be obtained by multiplying the channel number by another dimensionless constant - the squared ratio of the particle diameter to the width of the channel. Typically, R_p is much less than one, and this implies that the particle will match the speed of the fluid in the channel. This means the R_p has the additional reliance on the diameter of the particle, which makes it a slightly more effective method of quantifying the flow of the particle. Previous

research has suggested that the level of focusing increases with the R_p. An R_p that is too high will result in damage to the cells, but an R_p that is too low will not result in proper focusing.

$$De = Re(D_h/2r)^{½}$$

Equation 3. Dean Number

The Dean number is another dimensionless constant that places reliance on the centripetal forces occurring within a pipe. The major modification is the addition of the r (radius of curvature) term. As before, research suggests that the Dean number should be less than 50 to be effective at maintaining flow conditions throughout the channel, and numbers between 10 and 20 are the most efficient for proper cell focusing. Upon further analysis of the research, it was discovered that the ratio of particle diameter to channel width ought to be between 0.1 and 0.5 to conserve this effect. As such, the channel width of 50μm could maintain particles with a diameter between 5 and 25μm before focusing would no longer be effective. The balance between inertial lift and Dean drag force is what maintains the cell localization to a specific point in the channel. Information regarding the Dean number was important to the initial analysis of the model, but further data collection was decidedly more reliant on observing the effects of the resulting core velocity that is characterized by these constants. Once a particle diameter of 10μm was determined to remain consistent with the Skala Lab's typical cell size, it was merely relevant to acknowledge how the ratio reshapes the physical ability for the cells to remain stabilized.

2.4. Remodelling the Snake to observe width and pressure effects

In tandem with the creation of the sheath fluid design, a separate model was created using a simple sketch, extrude, and shell method which was used to demonstrate the effects of particle centering with constant fluid flow through the channel (this can be observed in Figure 3). The new model was intended to test the pure functionality of the new design without traditional sheath flow mechanics. Initially a simple one-off design, this became the standard for creating the Snake and went through many iterations before a final design was chosen based upon the DiCarlo paper's specifications and a thorough analysis of the ratio between the asymmetrical curves of the design. It was desired that there be a method of comparing the effects of alterations in the channel width on the ability of the design to focus the particle stream and maintain velocity. An initial model meant to maintain a rough channel width of 50 micron was constructed with a small turn width equivalent to the size of the channel and a large turn that is 150% wider. Taking one "monomer" of the channel to be one large and one small curve, the final design was elongated to 100 monomers and was scaled up within SolidWorks to fit 100 micron and 150 micron channel widths with the goal of running multiple input pressure based simulations simultaneously on each design.

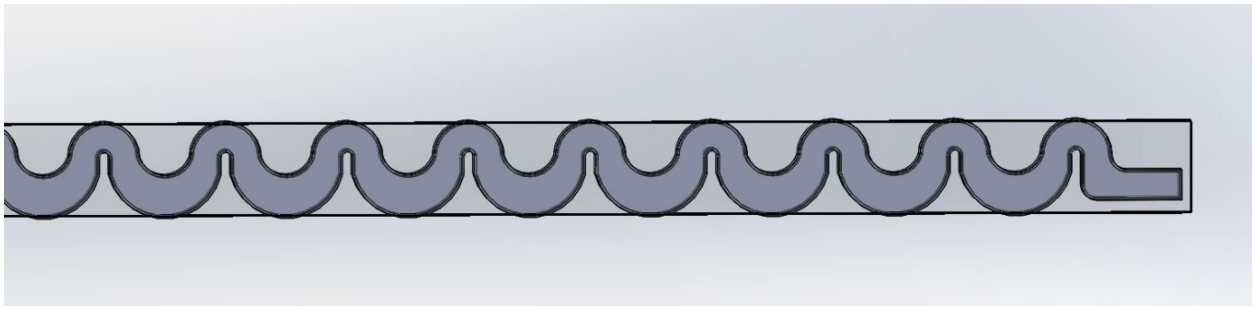

Figure 3. The layout of the updated Snake design used in testing for input pressure variations. The ratio of 1.5:1 for curved channel width was maintained for all three major design width variations, so the shape remains the same between them all

2.5. Particle Simulations

Particle simulations were done using the add in through Solidworks after the models had been created. Using the setup wizard, lids are placed on the ends of the designs to create a watertight shape. Next, each inner face (one for the inlet, one for the outlet) is selected and given a pressure. The inlet pressure will always be greater than the outlet pressure and will be variable. The outlet pressure will be set as atmospheric pressure (which is typically identified as 101325 Pa). A surface goal is set for volumetric flow rate at the outlet face. The fluid simulation will then run. After it is done loading, a particle injection study can be done. The injection gets selected and put on the inner inlet face with the number of particles set at 20, particle size set at 10μm, and polyethylene plastic beads selected to simulate the cells being used. After the particle injection study runs, it can be visualized or played as a movie for analysis. Further in depth analysis can be done by selecting the injection, exporting as an .xlsx file, and using the data about the beads from here. Analysis of the .xlsx file was done using the code in Appendix VI. A detailed protocol of the particle simulation is listed in Appendix IV.

2.6. Parametric Studies

Parametric studies were set up to run multiple particle simulations in a row without needing to manually start each trial. After a new parametric study folder is created, a simulation parameter needs to be declared. In this case, the inlet pressure was selected because this is the parameter that will be varied across the trials. From here, the variation is edited to include a start value of 101425 Pa, an end value of 201425 Pa, and a step size of 5000 Pa. The start and end values were determined based on the atmospheric pressure, and the capability of the Skala Lab's pump to eject pressures of up to 1 Bar (or 100000 Pa). The step size of 5000 Pa was chosen to limit the large number of runs needed to detail this range, however a more in depth analysis of certain pressures were run with step sizes of 1000 and 500 Pa. Next, an output parameter was declared, and this was our surface goal set in the Particle Simulations section above. Once this is done, the parametric study can be run. To load the results, the appropriate trial number folder was located under the parametric study folder. Within this trial sub-folder is a .fld file with the

particle simulation results for a specific trial number. A more detailed protocol for setting up and running the parametric simulation is listed in Appendix V.

2.7. Numerical data extraction, particle tracking, and analysis methods

Once a particle simulation has been completed, there are built in methods to the SolidWorks program that allow for all of the computational data to be extracted in numerical form. By outputting this data to a separate file, isolating the particle trajectory data near the terminal end of the channel becomes a matter of data parsing (a task which was accomplished through laborious efforts as well as through MatLab coding available in Appendix VI). Due to the manner in which the model was constructed, the plane upon which the surface of the channel rested coincided with the Y/Z plane, meaning that lateral focusing in either of these directions was analyzed for normality and statistical significance via the compilation of standard deviations at the various pressures being analyzed. Particle velocity could also be characterized via this method for reassurances from the initial visual analysis step during particle simulations. A trajectory plot as well as several histograms were constructed from each subsequent set of data in conjunction with a quick ImageJ cross-sectional image analysis and surface velocity plot mapping to help visualize the quantitative data for easier interpretation.

3. Results and Discussion

3.1. The initial results of the Funnel design

The results of the computational modeling for the Funnel design provided beneficial insight into its feasibility and functionality. The flow simulation modeling revealed information about the flow behavior of the core fluid diameter as it traveled into the channel. The modeling also revealed information on how cells would flow through the system. The parametric study on different inlet velocity speeds also provided information on how different speeds affected the flow.

The simulation of the Funnel design, as seen in Figure 4**,** shows that it was able to reduce the diameter of the core flow as it enters the channel. It was also shown that as the core fluid travels into the channel from the needle, it increases its velocity. This diameter reduction was not quantified. Having a better understanding of the reduction of core diameter would give better insight as to where the cells would be traveling down the channel. The cells would most likely stay within the flow of the core fluid, however. To provide more evidence of this, particle tracker simulations were used.

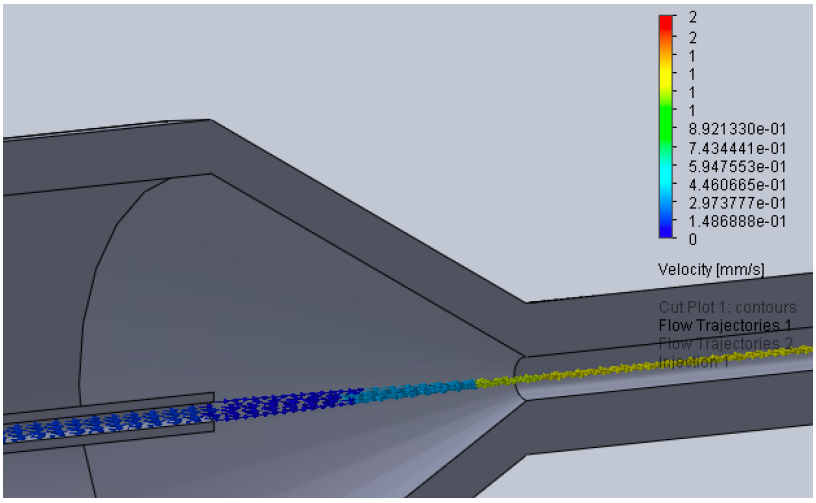

Figure 4. A cross sectional view of the Funnel design showing flow of the fluid coming from the needle.

The particle study shows how cells would behave as they traveled through the device, and it shows the cells being confined along with the core flow, seen in Figure 5. It also confirms that the cells are being centered within the channel, a fact further confirmed during the particle tracking stage of the testing procedure. Additional experimental testing would be needed to ensure that the cells are in fact staying within the area of core and if the model was correct.

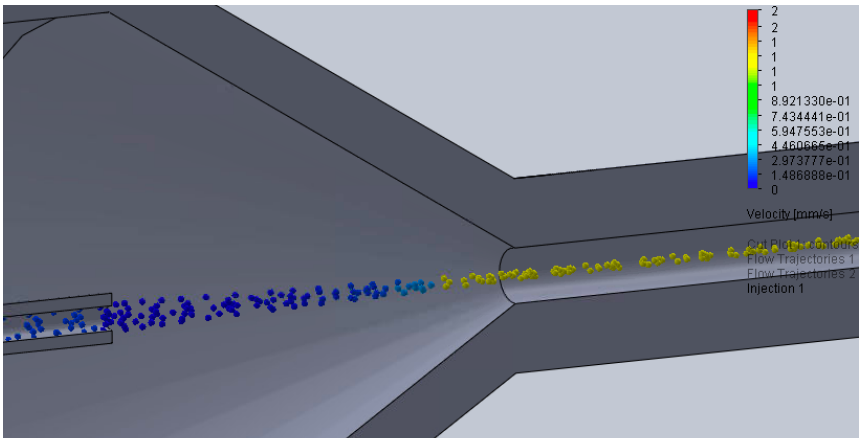

Figure 5. A cross sectional view of the Funnel design showing particles that represent cells flowing through the system from the needle.

To achieve the goal of having the velocity of the cells around 1-10 mm/s as they pass through the channel, some testing of different inlet velocities was simulated. First, the velocity of both inlets was varied to gain an idea of the effects that it would have, shown in Figure 6. The results revealed that the velocity of the sheath flow had a much greater impact on the flow in the channel while changing the inlet velocity of the cells had little to no impact. Following these results, the cell velocity was fixed while varying the sheath flow velocity to understand how it would need to be adjusted to get a final channel velocity of around 1-2 mm/s. The results

conclude that the velocity of the fluid in the channel was dependent on the sheath flow velocity. Another factor that would affect the velocity is the volume of fluid in the sheath flow which could be varied if more control was needed.

Velocity (Cells) [mm/s]	0.1	0.55	1	0.1	0.55	1	0.1	0.55	1
Velocity (Sheath Flow) [mm/s]	0.01	0.01	0.01	0.055	0.055	0.055	0.1	0.1	0.1
Velocity in the channel [mm/s]	1	1	1	7	7	7	13	13	13

Velocity (Cells) [mm/s]	0.1	0.1	0.1	0.1	0.1
Velocity (Sheath Flow) [mm/s]	0.001	0.005	0.01	0.015	0.02
Velocity in the channel [mm/s]	0.148	0.656	1	2	3

Figure 6. Table of final velocities in the channel that corresponds to a variety of velocities of the two inlets.

3.2. The effects of input pressure on particle velocity

The next step in characterizing the Funnel design was to determine the relationship between the pressure input and the velocity of the particles at the end of the Funnel. Since it was previously determined that the velocity does not change when the cell input pressure is changed, the cell input was kept 5 mBar higher than the sheath fluid pressure and then varied the sheath pressure. The cell input was kept 5 mBar higher so that there was no negative gradient of pressure that would cause fluid to exit the input. The particle simulation ran between 1 mBar to 100 mBar in increments of 10 mBar. The results of the particle velocities are shown in Figure 7. The graph shows a linear relationship (R^2 = .999) between the pressure applied and the velocity of the particles.

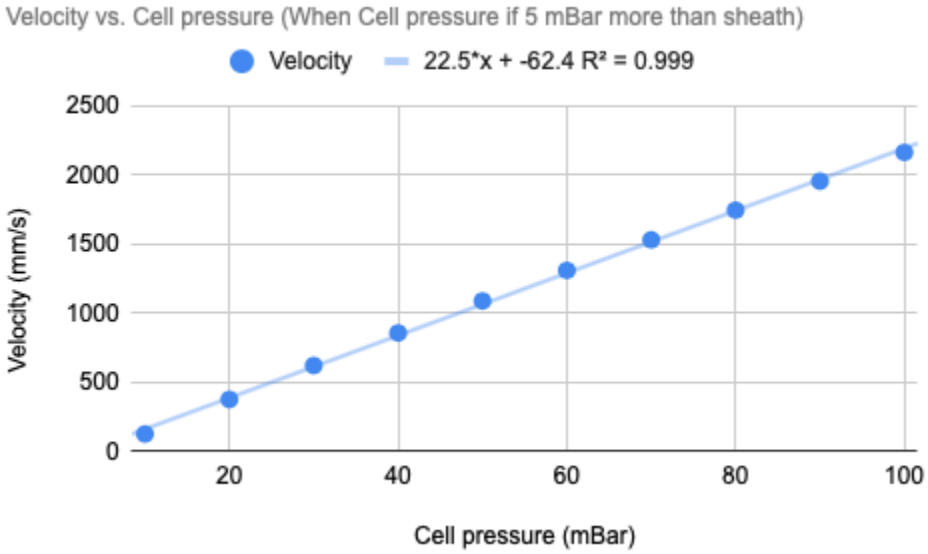

Figure 7. Graph of particle velocity in mm/s in relation to the pressure of the cell input.

3.3. Y/Z Centering of Funnel Design

A major goal of the device was to center and focus the cells into a single stream of cells. To measure the effectiveness of the Funnel design to accomplish this, the positional data of the particles were extracted. Each of the particles at the end of the channel were graphed to show where the cells would theoretically end up at the terminus of the device. Plots for 10 mBar and 100 mBar are shown in Figure 8. These two plots show that they are focused into a small area within the channel. It also shows that, at higher pressures, the cells become more confined. The spread of the particles was characterized by taking the standard deviation of the Y and Z components of each particle and comparing them to the other pressures as seen in Figure 9. The initial positions, at the beginning of the input, of the particles are included on the left to compare how confined they are before and after going through the device.

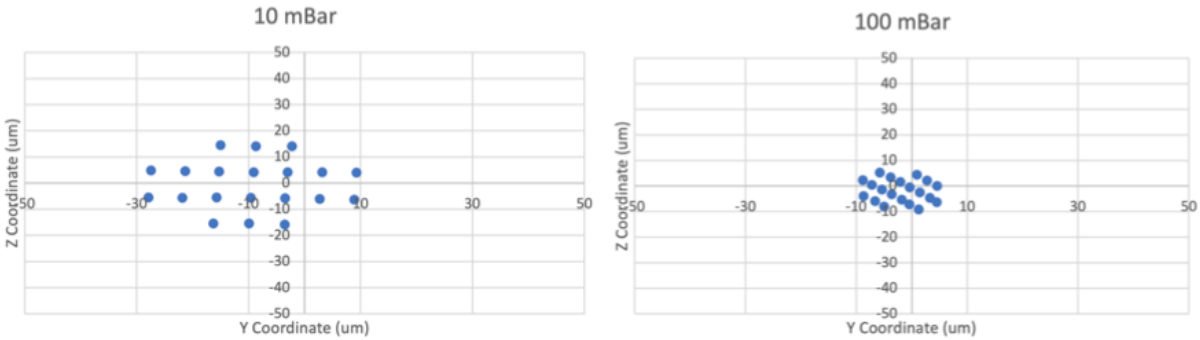

Figure 8. Graphs of the particle positions at the end of the Funnel design for 10 mBar (left) and 100 mBar (right). The origin of the graph is the center of the output channel.

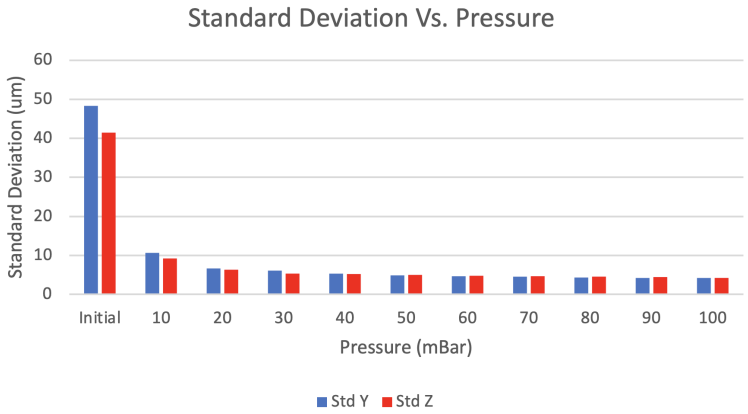

Figure 9. Graph of the standard deviations of the Y and Z spread of particles at each pressure.

The graph shows that it is able to focus and move the cells closer together. However, the change in the standard deviation plateaus. As the pressure increases, the focusing ability is not

significantly affected after 20 or 30 mBar. However the speed of the particles will still increase as shown in Figure 7. For reference, the cells are 10 μm, thus, in the 10 mBar graph the spread is about 4 cells wide where in the 100 mBar graph the spread is about 1.5 cells wide (or 40 and 15 micron respectively). Comparing this spread to the initial width of about 10 cells wide reveals the ability for the device to confine the cells.

3.4. The effects of inertial ordering in a sheath fluid environment

With reference to the sheath fluid-based Snake design, the bulk of the analysis was spent looking at qualitative data provided by the particle simulations. This was due to the search for a method to properly analyze the qualitative results of the Funnel Design as well as the various alterations that were made to the Snake in terms of frequency of turns, radius of curvature, speed of flow, and the presence of sheath flow. Figure 10a illustrates the resulting particle simulation that was produced. Cells appear to focus early on in the channel and, upon contact with sheath fluid, are focused further within the plane of the fluid and propelled at faster speeds towards the outlet port of the device.

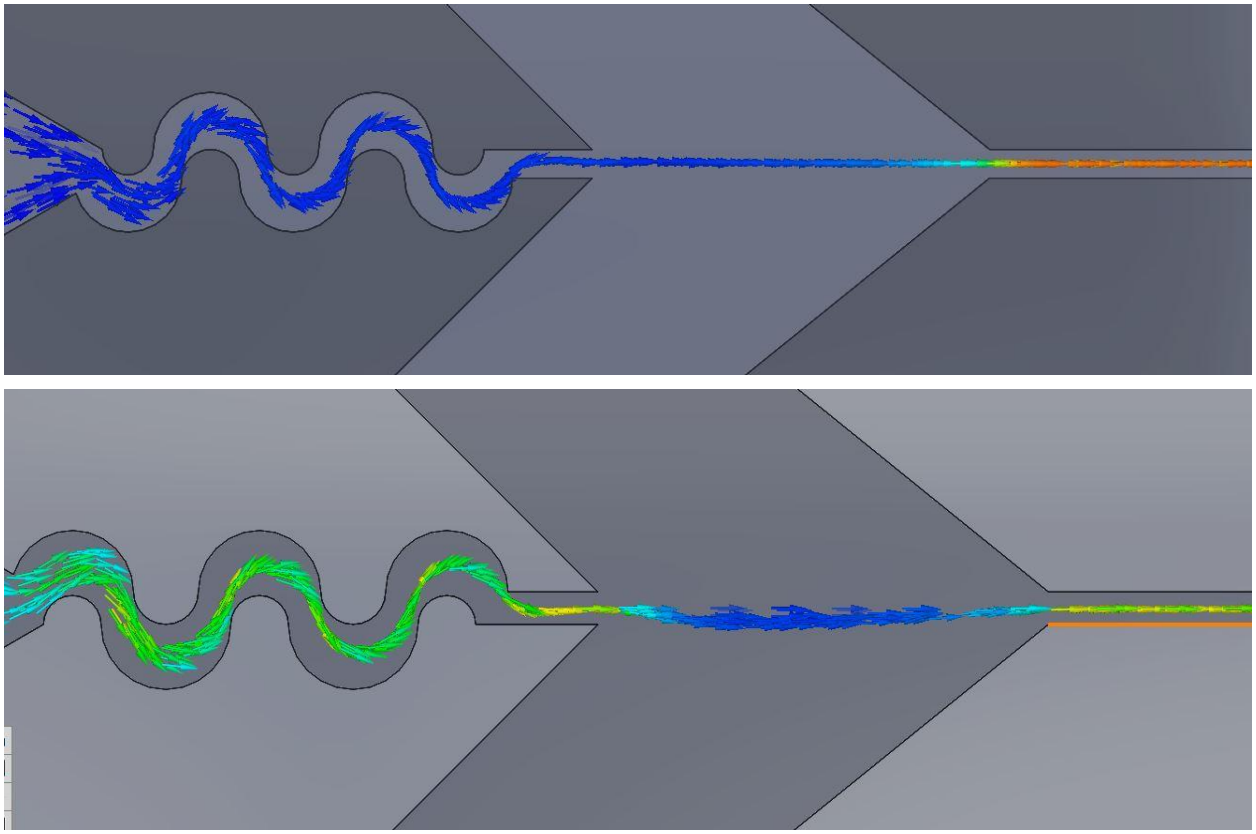

Figure 10. a) A visual representation of the XY plane of the particle simulation with sheath fluid. Increased focus can be observed upon contact with the sheath fluid. b) Removal of the sheath fluid shows a dramatic decrease in focusing before the channel width forces the cells back into a single-file stream

While the success of this design initially seemed to illustrate the feasibility of a shortened inertial ordering combination design, the clients pointed out that the majority of the focus was likely a direct result of the addition of sheath fluid and very little was actually being accomplished by the inertial ordering. Figure 10b shows the result of the sheath fluid being removed from the simulation parameters. Upon reaching a more open channel, the cells will expand to fill more space which reduces the effectiveness of the inertial focusing. It was decided that the inclusion of sheath fluid reduced the role of the inertial ordering mechanism entirely and did not serve as a sufficient improvement to the system as the velocity and focusing were mainly being controlled by the presence of the traditional sheath fluid system.

3.5. The effect of Dean drag using the remodelled design

Utilizing the revitalized design to follow-up on the initial testing stage, a quick set of simulations was run to test increases in velocity. Assuming the same principles described by the Dean drag equation hold true for the Snake, holding the cells at low input velocity and slowly increasing to a much larger velocity (almost 1.5 m/s in extreme cases) should show much clearer signs of focusing. This was indeed observed during the initial testing phase of the new model. Increasing the speed of the flow through the channel was able to increase the effectiveness of the inertial focusing. Reducing the width of the curves from an initial 100μm to 50μm accounted for speed changes in the Reynolds number calculation, bringing the particle constant (R_p) to about 3. This ensured that the Dean number was decreased to an appropriate level. Once the DiCarlo design was adapted, the effects of the channel's dimensions were more easily analyzed when looking specifically at the effect that the channel was having on fluid flow velocity.

3.6. Effect of fluid flow velocity on inertial control

The major source used for designing the Snake was the DiCarlo paper. In this paper, it is shown that a symmetrical, sine-wave design leads to the production of, what the paper calls, a Dean flow in which the curvature of the pipe and the combination of inertial forces leads to the production of two separate vortexes at either side of the channel, leading to the production of two separate particle streams that are guided by this vortex after a certain pressure amount is applied at the inlet. It was indicated in the paper that an asymmetric channel would restrict the production of such a flow to a single stream of particulate [9].

However, as noted in Figure 11, the production of a single high velocity flow stream at the center of the channel led to similar, particle stream-splitting results at higher pressures. At very low pressures, nearing 1 mBar, the particle stream is forced to stick to the surface of the flow stream, being guided by the core velocity without conforming to the same speeds. When pressure is increased, the actions of the Dean flow are seen to usher the particle stream into the center of the core fluid flow stream, increasing the velocity of the particles to nearly the maximum velocity of the fluid. Even further, increasing the pressure sees the particle stream leaving the influence of the core velocity, in favor of the more stable average fluid velocity range (represented by green in the figure). It is at this point that the asymmetrical design no longer

overpowers the effect of the Dean forces, and the particles are forced into two single file streams. This is seen across all channel width variations with smaller channels seeing an increased benchmark pressure for this split point. At 50µm of width, it takes 250 mBar of pressure before the particle stream splits while at 100µm it only takes 70 mBar.

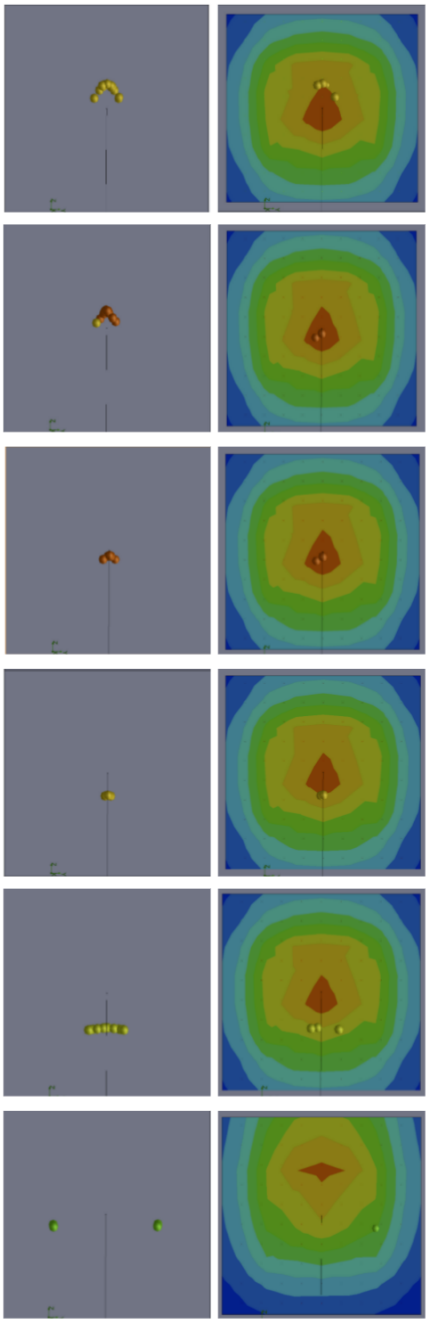

Figure 11. The effects of the core velocity pattern on the focusing of the cell stream for 1, 5, 15, 30, 50, and 1000 mBar in the 100µm channel design. The DiCarlo paper describes the Dean flow (as a direct result of the Dean calculations described earlier) as being responsible for shifts in velocity in curved

piping. Red colors represent the maximum channel speed while blue represents the minimum (for exact values for each, refer to images in Appendix IX)

The current applications of the specific type of cell sorting require the cells to fall into a single file line. Thus, it is important to note that the asymmetrical design only functions to keep the particles focused so long as the pressure does not surpass the ability of the channel to counteract the Dean force. Once this occurs, the particle streams will split, speed will match the average flow speed, and the streams will remain in a single file line, controlled entirely by the presence of a Dean vortex present at either side of the channel.

3.7. Variations in linear velocity with channel width

Velocity had the tendency to vary linearly with changes in pressure. This was an expected outcome to be sure. When comparing the velocity with channel width, specifically, there was another, equally expected outcome which also reared its head. For the same pressure applied across all three designs, the velocity of the particles at the outlet was also significantly higher when more volume was available. One interesting extrapolation of the velocity can be observed in Figure 12 where it is seen that, at certain pressure benchmarks, the slope of the linear relationship between the two variables drastically changes. For the 50 micron design, for example, the particle stream leaves the influence of the core flow stream at the point marked in red. It is also at this point that the first drastic slope change occurs. Further changes in slope are found to correspond with alterations in the channel's ability to redirect the central flow velocity as well as the particle's gradual conformity to the average fluid velocity of the channel.

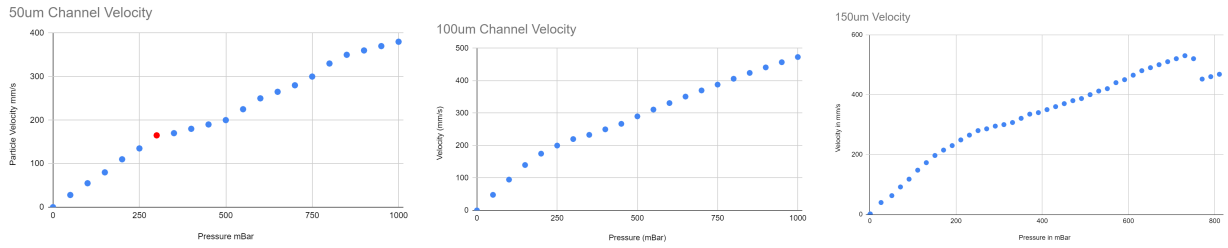

Figure 12. Graphical representations of the various linear relationships between velocity and pressure across the three major designs. Due to the location of its benchmarks, the alterations across the 50 micron channel are most clearly observed while, in the 150 micron snake, it can be seen that, at high enough pressures, the effect of the core fluid velocity is lost entirely and the particle speed drops to conform completely to the average flow speed.

Taking the 100 micron channel aside as an example, there can be found an adequate proof that the linearity of the relationship is much more accurate at small pressure inputs. Figure 13 represents a near perfect representation of the particle stream velocity relationship when the stream is just within the realm of influence of both the Dean forces and the core velocity. From 1-20 mBar, for every increase of a single mBar, the velocity increases by approximately 1.3 mm/s up until the point where influence is lost.

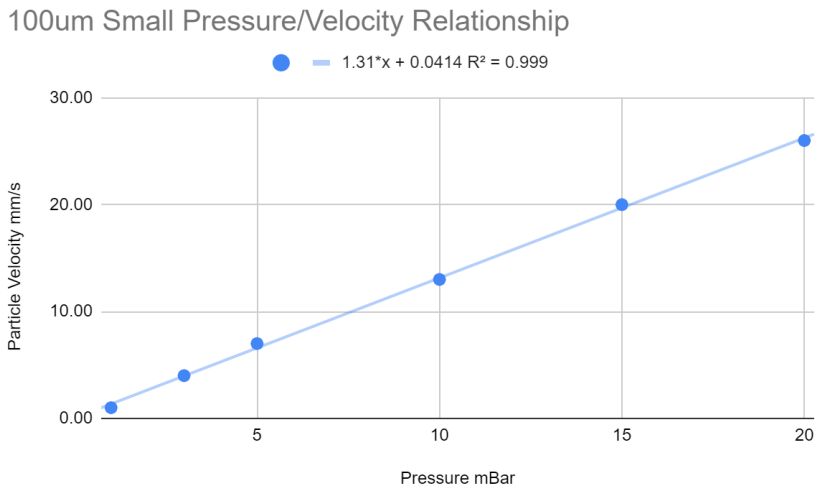

Figure 13. If assuming that the particle velocity does conform to a linear relationship at low pressure inputs, the relationship of the 100 micron channel shown above can be represented by the corresponding equation with an R-squared accuracy value of 0.999. After a certain pressure nearing closer to the "split-point", this relationship is altered.

3.8. Y/Z Centering in the Snake

Due strictly to the method of model construction, the face being analyzed at the terminus of the Snake ended up lying on the Y/Z plane. This meant that the majority of extracted data that was relevant relied solely on the Y trajectory and Z trajectory data that was presented by the particle simulation. Using the 100 micron channel as reference due to the client's initial design's attempt to replicate it (but knowing that each design conformed to the same patterns), a look at the general patterns being observed can be found in Figure 14 (with much more extensive graphing located in Appendix X and Appendix XI). From 1-15 mBar of pressure, focusing appears to be occurring on both axes due to the gradual merging of the particle stream with the central flow. At 15 mBar, the particle stream maintains position closest to the center of the channel with a center of mass maintaining within 3µm of the channel center in the Z direction and approximately 0.15µm in the Y direction (entirely dependent on the location of the central flow stream). After this point, dependence on the central flow stream begins to dip with Dean vortices taking a more active role. The most balance between all forces is achieved at 30 mBar where central focusing is reigned in to a minimum range of 3.16µm in Y and 0.42µm in Z (for comparison, the 50 micron channel sees this occurring somewhere between 150-200 mBar and reaches a minimum range of 0.35 and 0.09µm in Y and Z respectively).

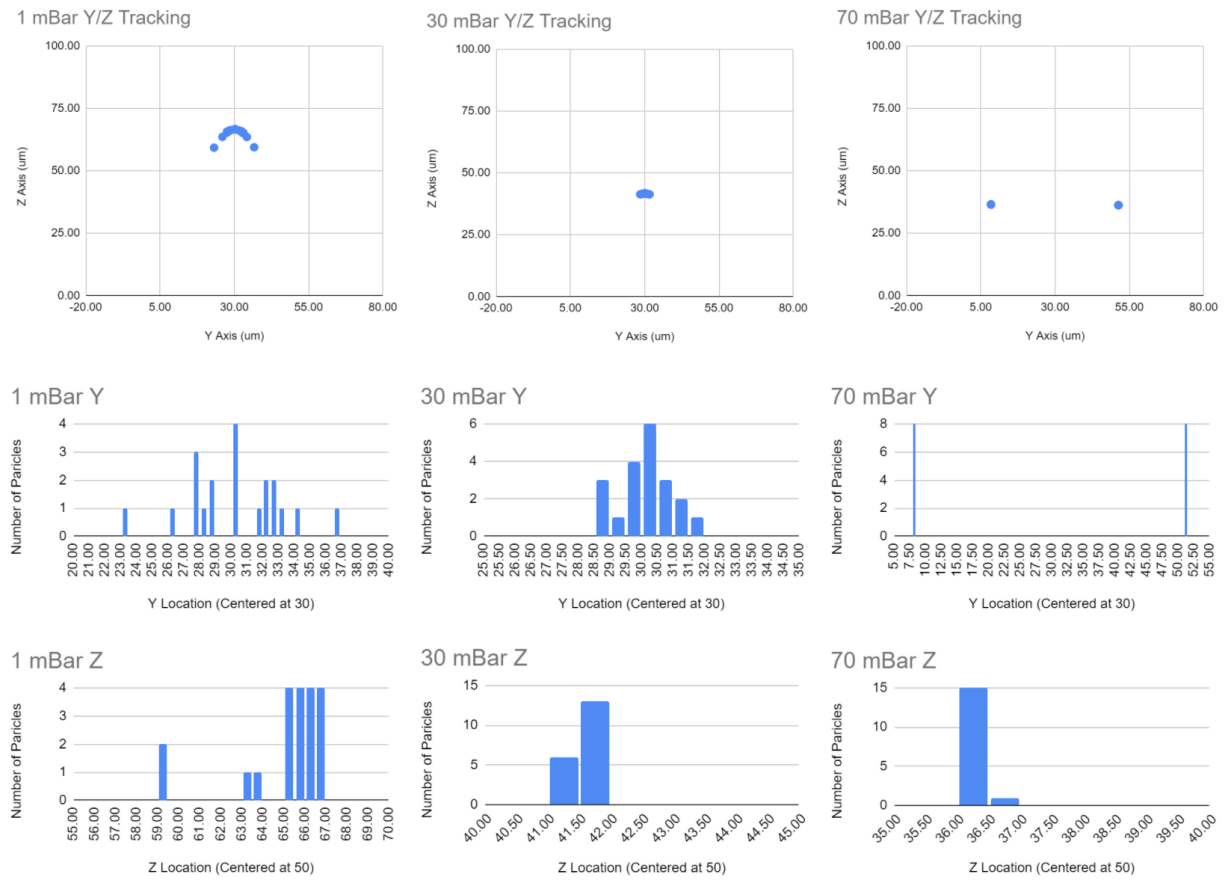

Figure 14. A comparison of the effect of pressure on the 100µm width channel design. Three main pressures are shown to represent the major stages of the process: 1-30 mBar shows the progress towards focusing while 30-70 shows the decline towards the split point. From 70 mBar and onward, the graphs all look nearly identical.

Once the 30 mBar optimal pressure zone has been surpassed, the particle stream gradually begins to lose its focusing power. By 70 mBar, the stream has been fully consumed by the average velocity stream (shown in Figure 11) and two separate particle streams have been formed with ever increasing velocity. Curiously, the Z direction remains focused with both secondary particle streams appearing to remain entirely single file throughout the duration of the pressure testing.

3.9. Overall impressions of inertial ordering channel effectiveness

Based purely on the data regarding Y/Z focusing, the power of inertial ordering seems to be relatively plausible when implemented at lower input pressures. The effect of increasing pressure on the channel has the effect of, not only increasing the velocity of the particle stream involved, but also eliminating the effectiveness of the concentrated streaming effect. At its peak, the 100 micron design demonstrated a focusing power that reduced the range below 4 micron in either direction. Given the overall particle size of 10 micron, this type of focusing seems to be a

reasonable reduction in stream diameter from initial randomly ordered methods without the use of sheath flow. Figure 15 demonstrates the effects of increased pressure on the ranges and standard deviations for the 100 micron design, clearly showing that maintaining pressures that are effective at keeping the cells moving at slow speeds without disrupting their structure is also an optimal method for generating minimal cell spread across the channel.

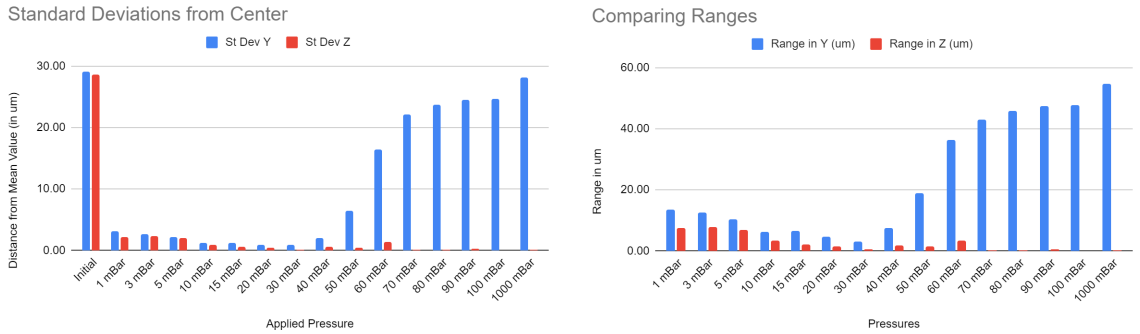

Figure 15. The standard deviations and ranges for the 100 micron design for various applied pressures. The initial bars included on the standard deviation graph are meant to represent the simulations initial particle placements at the inlet of the channel to provide a reference for how much the particulate spread was reduced.

A final test was conducted on the long term effect of the focusing. As was mentioned in the DiCarlo paper regarding the effects of the Dean vortex within the channel, it was expected that, over an extended distance, the particle stream would begin to conform towards one vortex or another (since two are typically formed in a typical curved channel). When the terminus of the 150 micron design was extended to be over 3cm in length, this exact effect was observed, with particle streams drifting towards whichever channel wall was closest at the original outlet position. This effect is hinted at in Figure 11 as a similar effect is responsible for distorting the velocity map at high input pressures (nearing 1 Bar) with the core flow velocity moving towards one wall or another. This effect, too, seems to be minimized at lower pressures, allowing the central velocity to continue in a central position with the cells remaining in focus. However, it is important to note that the full effect of this elongation was not tested, so the extent to which particles remain centered well after passing through the inertial ordering curvature is not known. For the purposes of microscopic analysis and cellular tagging, the distances should nonetheless suffice.

3.10. Comparisons in the effectiveness of the two methods

The traditional method of utilizing sheath flow to generate a particle stream through force is fully on display in the design of the Funnel. This active role plays clearly into the control of pressure on velocity. Alternatively, the more passive presence of fluid in the case of the Snake design allows for similar, albeit, more controlled functional properties with higher variation being seen among the various traits being analyzed. In the case of a velocity, a linear pattern is observed using both devices. However, in the case of the sheath fluid alternative, the relationship

is roughly 20x larger than for the Snake meaning, at low pressures, the passive role of the Snake still manages to produce greater reductions in overall speed (with respect to realistic changes in input pressure alone). When attention is turned towards the focusing ability of the two designs, the Snake is the clear winner in some areas while the Funnel earns a more consistent reputation. For the duration of testing, the Funnel design was able to retain a focusing diameter of roughly 15μm without ultimately failing at larger pressures. In fact, centering improved continuously up until 40 mBar where an optimal diameter was reached and persisted for all higher pressures. The Snake, on the other hand, could focus cells in a much tighter stream (nearing a single file line with an ultimate range of within 4μm of the center). Unfortunately, the tendency for this cell stream to split into two smaller streams at higher pressures is a detriment to the capabilities of the design (in spite of this, given the ability to focus velocity, it might just as well be irrelevant that higher pressures have an effect on the focusing power of the design given the low pressures that are likely to be used anyway). Ultimately, the decision between the two designs comes down to velocity control and what pressures the user has the capability of working with. If speed is of no consequence, the Funnel is the most plausible option. On the other hand, it appears as though the plausibility of the Snake to generate an optimal amount of focusing might far outweigh this option, but further testing will be necessary to ensure that this is a physical certainty.

4. Conclusions

This project resulted in the development of two unique designs to aid the Skala lab in cell sorting experiments. Of the two designs, the Funnel design was simpler to model due to the geometry and popularity of flow cytometry. Following modeling in Solidworks, flow simulations were performed to determine the ability for the sheath fluid to confine the cells to the center of the channel. Particle studies characterised outlet velocities at various inlet pressures as well as the confinement of the cells. Results were favorable and indicate that the design would be successful when fabricated.

Work on the Snake design consisted of modeling and simulations to investigate various iterations and dimensions of the design. The design was tested both with and without sheath fluid as well as with different inlet pressures. With the DiCarlo paper as a guide, alterations to the radius of curvature, width of the curved channel, and initial flow velocity were made to optimize the design for this application. Testing with particle tracking and parametric studies revealed the feasibility of the inertial ordering design at lower pressures.

5. Future Work

5.1. Further steps taken by the Skala Lab

The next phase of this project will likely include fabrication of both designs for further testing in the lab. Potential options for fabrication of the devices have been investigated and a number of options have been identified. The Skala lab has convenient access to a high resolution 3D printer that may be used for prototype development. Initial prototypes should be tested to ensure functionality and a leak free connection to the lab's pump set-up. Additional testing

should be performed to ensure the simulations are valid and collect further experimental data. After further testing of the prototypes, higher quality prototypes or final copies of the devices can be fabricated via custom microfluidics producer. At present, a version of the 100 micron channel design of the Snake, made out of PDMS through the use of soft-lithographic techniques, was generated by the Skala Lab for initial testing of the focusing power. Initial qualitative results are positive.

5.2. Physical data necessary for proof of simulation validity

After fabrication of the design prototypes testing should be performed in the lab to validate the results shown in the simulations. Experimental set up may include the use of fluorescently labeled beads to simulate cells that will flow through the devices. One of the first tests should include using a brightfield setting on the microscope to visually verify that beads are flowing in the center of the channel, if they are going through one-by-one, and to make sure they are flowing at the right speed. Another test would include using the laser to confirm that the beads are flowing through the window of integration and are within the focused laser. Testing should be performed at various pressures as done in the simulations to confirm that the simulations are a valid prediction for the behavior of the cells in the prototype.

Acknowledgements and Collaborators

This research was supported by members of the Skala Lab, specifically Dr. Melissa Skala, Emmanuel Contreras-Guzman, Dr. Kayvan Samimi, and Andrea Schiefelbein, without whom the project would not have been discovered by the BME Department. Support also came from the Biomedical Engineering Department at the University of Wisconsin-Madison, the team's advisor, Dr. Justin Williams, and the rest of the faculty responsible for maintaining the BME Design Program and its assets. Funding was provided for this project, but no money was spent.

Appendices
Appendix I: Project Design Specifications

Project Design Specifications

Team:

Josh Zembles
Sara Wagers
Caleb Heerts
Hunter Hefti

Date:

March 3rd, 2021

Function: The Skala lab has developed label-free optical signals to sort T-cells by activation state. The next step in their research requires a microfluidic chip to flow the cells at speeds that allow 100's of ms integration time on the detector. The device can be commercial or newly designed, and requires a number of specifications in order to integrate with their system. The function of the device should create single-file cell flow through the interrogation window with a stable core diameter of 20 μm to 50 μm while ensuring that stability is first maintained in the z direction. Cells should flow through the microfluidic device along with a PBS sheath fluid at a flow speed of 1 mm/s and up to 10x faster.

Client Requirements: There are a number of specifications that need to be considered in order to ensure that our design is fully compatible with the equipment used by the Skala Lab:

- The device should be able to fit within their microscope's stage insert
- The bottom of the flow cell must have 150 micron glass thickness while accommodating the 1 inch wide objective lens at a working distance of 0.2mm.
- This device should be created with a budget of $2000 in mind, aiming to save money as compared to custom microfluidics and the cost of flow cytometers.

Design Requirements:

1. <u>Performance Requirements:</u> The device must be able to maintain sufficient pressure to flow the cells and media through the channel at a consistently low flow rate. Ideally, the device will be effectively integrated with the pump system that the Skala Lab has already set up. The microfluidic chip should maintain consistent performance over time as it is intended to be a reusable device.

2. Safety: There are limited safety concerns regarding the development of this device. The device should pose no threat to the user if used correctly as all cells and fluids should be contained within the channel. When operating the device or handling any associated cell cultures, typical safety protocols should be adhered to.

3. Accuracy and Reliability: This device must operate accurately to ensure that cells are within the interrogation window for a suitable amount of time. The channel must reliably create a single-cell flow of 1 mm/s and must also limit the variance in z-direction of the cells as they flow through. An accurate device will ensure that experimental data is useful within and between experiments.

4. Life in Service: The life of a flow cell is vague as the potential for reuse is essential to its design. Laboratory glassware can be used indefinitely as long as proper maintenance is applied to keep the material clean. The design will likely be made from glass or quartz as listed below. These items are not particularly prone to a quick expiration. Prototype designs should have a lifespan of at least a few weeks in order for testing to be completed while the final design should have a lifespan that exceeds 10 years if necessary and if proper maintenance is applied.

5. Shelf-Life: In conjunction with the life in service, the flow cytometer cell should be designed in such a way that parts do not degrade while in use. As such, while not in use, the cell should be able to withstand an extended period of resignation in storage that surpasses the lifespan of a cell that is in continuous circulation. This assumes that, prior to storage, proper sterilization techniques using ethanol are employed to prevent mineral build-ups or the proliferation of any residual cells.

6. Operating Environment: Elements of the cell will be exposed to a pulsed laser and should be able to withstand such exposures. Placement under a microscope or under other varieties of imaging equipment may also be possibilities. Pumps are used to produce the pressure that powers the transport mechanisms responsible for pushing fluid and cells through the cell which should also be accounted for. General lab temperatures and light exposures should also be accounted for if necessary.

7. Ergonomics: The microfluidic cell functions similar to a glass slide used for microscope viewing and can be placed over the laser in a manner that is similar. The human hand is capable of picking up objects that are 1 mm thick with relative ease and only two fingers will be required to pinch together enough strength to pick up and hold the cell. Other elements such as the pump have already been designed ergonomically in a fashion that allows for the control of pressure and flow to remain in the hands of the user.

8. Size: The objective access window that is meant to carry the Quartz/Glass capillary is roughly 3.5 cm long while the PDMS that currently acts as the inlet and outlet are nestled at either end of the tube. The size of the current cell is about as thick as a 1mm glass slide but can likely be thicker up to ~ 2.5 mm while the whole of the device is 9.6-9.75 x 2 cm in overall size. The current laser is set up to accommodate objects roughly this size so the length of the overall cell should not exceed 10 cm in length and not much more than 2 cm in width.

9. Weight: A reasonable weight to set the design of the cell can be estimated as less than 15 grams. Glass can be reasonably approximated as having a density of 2.5g/cm^3 while quartz has a density of 2.43g/cm^3 and PDMS has a density of 0.965g/cm^3. Using all of these measurements in various combinations using the estimated maximal size of the object above, all calculations yield potential weights that are near or smaller than 15 grams. A device made entirely of PDMS would weigh approximately 5 grams. As such, the weight of the cell is expected to fall near one of these measurements.

10. Materials: The materials used for the design should be biocompatible or bioinert. They should not interact with the cells, cell media, or other solutions such as PBS, DI water, or clean water in order to stop any contamination from occurring. Additionally, the materials used should allow light to pass through uninterrupted for measurements being taken. Materials suggested by the client include either quartz or glass, however for prototypes, PDMS may be used due to its ease of fabrication. The material should be able to be reused and cleaned either with ethanol or an autoclave.

11. Aesthetics: The focus of this design is more on functionality. Being able to align the cells with a certain speed is the main importance meaning aesthetics aren't a major concern. The materials shouldn't be sharp when touched and the design as a whole should be relatively small to fit on the stage of the lab's microscope. Additionally, the material chosen must be transparent to allow light to pass through.

Production Characteristics:

1. Quantity: For the semester, only one product is needed, but if a successful design is found, then more could be produced for analyzing multiple groups of cells at once.

2. Target Product Cost: The client has set a budget of $2000 for the prototype. They are hoping to create a device more cost effective than a custom flow cytometer that can be produced with prices ranging upwards of $4000 [1].

Standards and Consumer Characteristics:

1. Standards and Specifications: There are no federal regulations concerning this device since it is being specifically designed for the clients use. However, the device needs to be sterilized to ensure no contamination.

2. Patient or User-related Concerns: It is incredibly important that this device will maintain sterility and work accurately as it will be used for research experiments. Care should be taken to ensure that cells from different batches are separated and treated as such.

3. Competition: Currently most cell sorting microchips [2] use weight or size as the factor to separate different cells. These kinds of chips will not work since they depend on multiple types of cells while the clients have one type and are either fluorescent or not. The cell sorting techniques that are based on fluorescence are an all-in-one machine. The client only wants the microchip which allows cells to be centered in a stream so their custom laser can be used to identify each cell. Microchips that consist of small channels are available on the market that allow for a stream of cells to flow through a narrow channel under a microscope [3]. However, these cells are not centered within the channel for the laser.

References:
[1] “Custom Quartz Flow Cell Manufacturing,” *FireflySci Cuvette Shop*. [Online]. Available: https://www.fireflysci.com/custom-quartz-flow-cell-manufacturing. [Accessed: 17-Sep-2020].
[2] Microfluidic Chip-Based Gentle Cell Sorter, Single Cell & Cluster Dispenser | On-chip Bio. 2020. *On-Chip Sort CONSUMABLES : MICROFLUIDIC CHIP | Microfluidic Chip-Based Gentle Cell Sorter, Single Cell & Cluster Dispenser | On-Chip Bio*. [online] Available at: <https://on-chipbio.com/product-onchip_sort/microfluidic-chip/> [Accessed 17 September 2020].
[3] “Straight Channel Chips - Glass,” *microfluidic ChipShop*. [Online]. Available: https://www.microfluidic-chipshop.com/catalogue/microfluidic-chips/glass-chips/straight-channel-chips-glass/. [Accessed: 17-Sep-2020].

Appendix II: Preliminary Designs

Plinko

The Plinko design is inspired by a pricing game from The Price is Right. The object of the game is to strategically drop round disks from the top of a peg board in an effort to guide their motion to a specific spot at the bottom of the board. While the motion appears to be random, a specific set of mathematical and physical principles guide the disk towards an intended location. The parameters that define the motion of the disk can be the angle of trajectory, the shape of the peg, the shape of the object being dropped, or even the weight of the object [1]. Predictability in the behavioral patterns of objects colliding with pegs on the plinko board provided inspiration for a channel widening technique that uses the same principles. The introduction of obstacles in a channel is not a new technique in microfluidics. Studies have been carried out on the disruption of diffusionally symmetry using ratchets and have shown that objects of varying sizes display predictable motion when flow is asymmetrically disrupted [2].

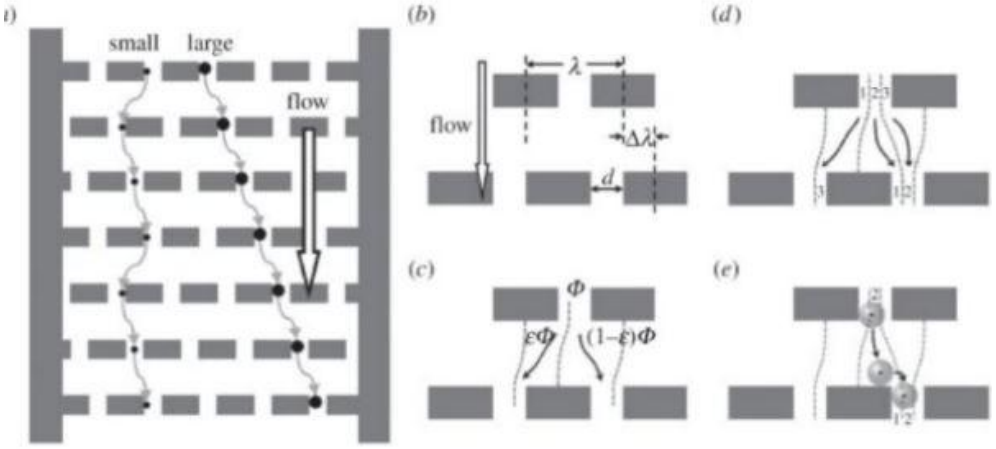

Sturm *et al.*, *Interface Focus*, **2014**;4(6):20140054. doi:10.1098/rsfs.2014.0054.

Figure 1: A diagram of flow passing through a channel with Brownian ratchets inserted. The basic principle of large particles flowing in an orderly fashion is highlighted.

Using these principles as the basis of the design, the main function of the Plinko concept's introduction to the cellular inlet is to guide the flow of the cells into a central position. Either through the introduction of randomly placed rods into an expanded channel or by directed placement of ratchets aiming cells towards the center of the channel prior to constriction, cellular focusing would be achieved while increasing the volume of PBS flow. Possible implications of this might be the ability for restricted flow or the integration of sheath fluid outlets to slow fluid flow down in tandem with inertial centering.

Funnel

Typical flow cytometry chips are designed with the intent to usher cells towards an objective. The most typical method for driving the sample is through the use of sheath fluid which, in a typical cell, arrives from side channels and converges upon the cellular inlet to carry the sample forward. Sheath fluid designs are frequently used in a two dimensional placement where fluid arrives from one or two directions [3]. While remaining a staple of the experiment, the two dimensional sheath fluid flow has the potential to introduce turbulent flow at the point where convergence occurs.

Alternatives to the two dimensional design commonly include three dimensional alterations. Funnel designs involve the utilization of a cone shaped sheath fluid inlet which allows for complete encapsulation of the incoming cell sample. In these cases, a core diameter is formed in which the cells are centered in all directions within the channel which is guided by laminar flow on all sides in the form of the sheath fluid. For this reason, the Skala Lab has already experimented with variations in a conical design.

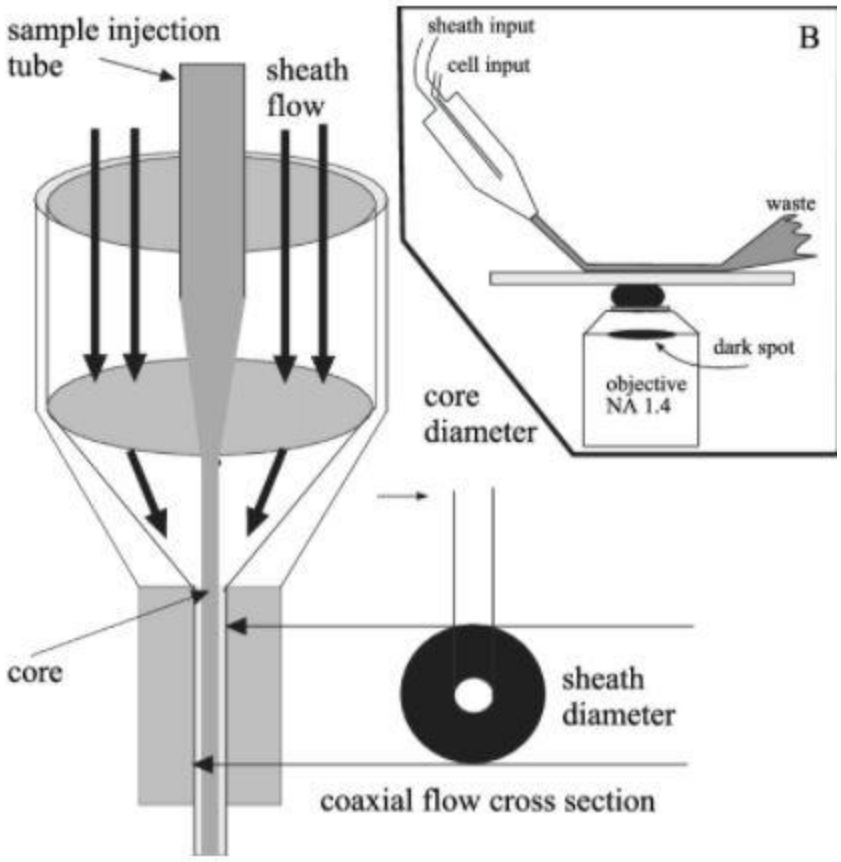

Figure 2: A typical conical shaped Funnel design which incorporates angular positioning to bolster fluid speed.

As shown in Figure 2, the Funnel design is typically accompanied by an incline in order to induce the fluid and accurately flow on all sides of the cone. While this is beneficial for generating the centering effect, if a kink is involved at the objective transition point, turbulent flow might interfere with the potential benefits of this effect.

Snake

The main design consideration behind the Snake design is the property of inertial lift. When laminar flow is made to pass through a channel that does not generate uniformly parallel streamlines, flow will seek out a path of least resistance. This displays itself in an outlet streamline which is uniformly centered towards the center of the channel. This idea was implemented into a microfluidic device by Di Carlo in 2007, and when an asymmetric design was implemented, a result that bears close resemblance to Figure 3 was produced [4].

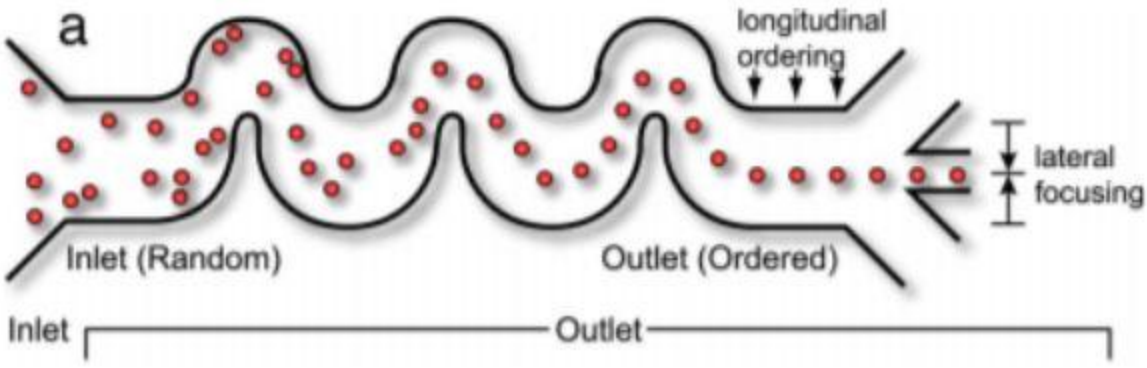

Figure 3: A schematic of a sample prototype for an asymmetrical serpentining channel. The summation of inertial lift forces encourages cells to form a line as they take the path of least resistance towards the outlet.

The snake design was expanded and the concept of inertial ordering was added to a set of potential improvements to cell sorting [5]. Most designs concentrate on cell ordering prior to the addition of sheath fluid. One such design even incorporated an asymmetric squiggle pattern in an effort to create order from the sample directly [6]. But it was hypothesized that adding the sheath fluid prior to entry into the inertial ordering system would allow cells to avoid potential turbulence and order the fluid prior to observation by the laser.

References:

[1] "Plinko," *The Price Is Right Wiki*. https://priceisright.fandom.com/wiki/Plinko (accessed Oct. 07, 2020).

[2] J. C. Sturm, E. C. Cox, B. Comella, and R. H. Austin, "Ratchets in hydrodynamic flow: more than waterwheels," *Interface Focus*, vol. 4, no. 6, p. 20140054, Dec. 2014, doi: 10.1098/rsfs.2014.0054.

[3] A. Cossarizza *et al.*, "Guidelines for the use of flow cytometry and cell sorting in immunological studies," *Eur. J. Immunol.*, vol. 47, no. 10, pp. 1584–1797, 2017, doi: 10.1002/eji.201646632.

[4] D. D. Carlo, D. Irimia, R. G. Tompkins, and M. Toner, "Continuous inertial focusing, ordering, and separation of particles in microchannels," *Proc. Natl. Acad. Sci.*, vol. 104, no. 48, pp. 18892–18897, Nov. 2007, doi: 10.1073/pnas.0704958104.

[5] P. P. A. Suthanthiraraj and S. W. Graves, "Fluidics," *Curr. Protoc. Cytom. Editor. Board J Paul Robinson Manag. Ed. Al*, vol. 0 1, p. Unit-1.2, Jul. 2013, doi: 10.1002/0471142956.cy0102s65.

[6] A. A. Nawaz *et al.*, "Intelligent image-based deformation-assisted cell sorting with molecular specificity," *Nat. Methods*, vol. 17, no. 6, Art. no. 6, Jun. 2020, doi: 10.1038/s41592-020-0831-y.

Appendix III: Preliminary Design Evaluation

Design Matrix

To aid in the consideration of preliminary designs, the team created a design matrix with weighted categories. The most important criteria considered were the Speed Reduction and Positioning. Speed Reduction is a crucial component of the design as it is necessary for the cells to slow down enough to be properly read by the laser. The Plinko design scored highest in this category because the cells will reduce in speed as they bounce around. The Snake design was the next highest scoring as going through the turns should also reduce the velocity whereas the Funnel design does not consider the need to reduce speed.

The Positioning criteria is as important as Speed Reduction because the cells need to be centered in the x, y, and z axes in order to have consistent readings by the laser. The Snake design scored highest in this category as it was designed specifically to align the cells when they come out of the curves. The other two designs did not score as highly as their alignment mechanisms are not as precisely designed. All three designs may face issues when aligning the cells in the z axis.

Ease of Fabrication is the next highest weighted category because a device that is easier to fabricate can streamline the development process as well as reduce the amount of work that the client will need to do to produce more microfluidics in the future. The Funnel design is the simplest and would be most straightforward to fabricate, followed by the Snake, and finally the Plinko. The client has considered fabrication by an outside vendor which can be expensive, so a simpler design may help to reduce those costs.

The next criteria considered is the Reusability/Sterility. These ideas go hand in hand as it is important that the device can be properly sterilized in order to be used again. The client will sterilize the device by running ethanol and purified water through the device. The Plinko design will likely be the most difficult to properly sterilize as there are many surfaces on which particulates or contaminants could get caught. The other two designs feature smooth channels that should be sterilized easily.

The Manufacturing Cost of the device should be kept to a minimum. This category was weighted lower than others because the cost is not a major concern of the clients, but cost should be reduced wherever possible. All three designs should have comparable manufacturing costs. Finally, the safety of each design was considered, and none of the designs should pose any threat to the user if properly fabricated.

Design Criteria	Plinko		Funnel		Snake	
Speed Reduction (25)	5/5	25	3/5	15	4/5	20
Positioning (25)	3/5	15	3/5	15	4/5	20
Ease of Fabrication (20)	3/5	12	5/5	20	4/5	16
Reusability/Sterility (15)	4/5	12	5/5	15	5/5	15
Manufacturing Cost (10)	5/5	10	5/5	10	5/5	10
Safety (5)	5/5	5	5/5	5	5/5	5
Total (100)	79		80		**86**	

Figure 1: Design Matrix of the three designs discussed above. Criteria are outlined on the left. Each criteria contains a score out of 5 and a weighted score for each design.

Appendix IV: Particle Simulation Protocol

Running a basic particle study consists of the following steps:

1. Setting up the model in SolidWorks
    a. Through importation or through the application of the part making process built into a SolidWorks, a new model needs to be implemented in order to run the particle simulation
2. Selecting the parameters
    a. In order to run a flow simulation using the build in software, the model needs to be considered water tight during the mesh setup process. Using the setup wizard makes the process easy, ensuring that the fluid involved is water and that atmospheric pressure of 101325 Pa is present at the initial setup
    b. A gray cube will represent the fluid simulation parameters of confinement. Adjusting the size of this shape will tell the simulation what is supposed to be included in the mesh and where the fluid is meant to be located and maintained
    c. A lid making tool can be used if the model includes any open ports where an inlet or outlet might be located. These lids can then be used to set up the fluid flow parameters, setting a static pressure at the inside face of both lids. The outlet must maintain an atmospheric pressure while the inlet can be varied to any degree.
3. Setting up a surface goal

    a. Once the fluid has pressure designations on the inside faces of each lids, a surface goal to analyze volumetric flow rate can be set at the outlet face where the particles are meant to flow.
    b. Setting up any kind of goal will likely do the trick, but this ensures that data on particle trajectories, fluid velocities, and all other relevant data is actually collected and the simulation can be run.
4. Avoiding errors
    a. Since the model must be water tight, there will be a variety of error messages that could pop up at any time. The model must be within a standard of perfection prior to implementation of the simulation, and it will not run without the above guidelines being met
5. Setting up a particle injection
    a. If the results are not already loaded from the resulting flow simulation file, these can be accessed via your individual file library, loading the .fld file should be enough.
    b. The option to set up a particle simulation should be clearly labeled in the results toolbar and, once the injection has been selected, the inner surface of the inlet must be selected.
    c. There are multiple options available for particle injection parameters. For our purposes, setting the particle number to 20 and the particle size to 10um (using a polyurethane or polyethylene plastic to simulate cell density) will work just fine. The particles can then be displayed via arrows, pipes, or dots, with movement physics depending on the computer's processing power and graphical capabilities.
    d. The resulting images can be captured for analysis - extraction of data to an excel file is simple, and capturing the trajectory values near the terminal end for further analysis can be simplified by following the code in Appendix VI.

Appendix V: Parametric Simulation Protocol

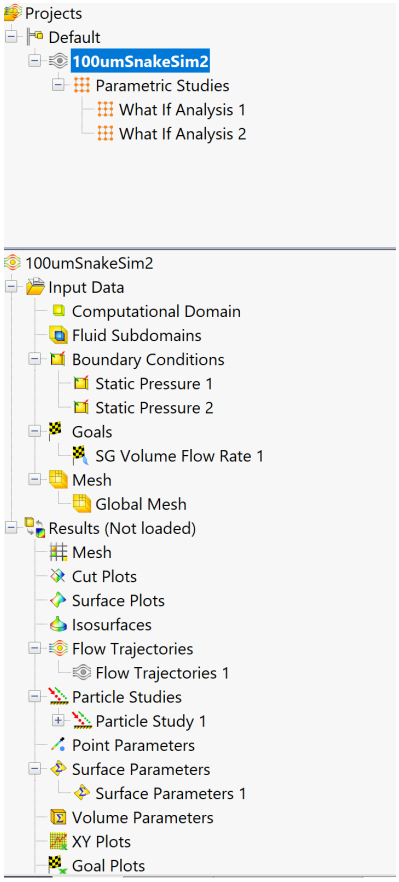

When starting a parametric study, you'll want a few parameters in place ahead of time. Both static pressures should be placed at either side (one set at atmospheric pressure and another set at a 1 mBar to initially test the functionality and ensure no errors pop up) and a surface goal for Volume Flow Rate should be set at the surface that has atmospheric pressure. With these in place, it helps to run a quick test to get the particle study set up ahead of time, so that everything is properly in place prior to the start (this isn't necessary as any of the results can be set up after the fact, but this way you don't forget).

After right clicking the name of the study (highlighted in blue above), you will click "New Parametric Study" and a table will load in at the bottom of the screen which says "What if Analysis".

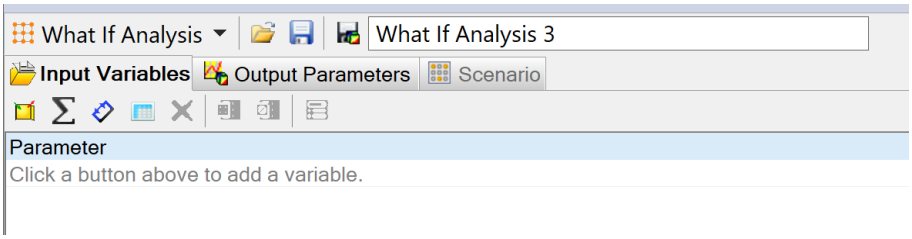

From here, click the first button just under "Input Variables" which prompts you to "Add Simulation Parameters". This opens the following tab in the lower right hand corner of the screen:

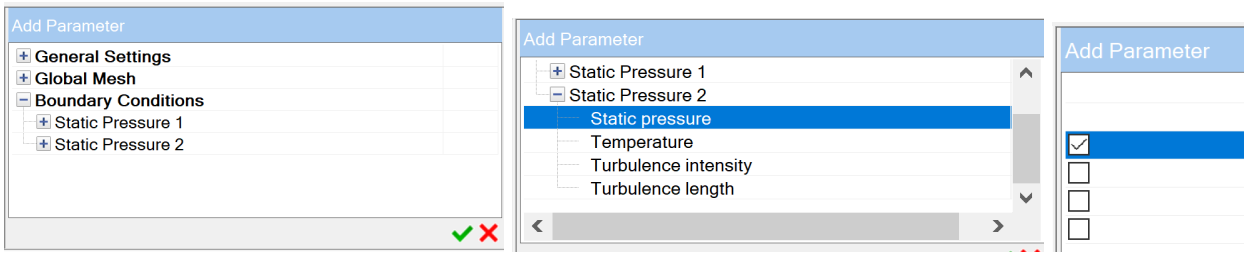

Once open, check the box for static pressure (for me, the input static pressure was set as "Static Pressure 2") so that the input is officially selected and press the check mark. This should reflect in the table:

Parameter	Current Value	Variation Type	#	Values
Static pressure (Static Pressure 2)	101425 Pa	Discrete Values	1	101425

Next, right click on the "Discrete Values" and select "Edit Variation". This should pull up a new menu similar to the last. By clicking on the 3rd icon within the table, you should see a screen that allows you to input the lowest value and the upper value and input the step size:

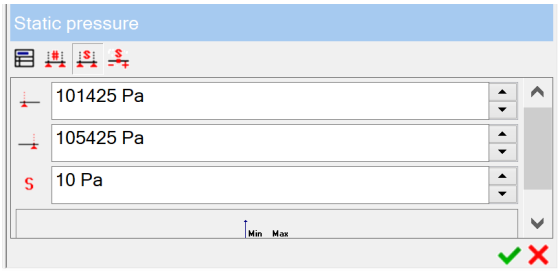

By clicking on the checkmark, the screen should be updated like this:

Parameter	Current Value	Variation Type	#	Values
Static pressure (Static Pressure 2)	101425 Pa	Range with Step	401	101425, 101435, 101445, 101455, 101465, 101

Next, you'll maneuver to output parameters and click on the checkered flag icon.

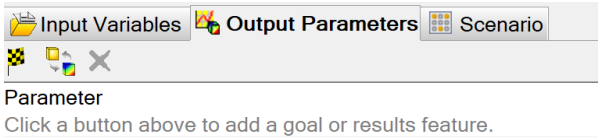

This pulls up yet another menu that lists all of the goals that you selected from the initial setup stage: in our case, only the Surface Goal will appear. Selecting this ensures that there is actually something to run so that data can be collected for each trial.

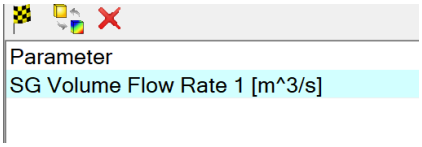

Once this has been selected, the Scenario tab will update to show the following:

Input Variables | Output Parameters | Scenario | Goals

Run

Summary	Design Point 1	Design Point 2	Design Point 3	Desig
Static pressure (Static Pressure 2) [Pa]	101425	101435	101445	10
SG Volume Flow Rate 1 [m^3/s]	?	?	?	
Status	Not calculated	Not calculated	Not calculated	Not c
Run at	[auto]	[auto]	[auto]	[a
Number of cores	[use all]	[use all]	[use all]	[us
Recalculate	☐	☐	☐	
Take previous results	☐	☐	☐	
Save full results	☑	☑	☑	
Close Monitor	☑	☑	☑	

And a Goals tab will have appeared which displays the selected result (in this case, the surface goal. The surface goal for volume flow rate will appear inverted and can be used to calculate, manually, the average velocity of the fluid at the surface. Which is technically useless, but at least now simulations can run):

Input Variables | Output Parameters | Scenario | Goals

Summary | Table | Value

Goal	Design Point 1	Design Point 2	Design Point 3	Desigr
Static pressure (Static Pressure 2) [Pa]	101425	101435	101445	10145
SG Volume Flow Rate 1 [m^3/s]				

When all of this is displayed, you can return to the Scenario tab and click Run. This will launch the simulations to begin the calculation process which, when running correctly, will begin to look like this:

Design Point 14	Design Point 15	Design Point 16	Design Point 17	Design Point 18	Design Point 19
166325	171325	176325	181325	186325	191325
-3.47094326e-09	-3.65926297e-09	?	?	?	?
Finished	Finished	Calculating...	Not calculated	Not calculated	Not calculated
This computer	This computer	This computer	[auto]	[auto]	[auto]
8	8	8	[use all]	[use all]	[use all]
☐	☐	☐	☐	☐	☐
☐	☐	☐	☐	☐	☐
☑	☑	☑	☑	☑	☑
☑	☑	☑	☑	☑	☑

The speed at which iterations run is dependent on the amount of cores that are being used. My computer from last week was running with only 4, and the process of computing 12 Design Points took roughly 6 hours or more. Today, I ran a new simulation using step sizes of 50 mBar or 5000 Pa for 21 total Design Points, and it only took 2.5 hours running on 8 cores. Either way, I left it alone both times and the process carries out automatically without the need to clone or manually reset the Static Pressure. Once the simulations finish, click the green checkmark to ensure everything is saved under the What if Analysis.

Loading the Results

Once the simulations complete, each result is preserved in a file folder saved to whatever your Solidworks has been told to save things to. So you can left click on the results tab and click “Load from File”

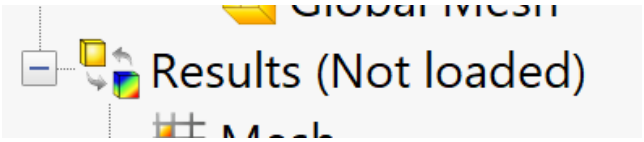

Upon hitting load from file, it should take you directly to the folder containing the information from that particular simulation automatically. If you ran a test run, a .cpt and .fld file will appear below the folders (no idea if there is a reason for these to be here otherwise). In my image below, the first parametric study listed was for the original 12 data points while the recent Parametric Study 2 is today’s 21 data point study.

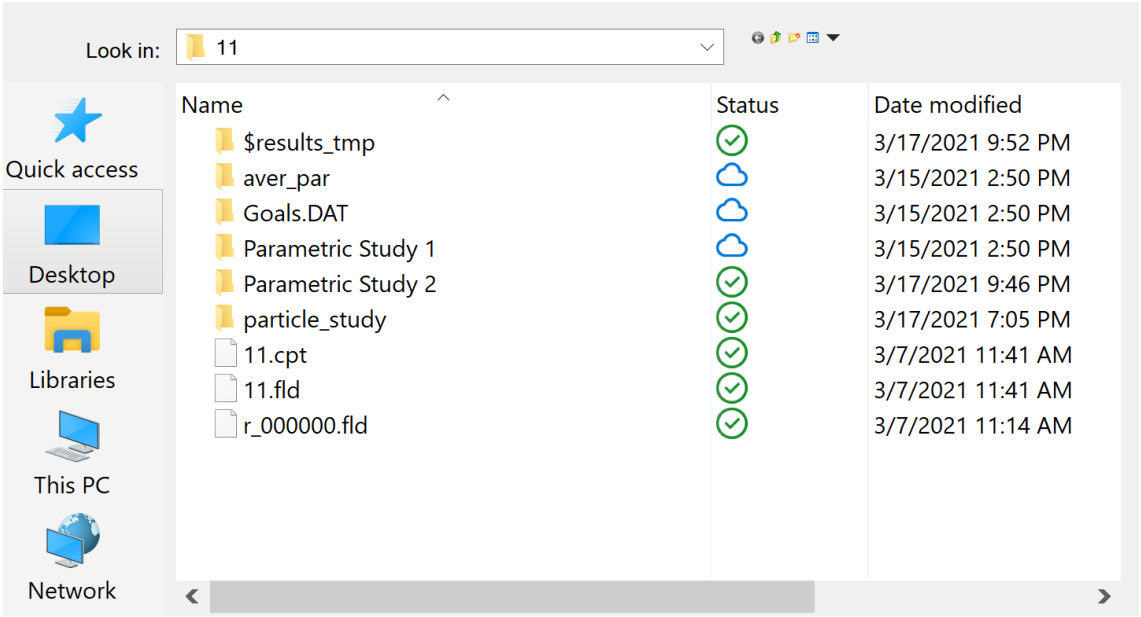

Also of note: the particle study. I usually set this up ahead of time, but it should not matter. In either case, once you set up a study, it will remain the same between file loads. So you should be able to casually switch between files.

Upon clicking the new Parametric Study folder, numbered folders will appear in accordance with the number of data points. If you don't want to rename all of the folders, it is helpful to have the What if Analysis table pulled up at the bottom to remind yourself which pressure is which as you select from a folder.

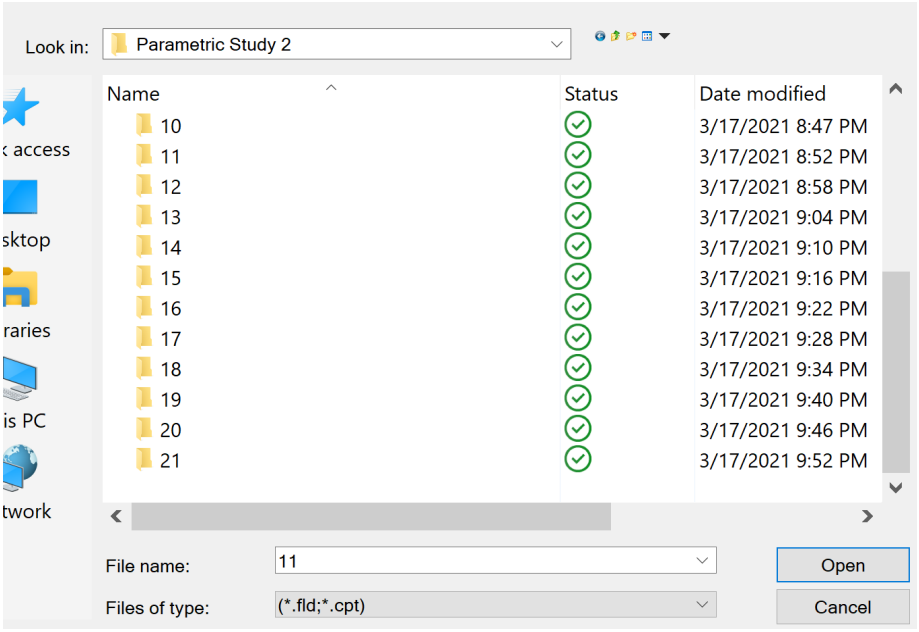

Opening any one of these folders will allow you to access another familiar looking folder setup (this whole thing is very Russian Nesting Doll, feels so unnecessary but what can you do). The important file that Solidworks cares about is the .fld file. So you can open that and all of the data will load from the respective simulation with that particular pressure, easy peasy. Any alterations can easily be observed if you look at surface speeds or just load in the particle simulation and load between the various folders real quick.

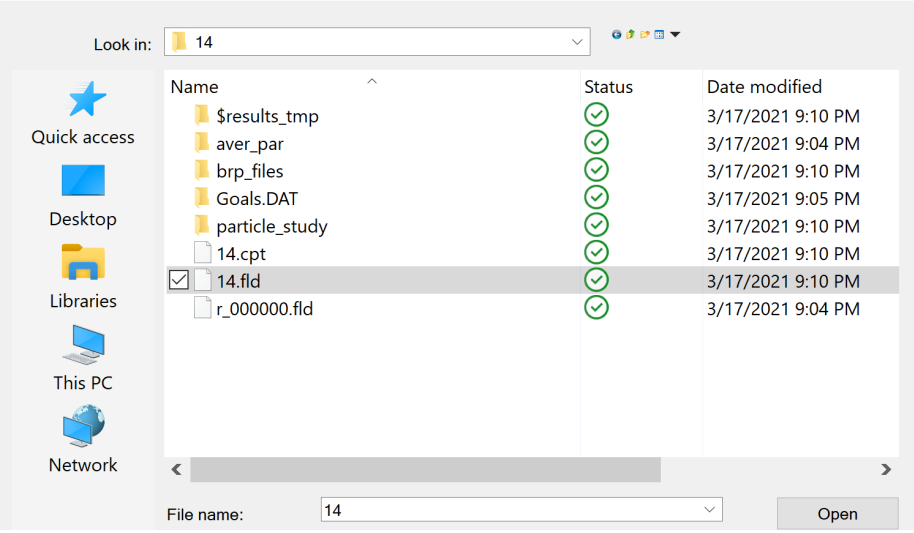

You should be able to switch between files even when the particle simulation is loaded in. That way the framing can stay consistent between shots when the particle simulation is paused. Additionally, (at least, with the 100um) adding a surface parameter analysis can help to better approximate the speed of the particle by comparing the color and the average/max/min velocities to see what physically makes sense. In this case, the pressure far exceeds the cutoff for single file focusing, so two streams appear and match closely with the average velocity (when focusing is proper, the maximum velocity seems a better approximation, but, since these particles are very green, it's probably about 0.351m/s which is probably more accurate than just going with 0.307 from the legend).

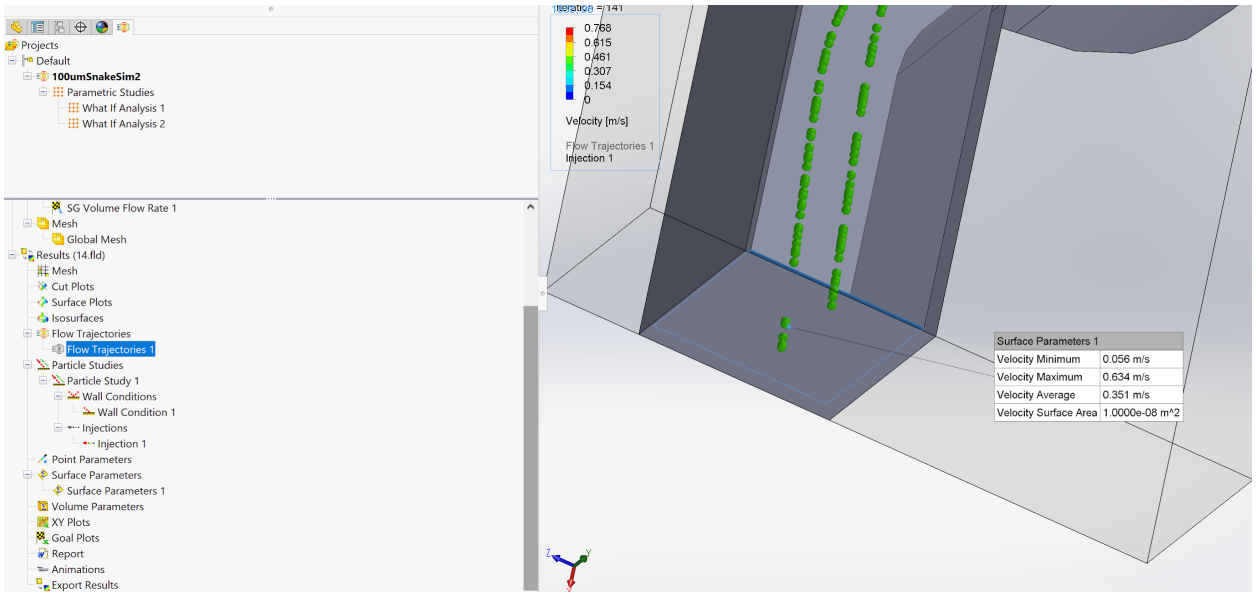

Appendix VI: Data Parsing MatLab Code

```
%%
clear all
% ask = uigetfile('*','Select the file to open');
% data = importdata(ask,'\t',1);
%%
ask = uigetfile('*','Select the file to open');
```

```
data1 = readmatrix(ask);
mBar = rmmissing(data1,1);

%%
%points = (1:20);
[A,B] = size(mBar);

%%

P = 1;
for k = 1:A-1; %A
   if mBar(k,1) > mBar(k+1,1)
      endpoints(P) = k;
      P=P+1;
   end
end
endpoints(P) = A;
%%

[C,D] = size(endpoints);

for i = 1:D;
   j = endpoints(i);
   while mBar(j,1) >= 0.024484
      j=j-1;
   end
   points(i) = j;
end

for r = 1:D;

   Y(r) = mBar(points(r),2);
   Z(r) = mBar(points(r),3);
end


cords = [Y',Z'];
```

Appendix VII: First 100um Parametric Study - Velocity examinations

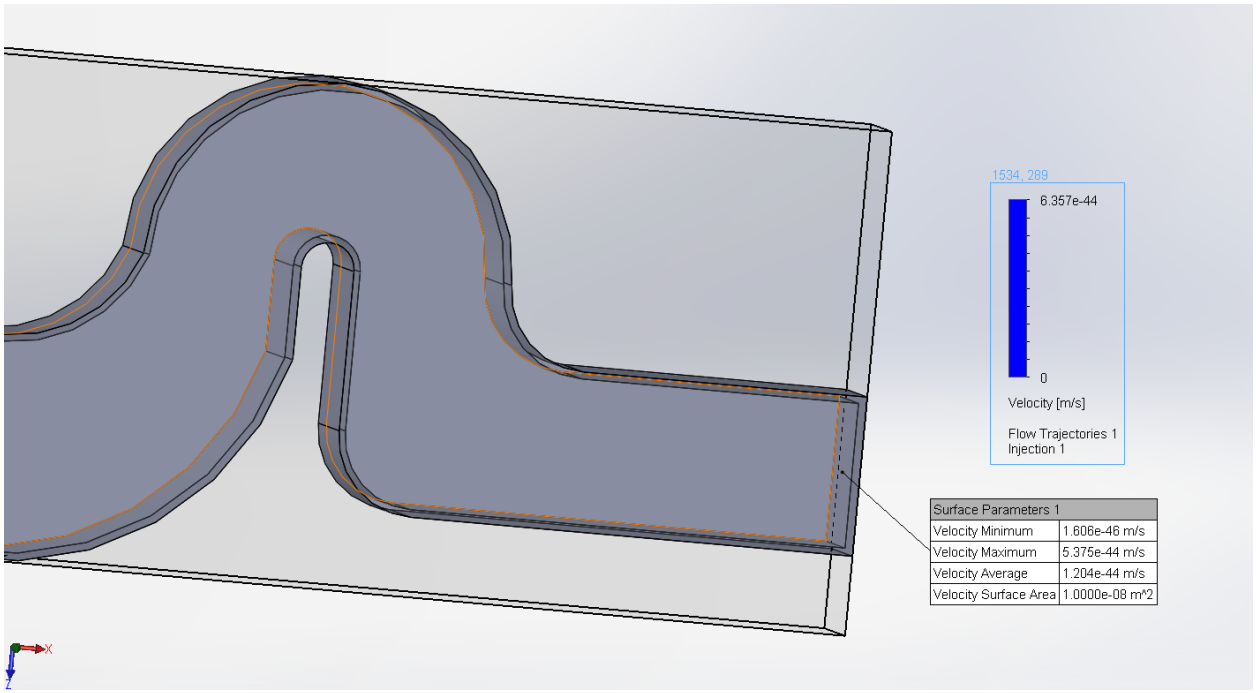

Figure 1. The model at 0 mBar, demonstrating a very low velocity. Particle simulation is on, yet none reach the end.

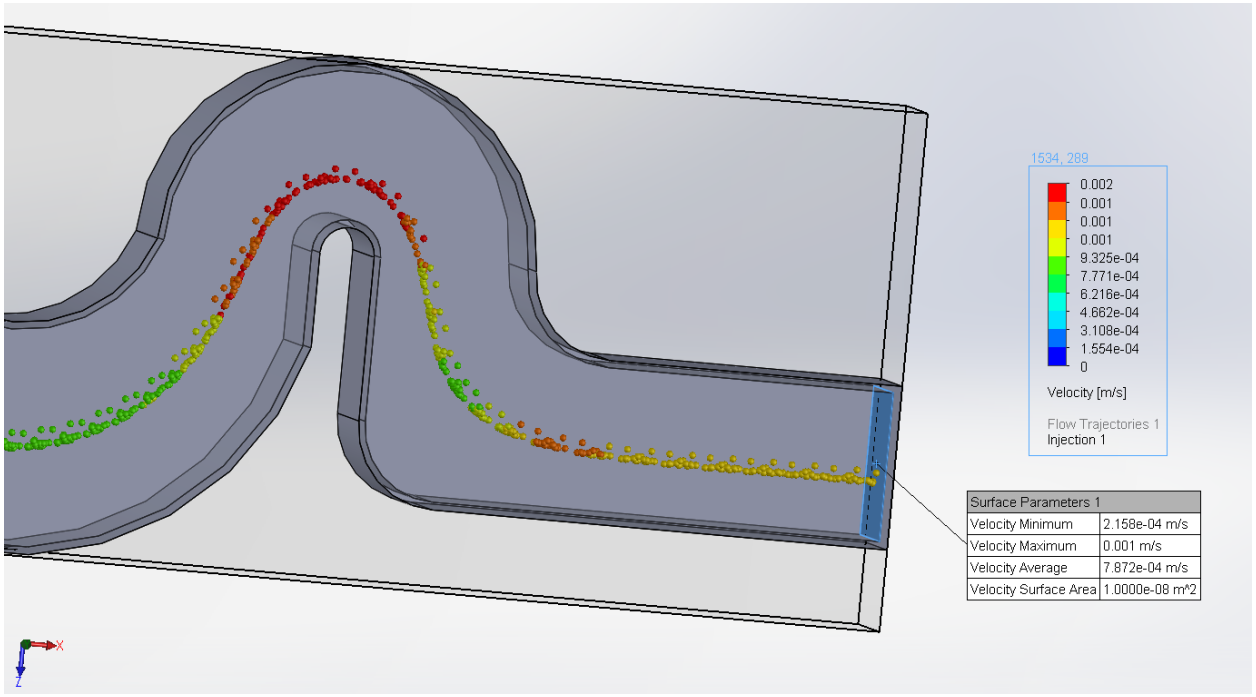

Figure 2. The model at 1 mBar. Has a maximum velocity of 0.001 m/s or 1 mm/s. This appears to approximate the velocity/color of the particle stream and will be used to describe it from here on.

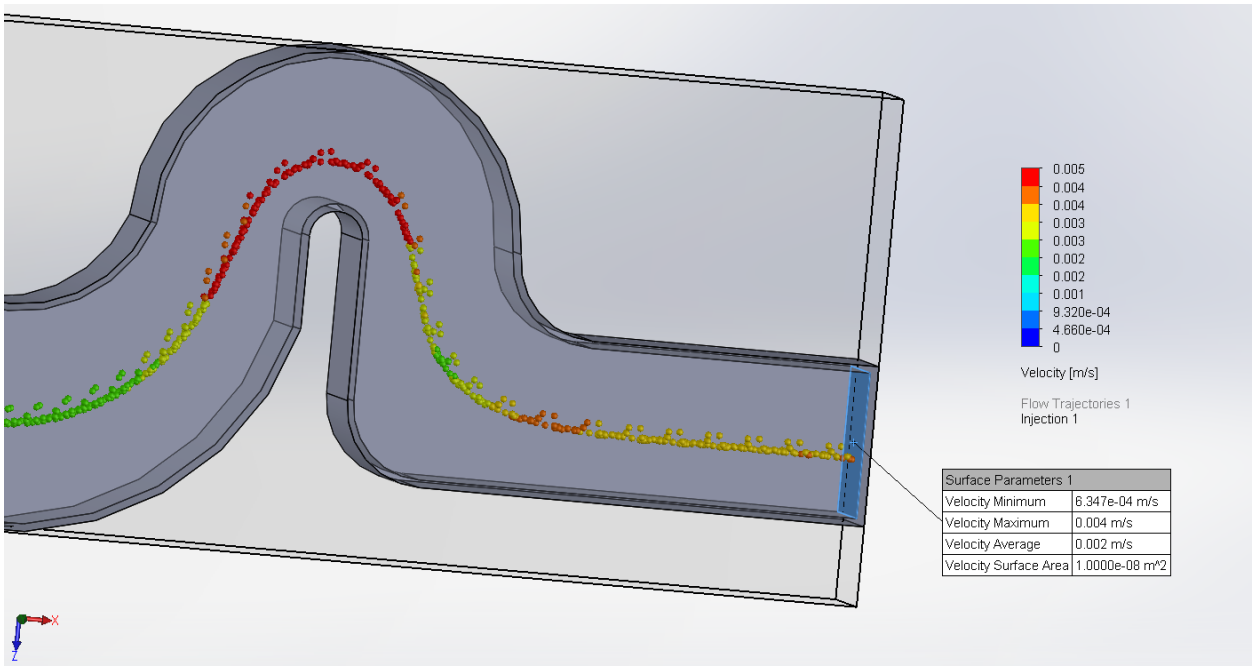

Figure 3. The model at 3 mBar. Has a maximum velocity of 0.004 m/s or 4 mm/s.

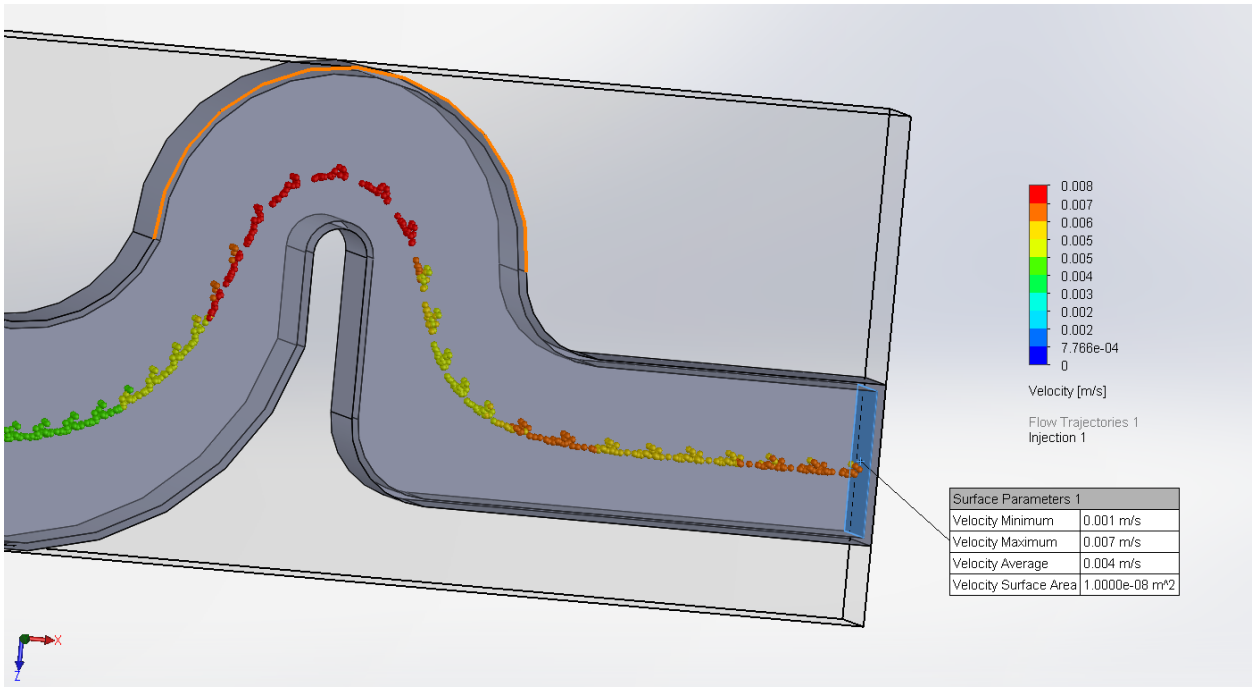

Figure 4. The model at 5 mBar. Has a maximum velocity of 0.007 m/s or 7 mm/s.

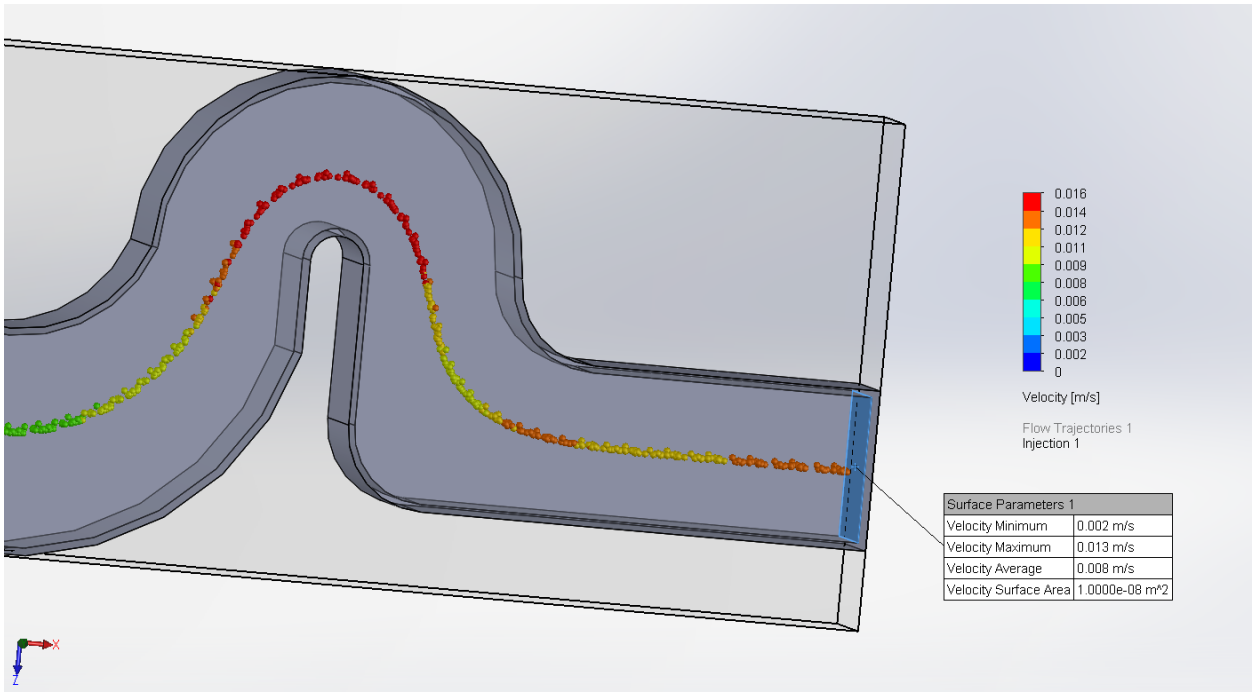

Figure 5. The model at 10 mBar. Has a maximum velocity of 0.013 m/s or 13 mm/s.

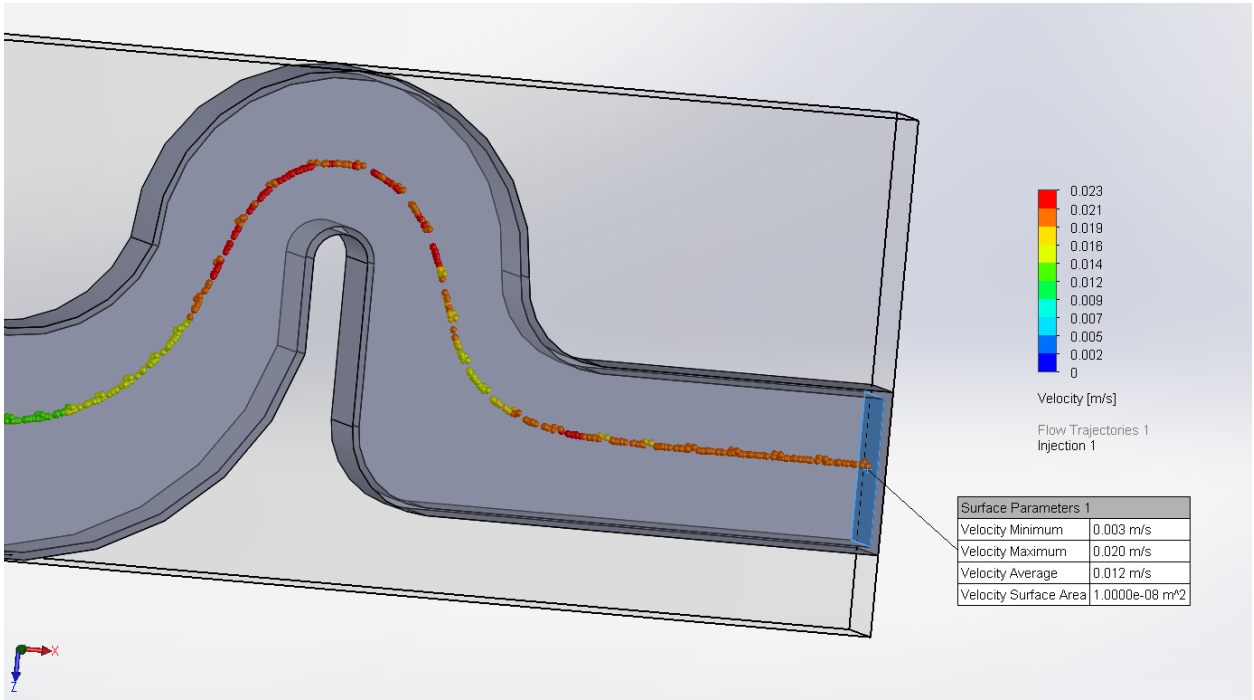

Figure 6. The model at 15 mBar. Has a maximum velocity of 0.02 m/s or 20 mm/s.

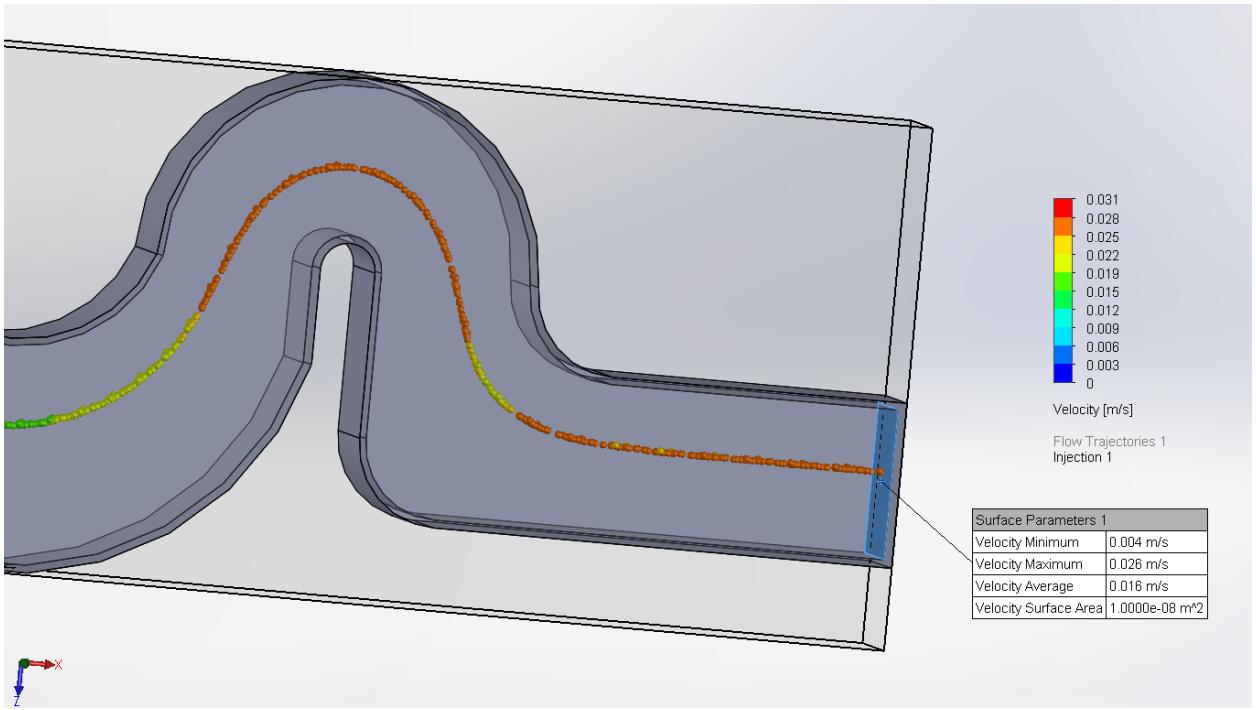

Figure 7. The model at 20 mBar. Has a maximum velocity of 0.026 m/s or 26 mm/s.

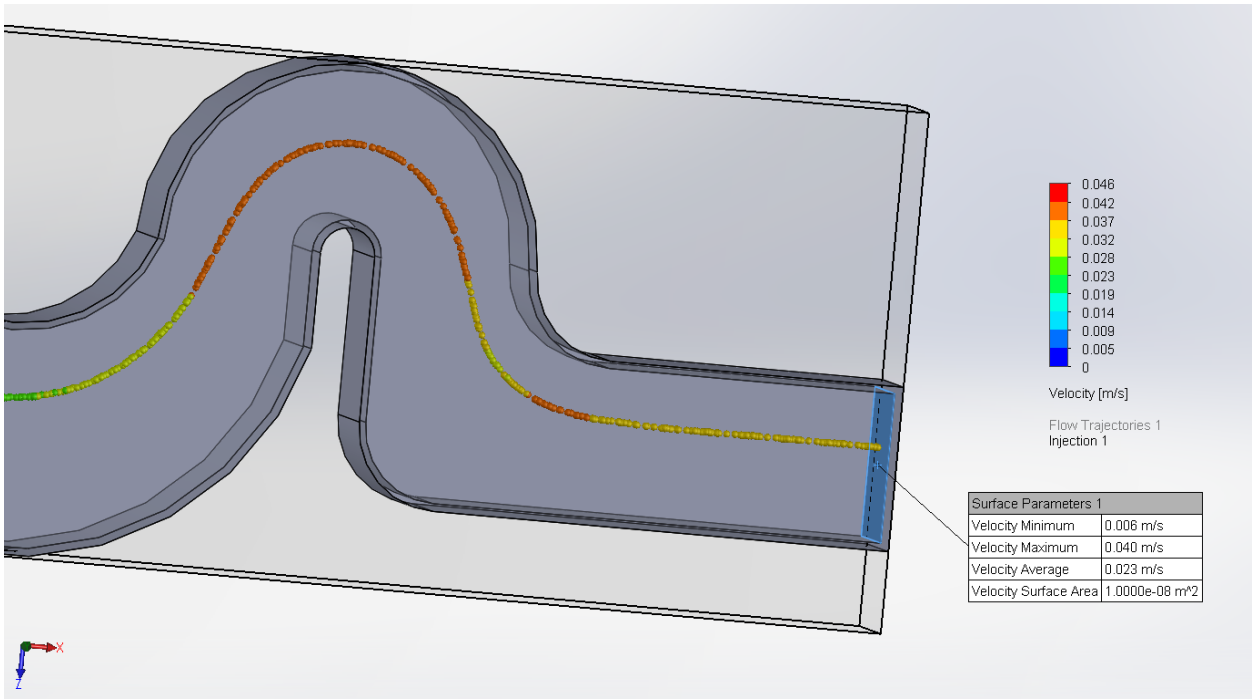

Figure 8. The model at 30 mBar. Has a maximum velocity of 0.04 m/s or 40 mm/s. Running a flow trajectory simulation seems to indicate that maximum velocity points nearly surround the particle's contact point on the indicated surface.

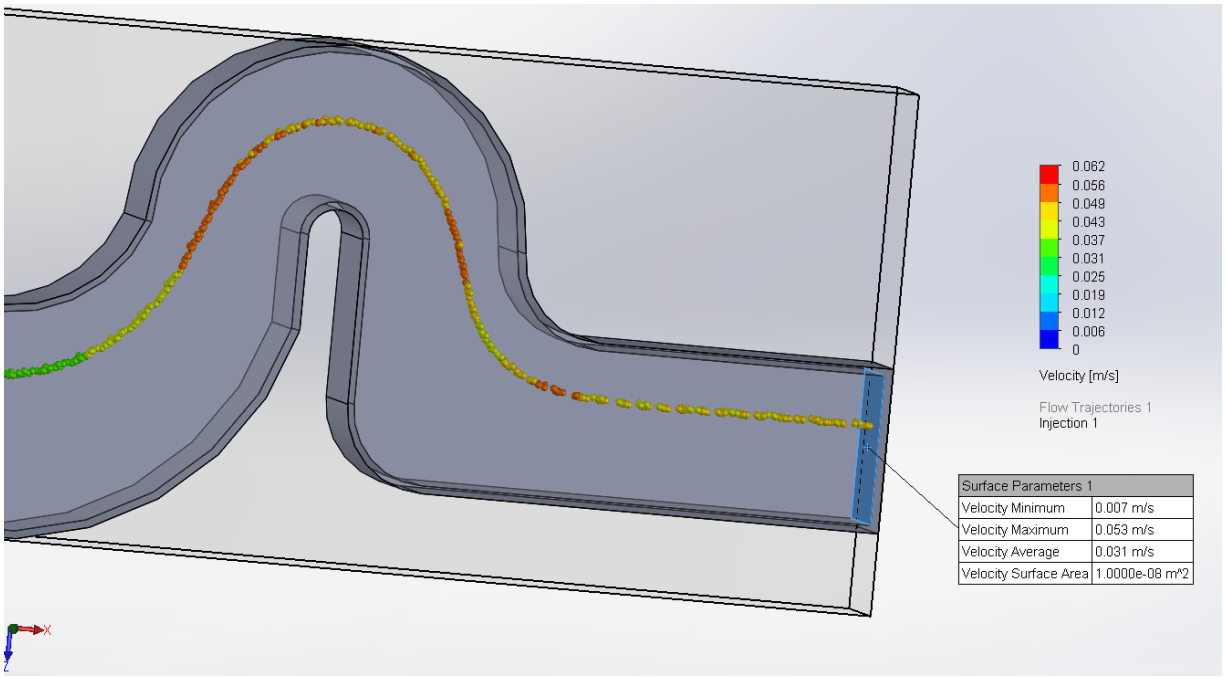

Figure 9. The model at 40 mBar. After this point, focusing becomes less optimized. The maximum velocity also appears to no longer mirror the particle velocity which seems to be closer to 0.043 m/s or 43 mm/s.

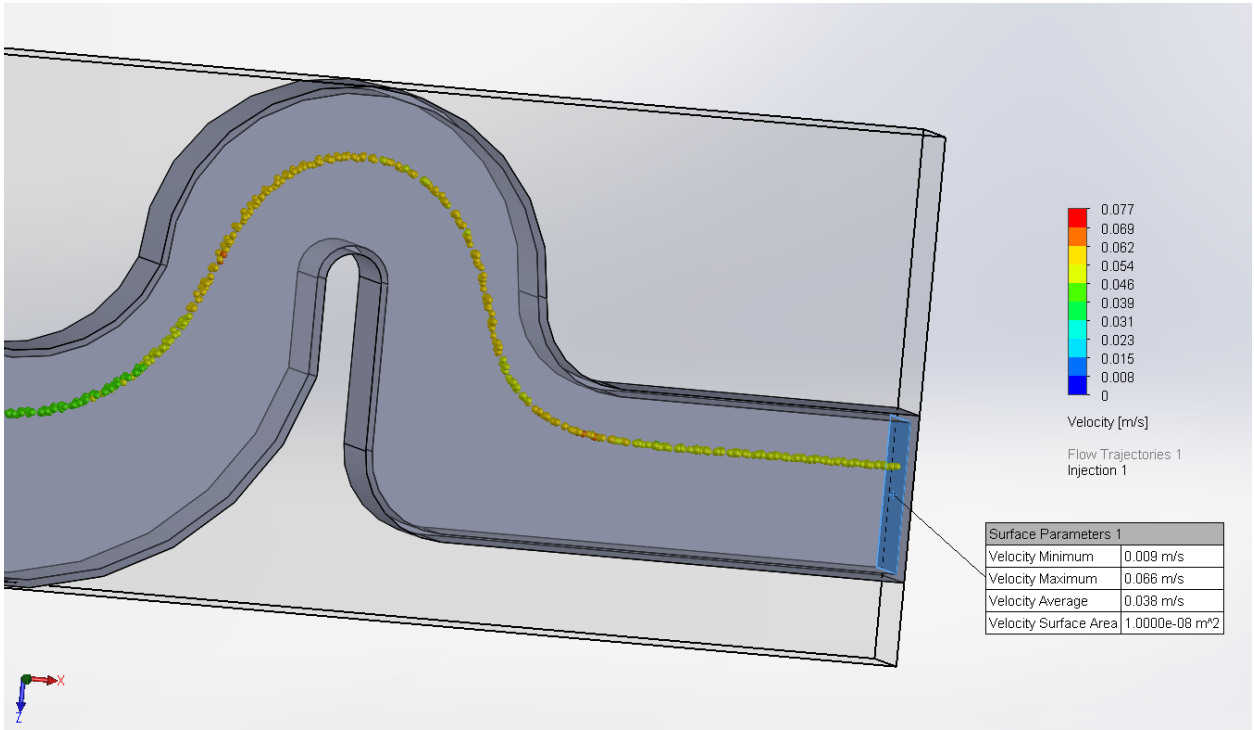

Figure 10. The model at 50 mBar. The particle stream is no longer focused and is more spread out. Particle velocity is certainly not 0.066 and appears to start approaching the average velocity instead. It is now about 0.047 m/s or 47 mm/s.

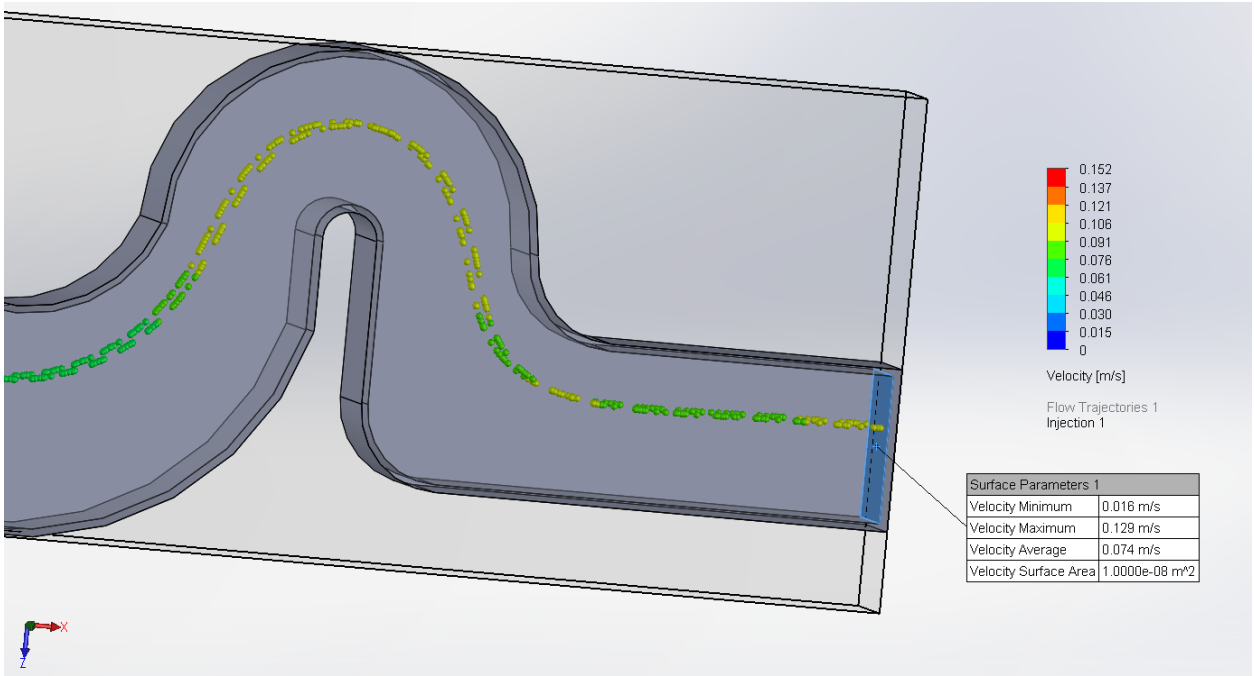

Figure 11. The model at 100 mBar. There are now two distinct streams of particles which are moving at the same velocity. Both are much slower than the maximum velocity as well and seem to fall at about 0.092 m/s or 92 mm/s.

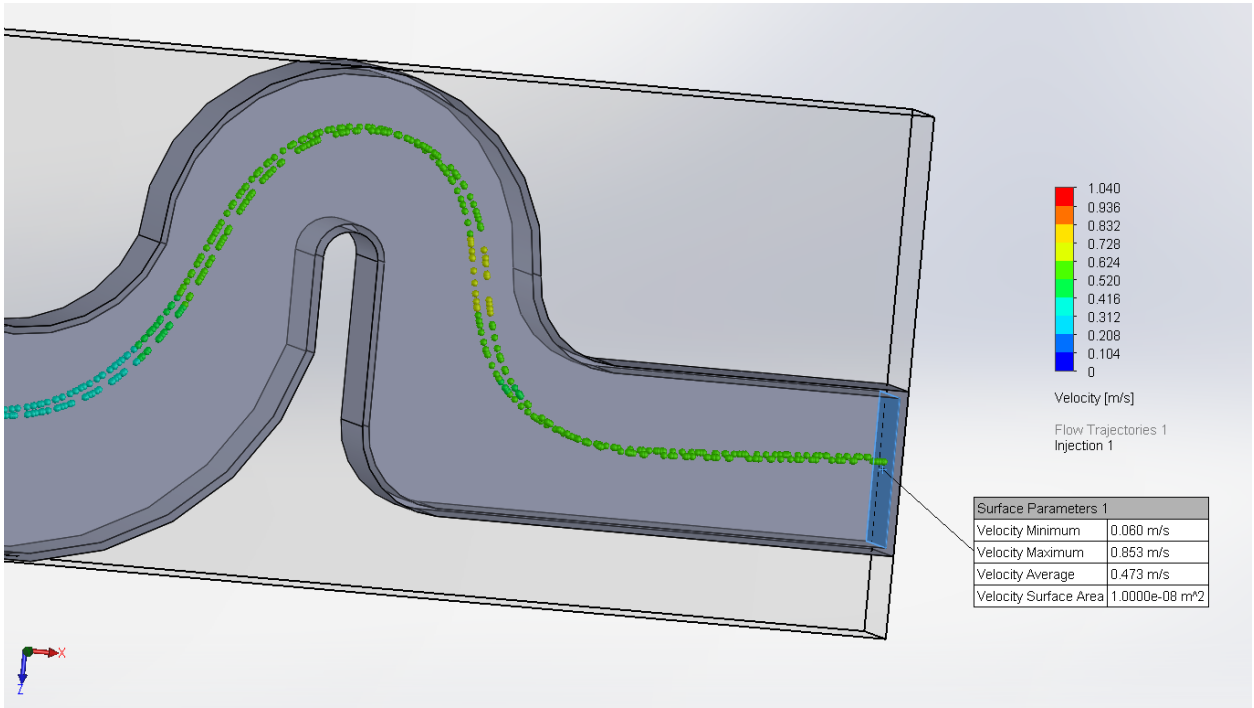

Figure 12. The model at 1000 mBar or 1 Bar. The two streams are now almost uniformly distinct and completely focused. They are contacting the barrier at the same Z locations, but are no longer focused in the Y direction. Speed also seems to be completely matched to the average velocity of 0.473 m/s or 473 mm/s. When running a flow trajectory simulation, the maximum velocity is observed to be below the particle flow, hitting at a lower point on the Z axis.

Appendix VIII: 100um Expanded Parametric Study

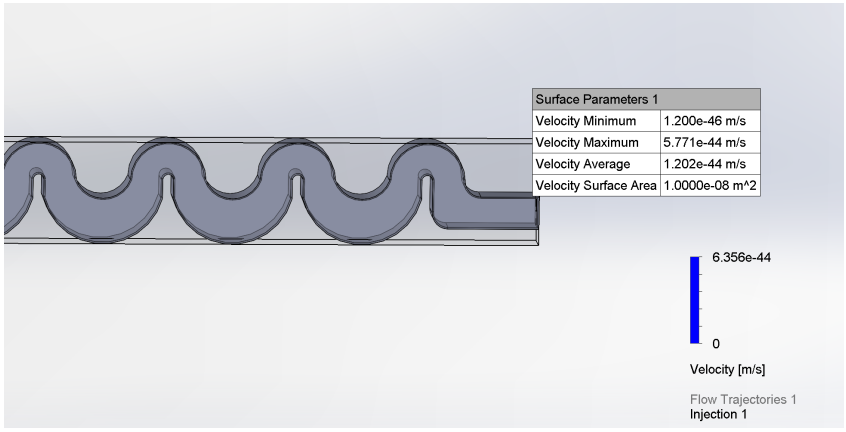

0 mBar - ~0 m/s

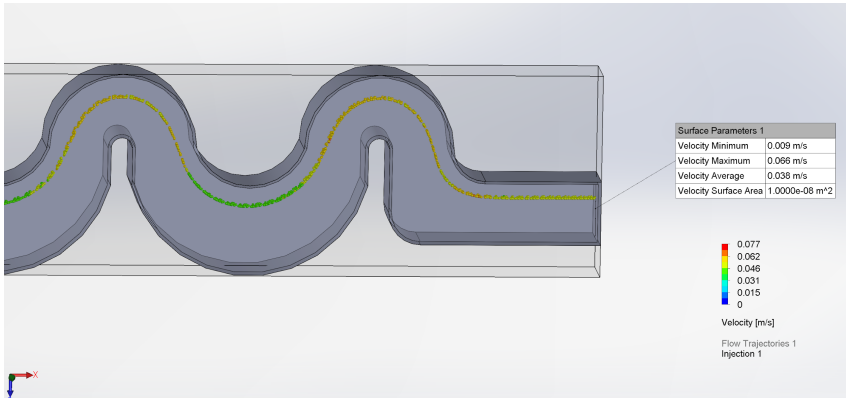

50 mBar - ~0.048 m/s

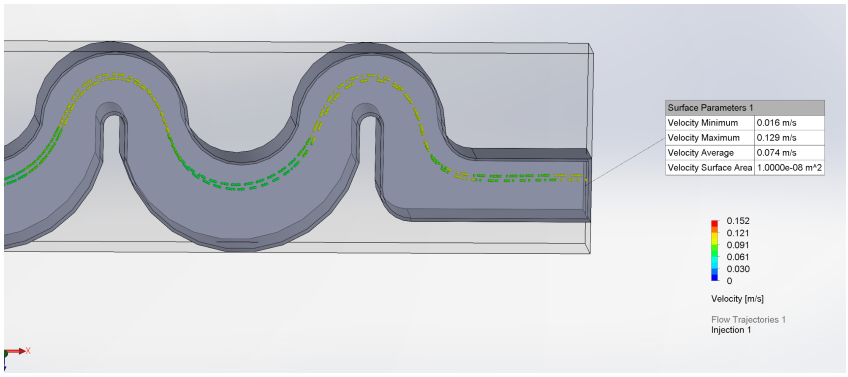

100 mBar - ~0.095 m/s

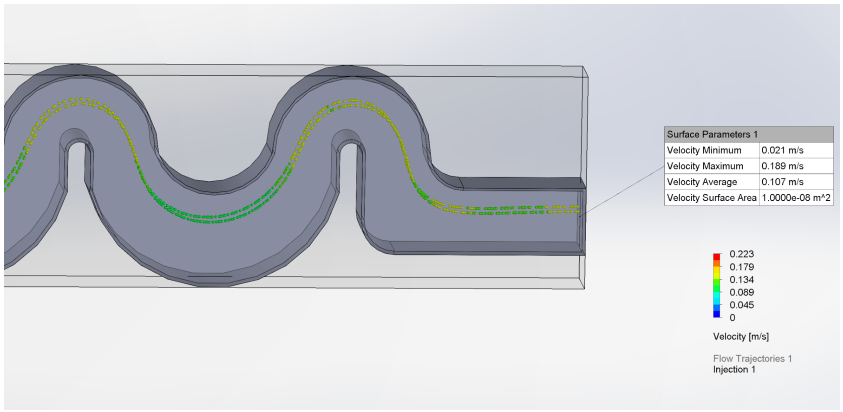

150 mBar - ~0.140 m/s

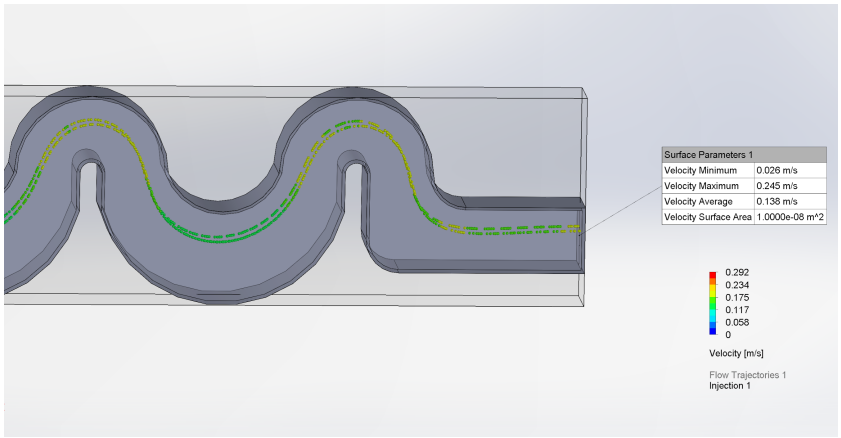

200 mBar - ~0.175 m/s

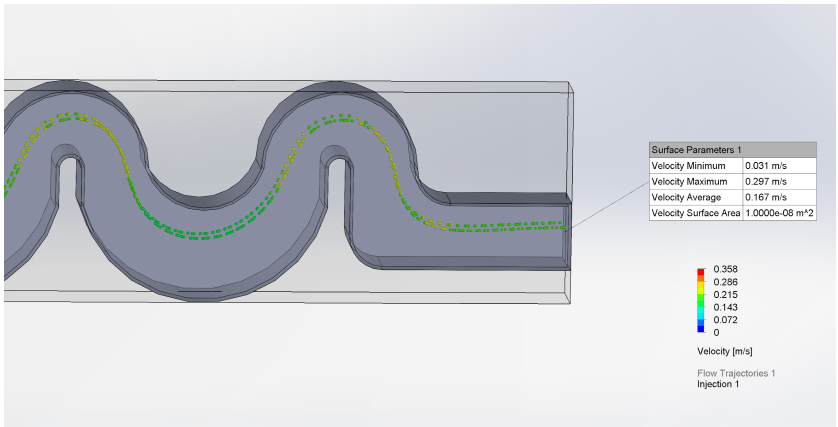

250 mBar - ~0.200 m/s

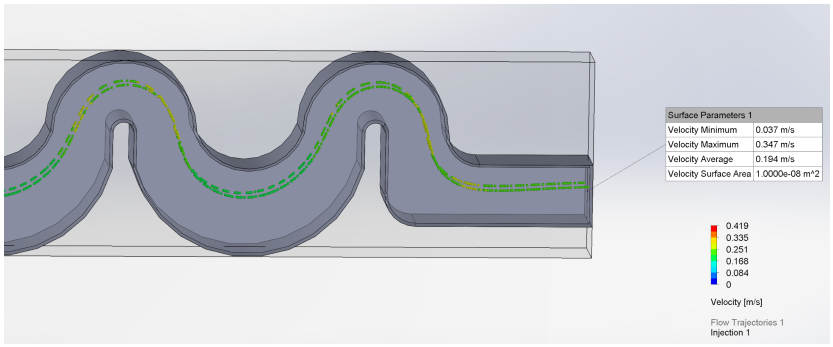

300 mBar - ~0.22 m/s

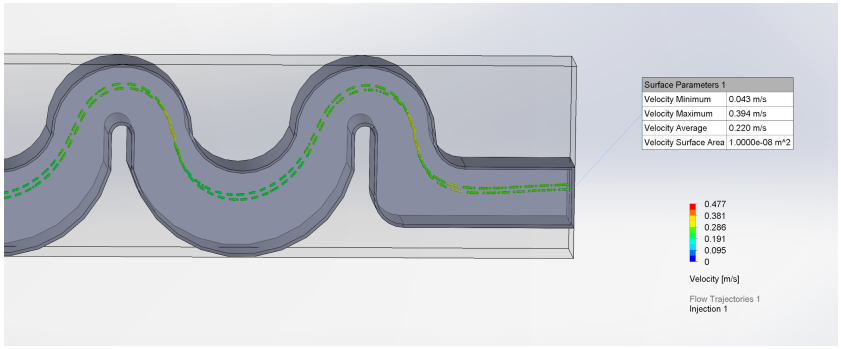

350 mBar - ~0.233 m/s

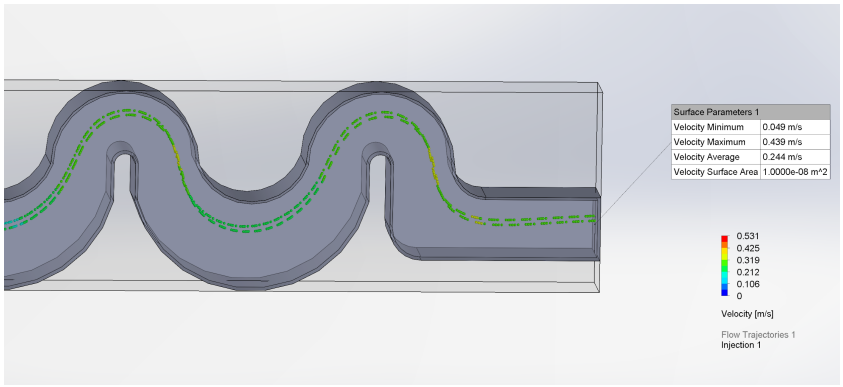

400 mBar - 0.244 m/s

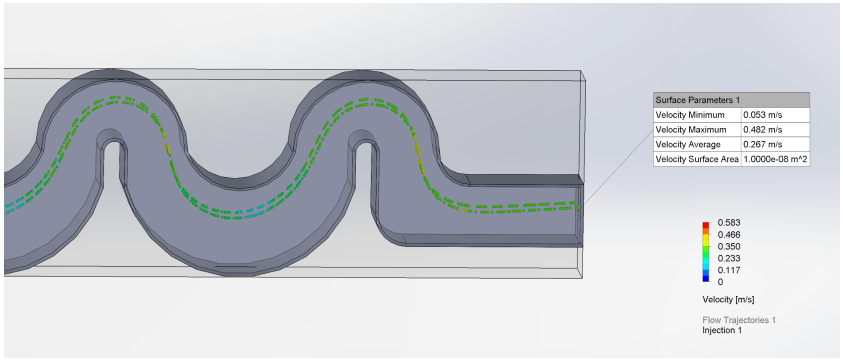

450 mBar - 0.267 m/s

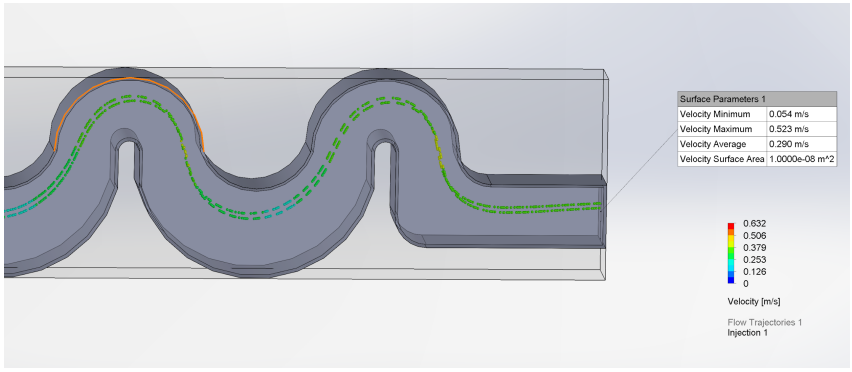

500 mBar - 0.29 m/s

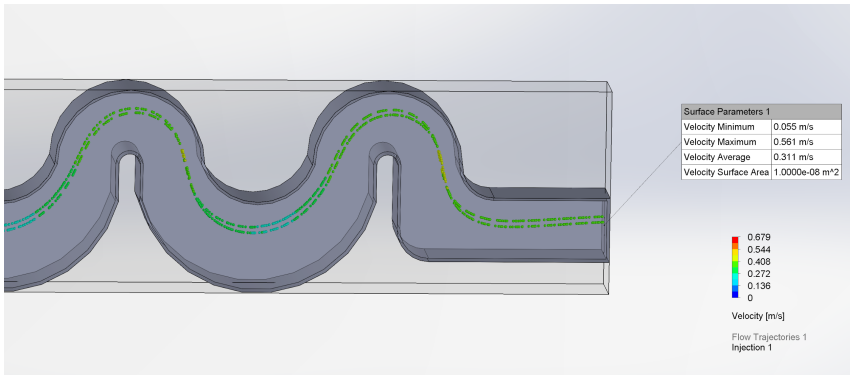

550 mBar - 0.311 m/s

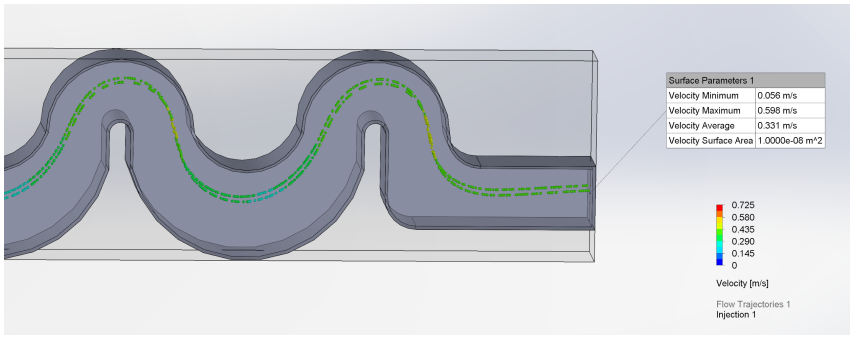

600 mBar 0.331 m/s

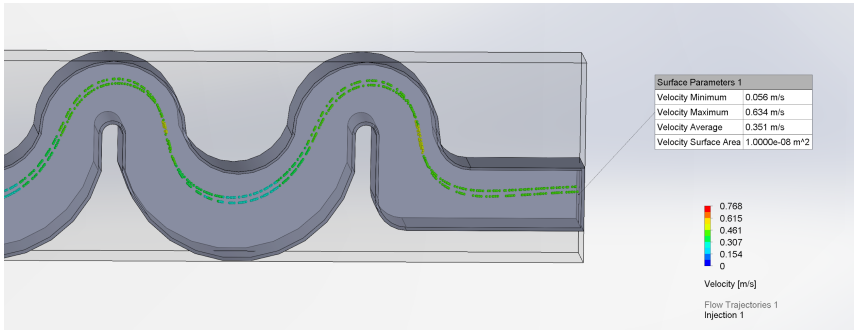

650 mBar - 0.351 m/s

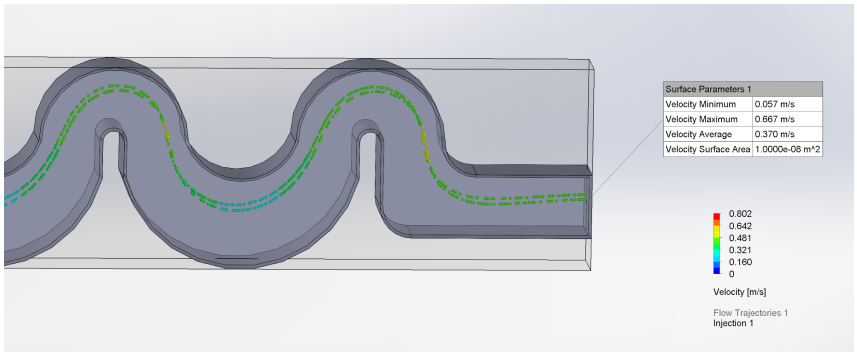

700 mBar - 0.370 m/s

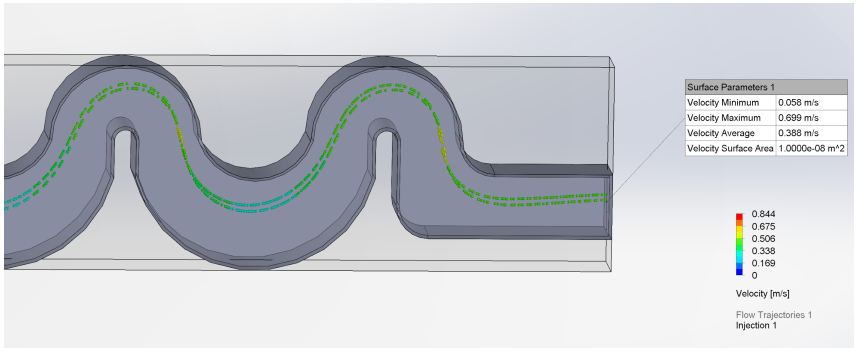

750 mBar - 0.388 m/s

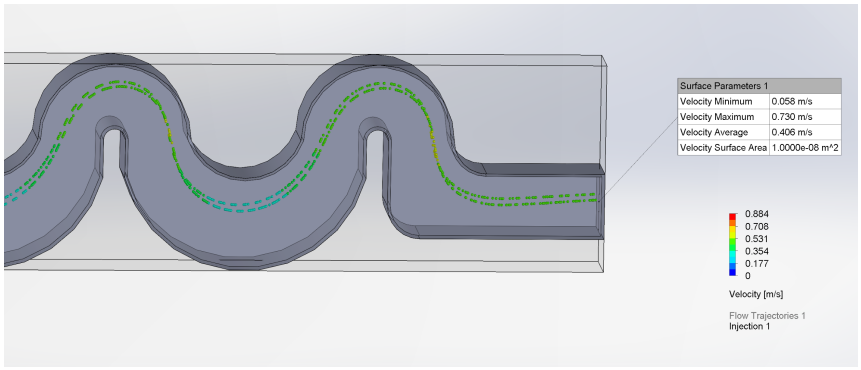

800 mBar - 0.406 m/s

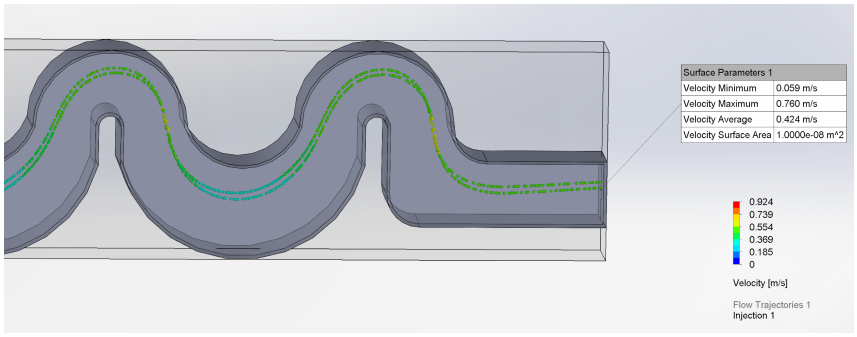

850 mBar - 0.424 m/s

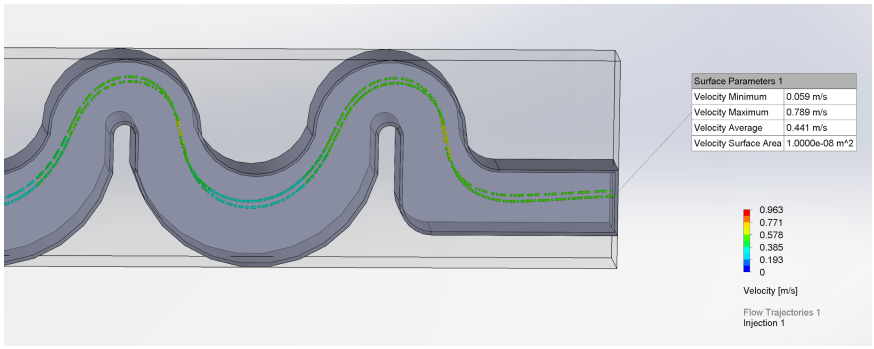

900 mBar - 0.441 m/s

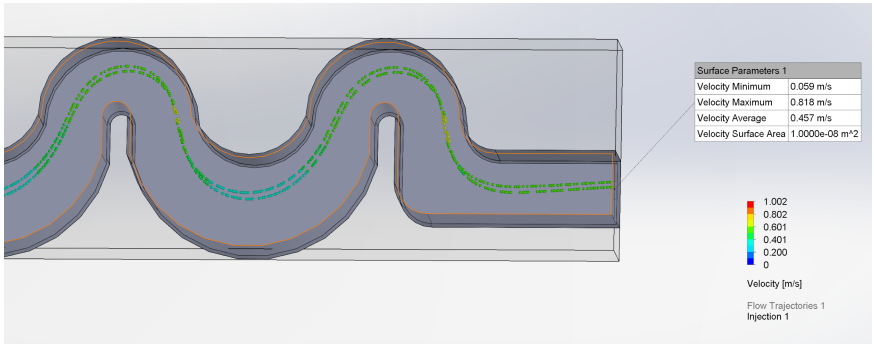

950 mBar - 0.457 m/s

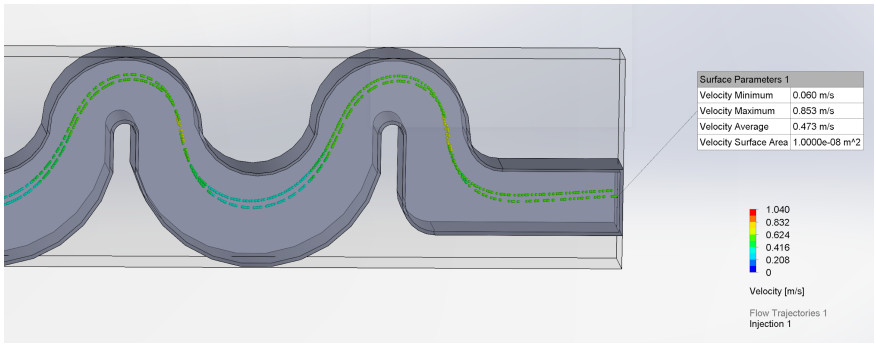

1000 mBar - 0.473 m/s

Appendix IX: 100um ImageJ Cross-sections

Pressure, Speed of Particle, Particle Distance from Center, Area of Particle Sim, Farthest Particle from Center Particle (i.e radius of error)

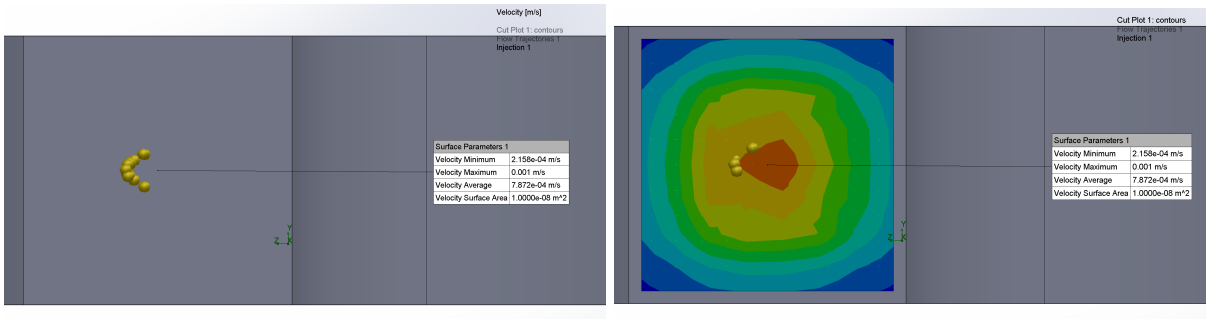

1 mBar, 1 mm/s, 12.75 um, 145 um^2, 11.5 um

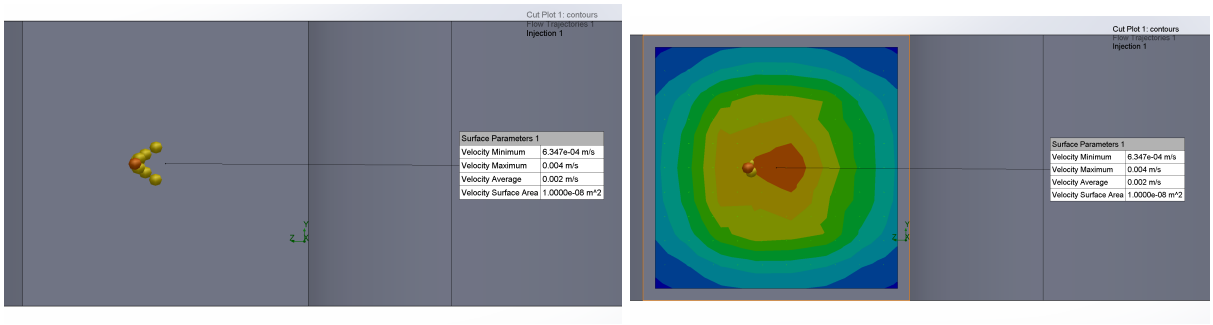

3 mBar, 4 mm/s, 11.1 um, 100 um^2, 11.5 um

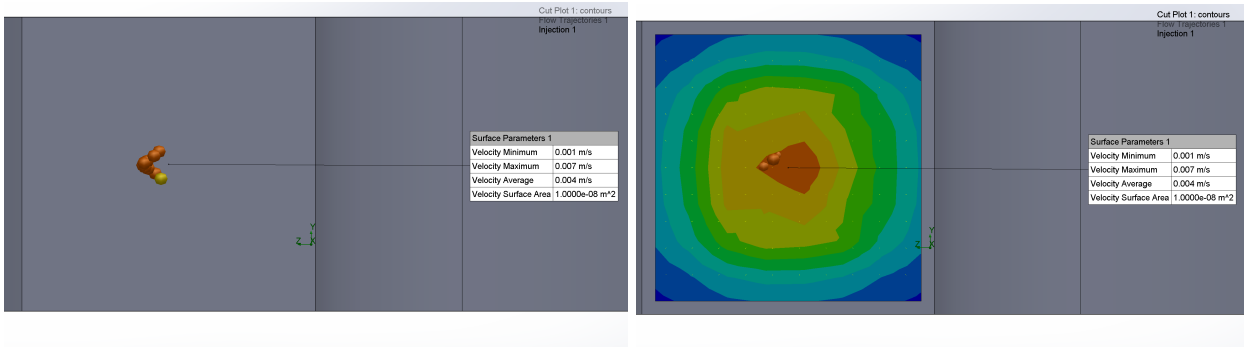

5 mBar, 7 mm/s, 9 um, 98.6 um^2, 10.25 um

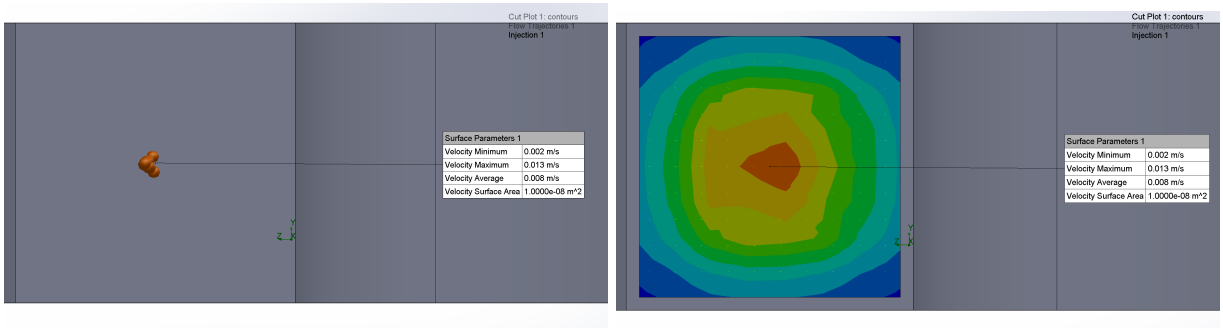

10 mBar, 13 mm/s, 5 um, 67 um^2, 6 um

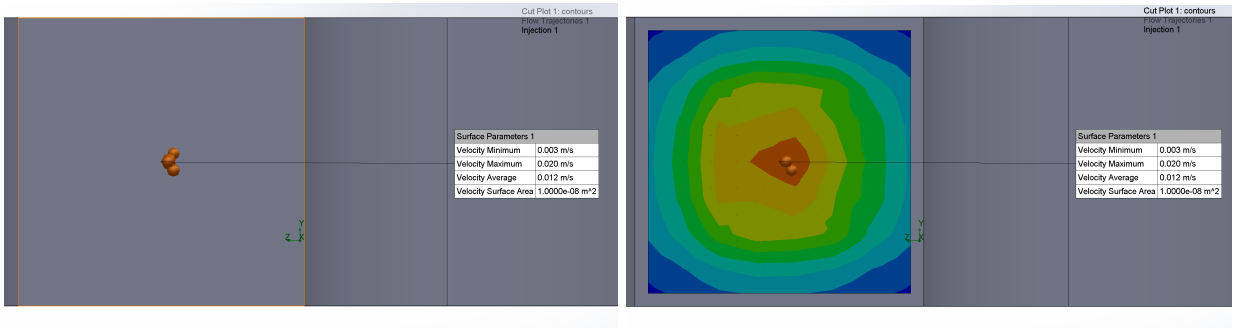

15 mBar, 20 mm/s, 2.5 um, 53.5 um^2, 5.5 um

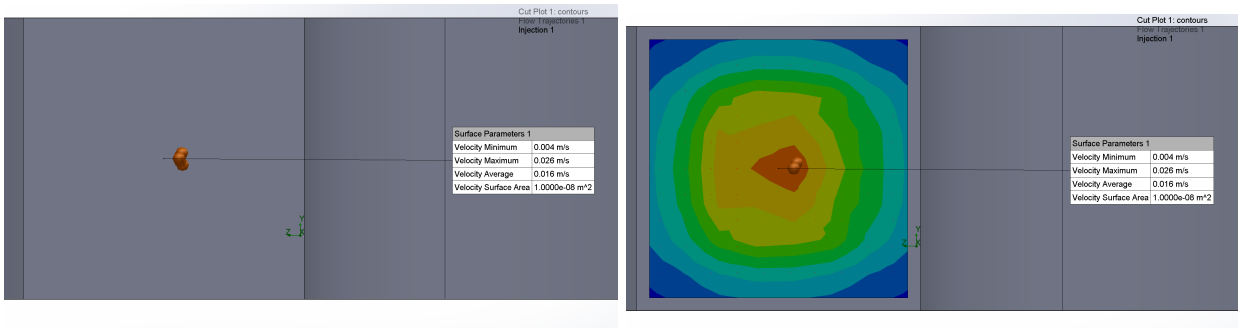

20 mBar, 26 mm/s, 6 um, 42.1 um^2, 5 um

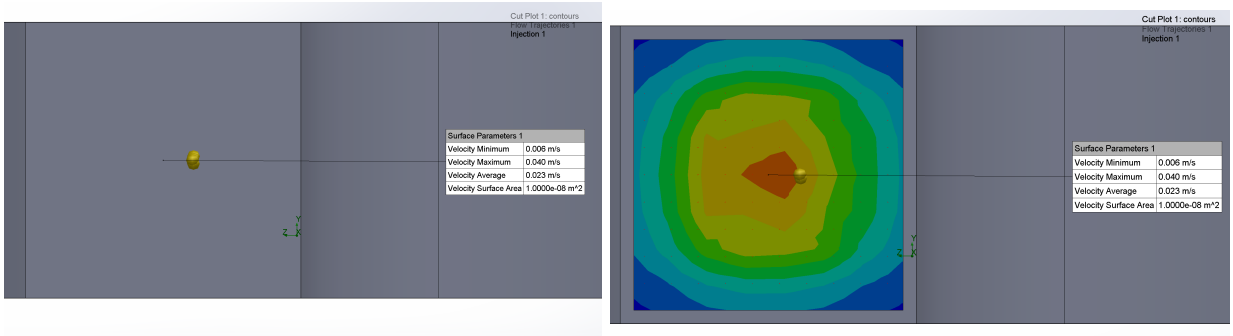

30 mBar, 40 mm/s, 11.3 um, 35.3 um^2, 3.5 um

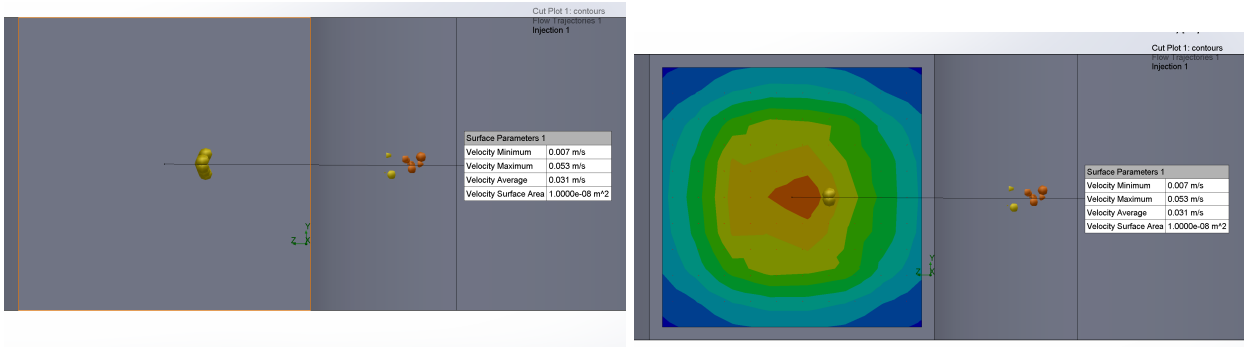

40 mBar, 43 mm/s, 13.4 um, 50.7 um^2, 6.7 um

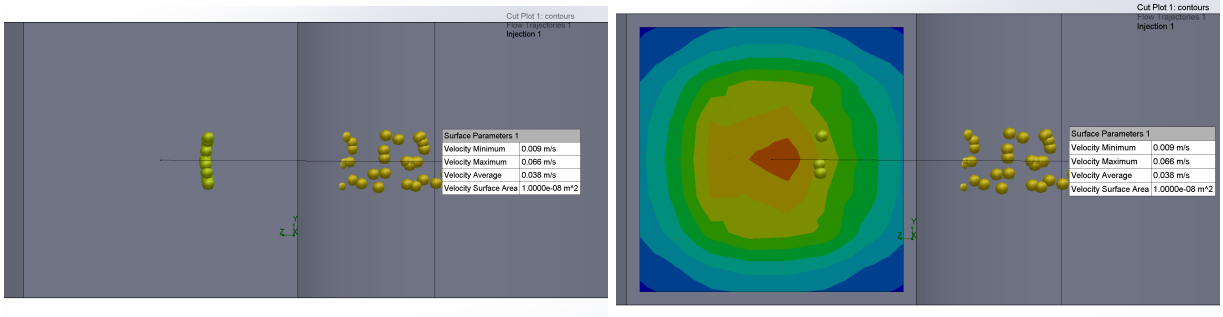

50 mBar, 48 mm/s, 18 um, 103 um^2, 11 um

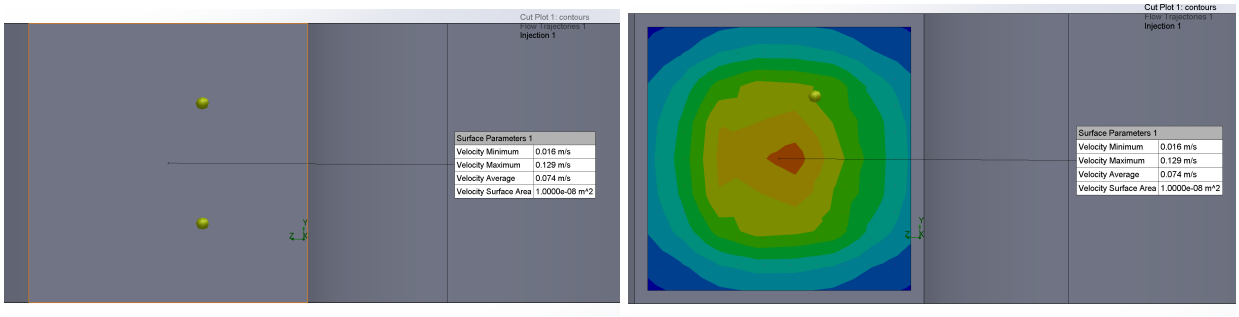

100 mBar, 95 mm/s

Particles no longer in line; Distance from Center: 27 um, Distance from Each Other: 47 um

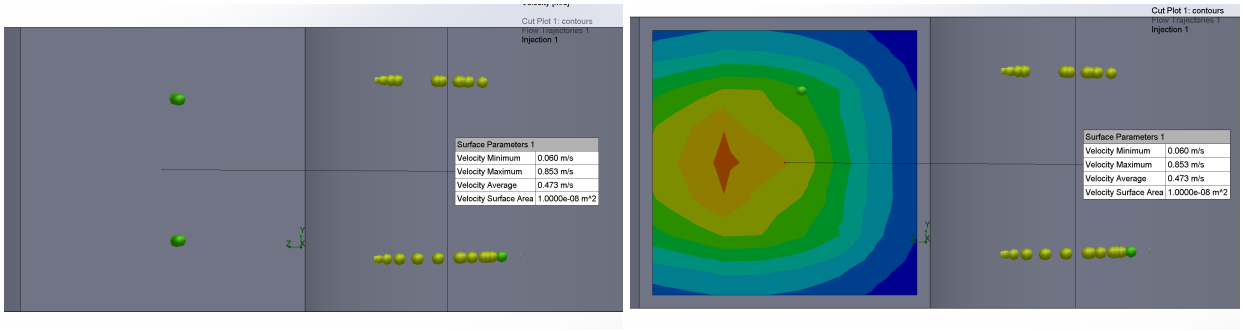

1000 mBar, 473 mm/s

Particles no longer in line; Distance from Center: 28 um, Distance from Each Other: 55 um

Appendix X: Y and Z trajectories for 100um

Z Trajectory Y Trajectory

1 mBar

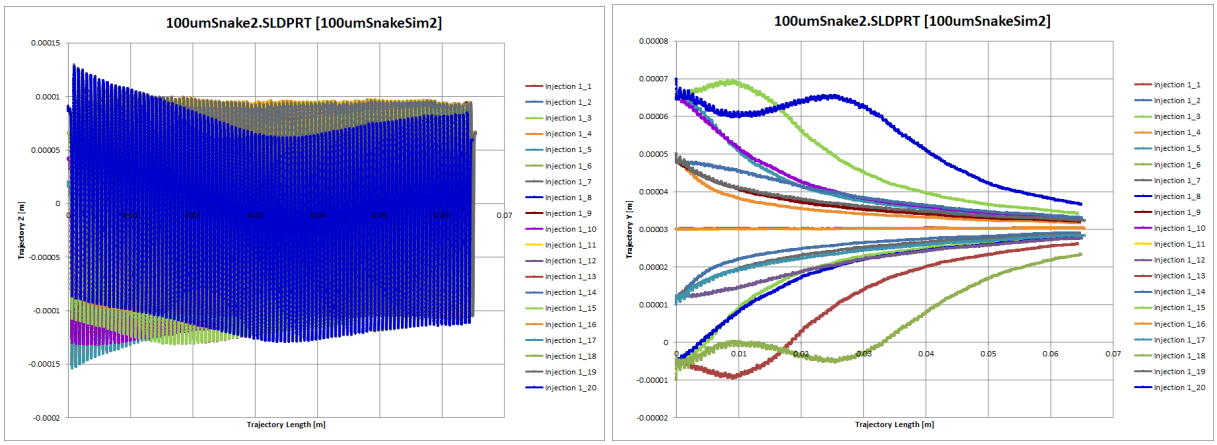

3 mBar

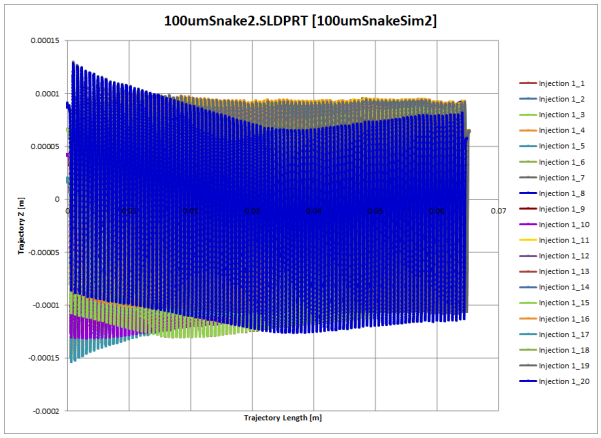

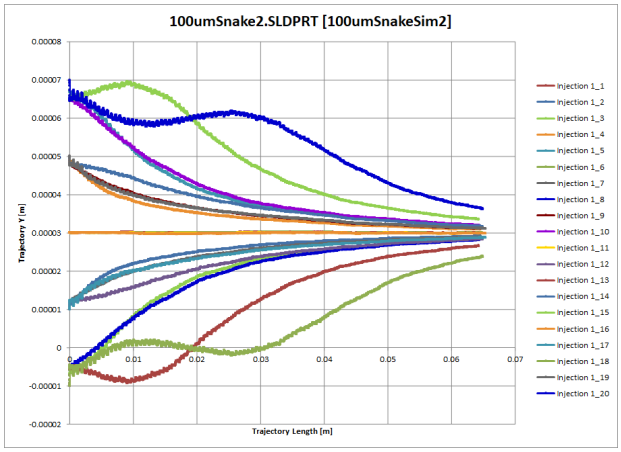

5 mBar

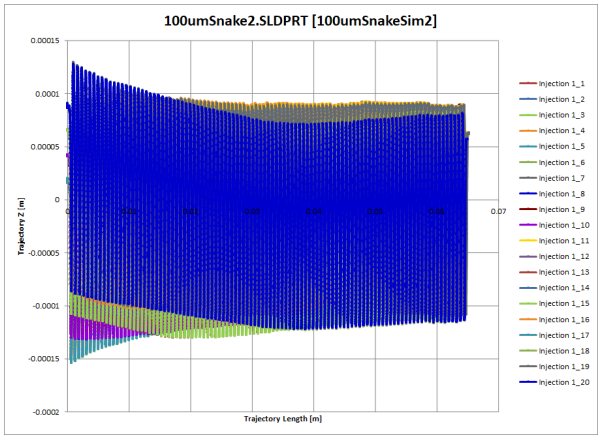

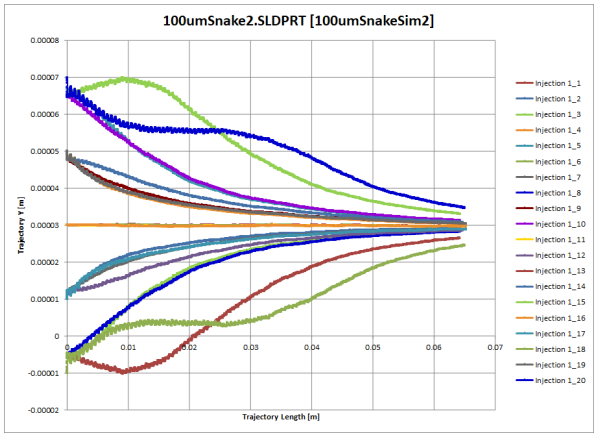

10 mBar

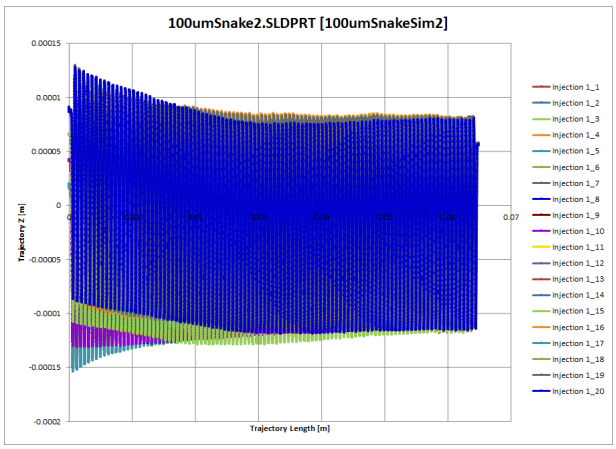

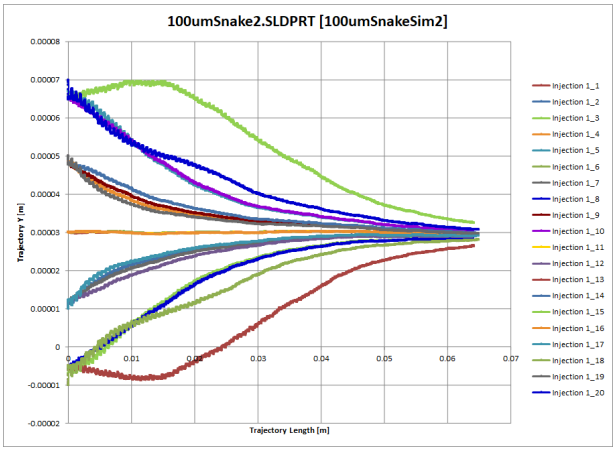

15 mBar

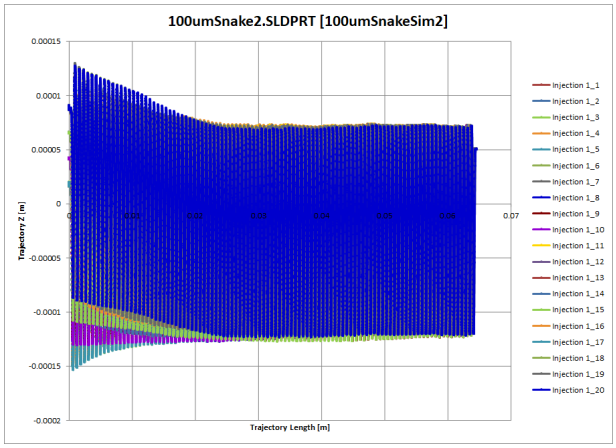

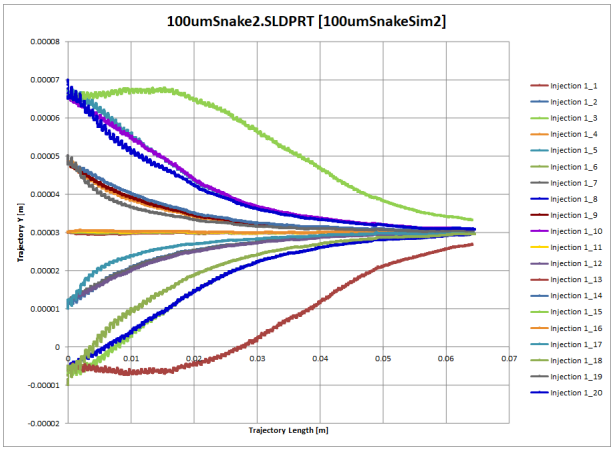

20 mBar

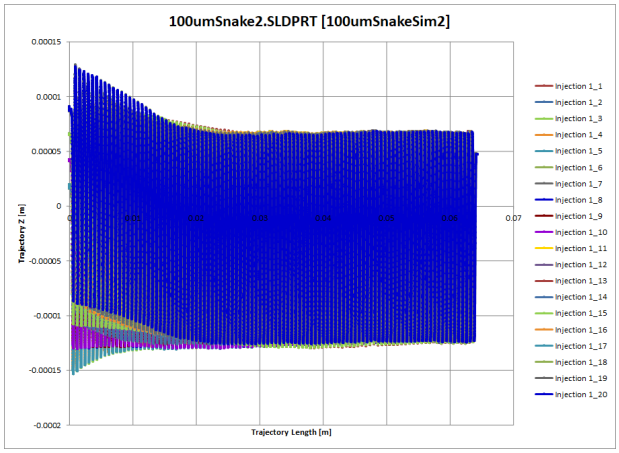

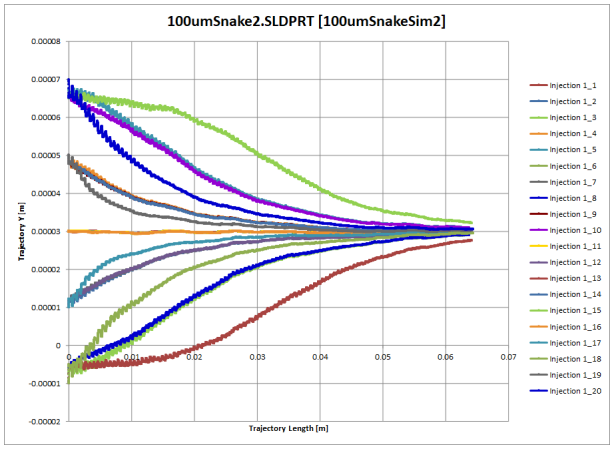

30 mBar

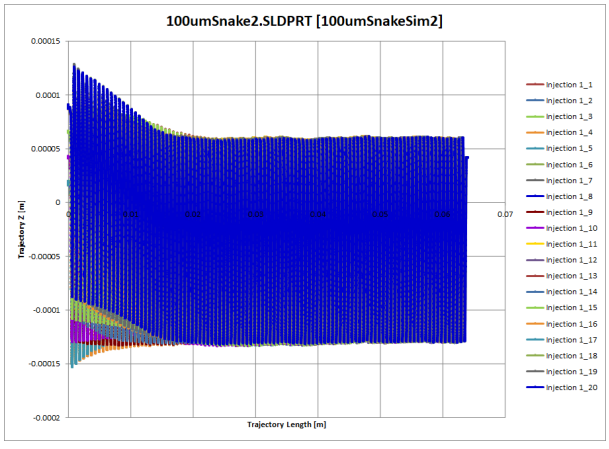

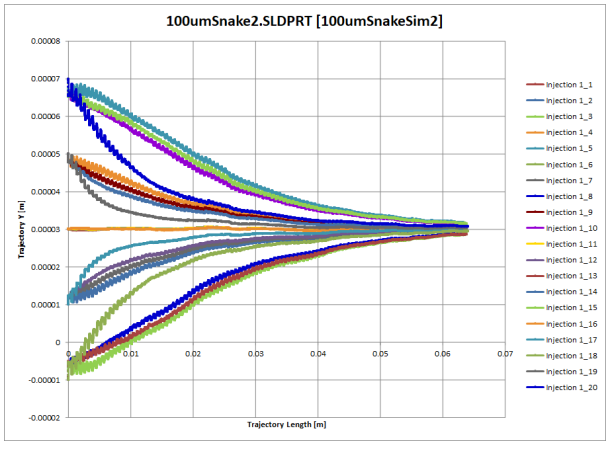

40 mBar

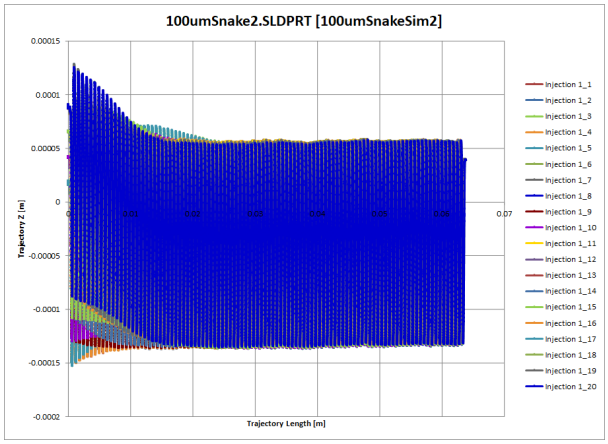

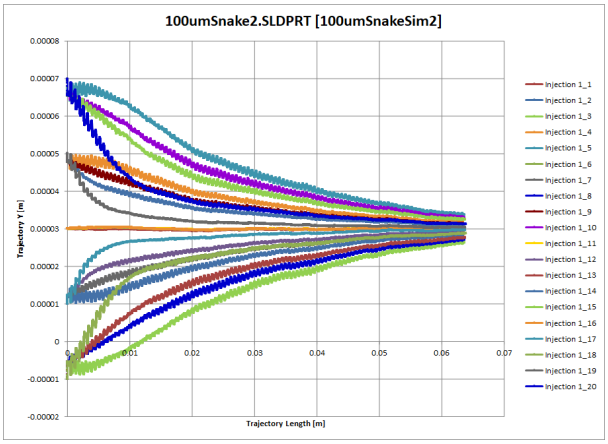

50 mBar

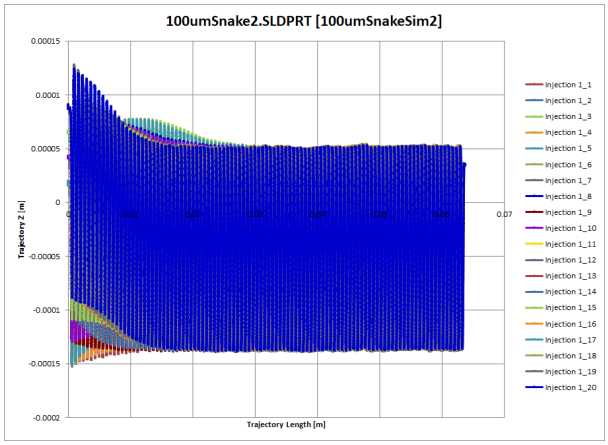

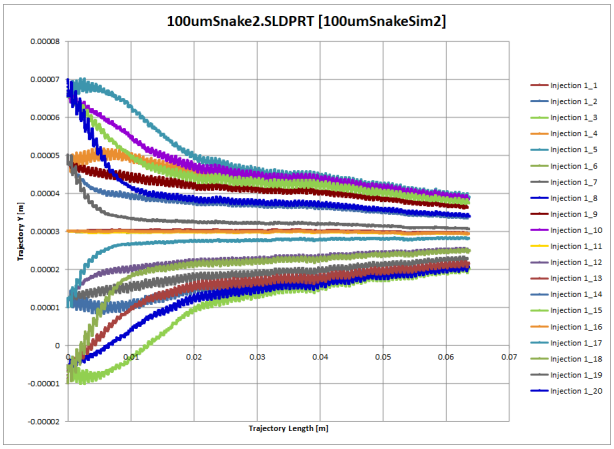

60 mBar

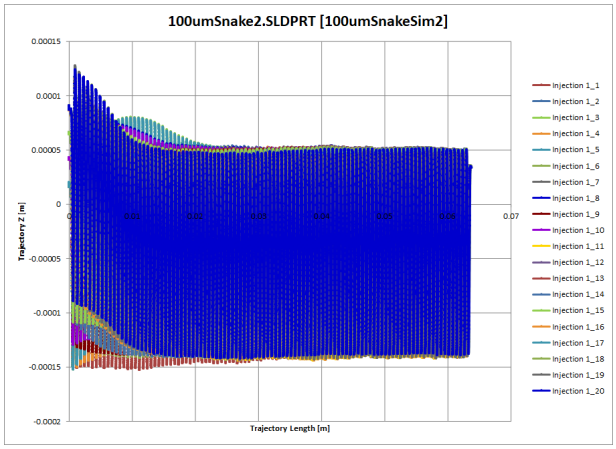

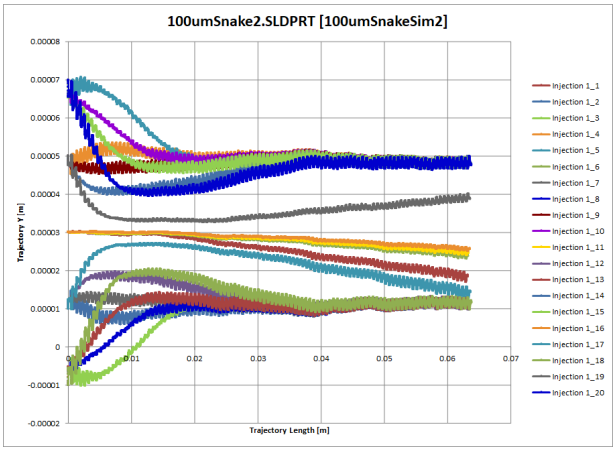

70 mBar

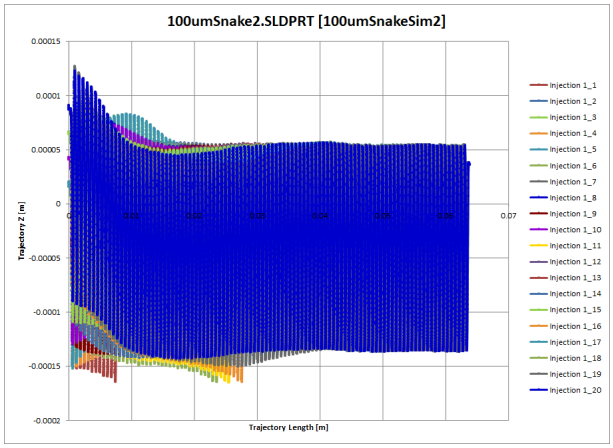

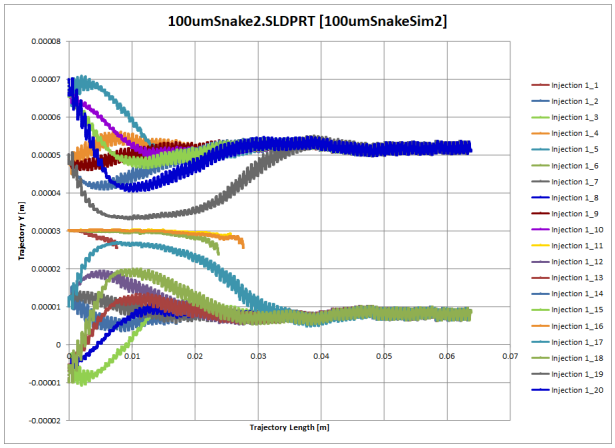

80 mBar

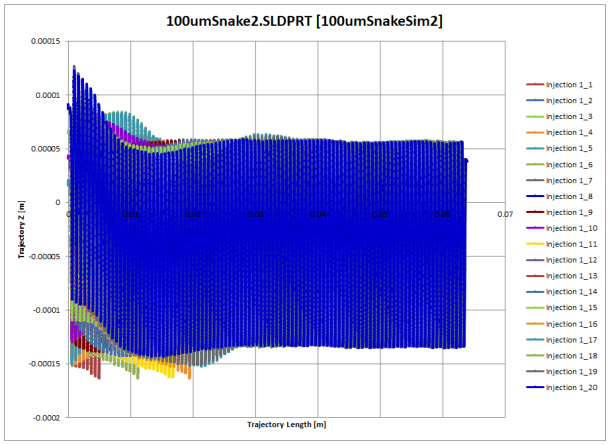

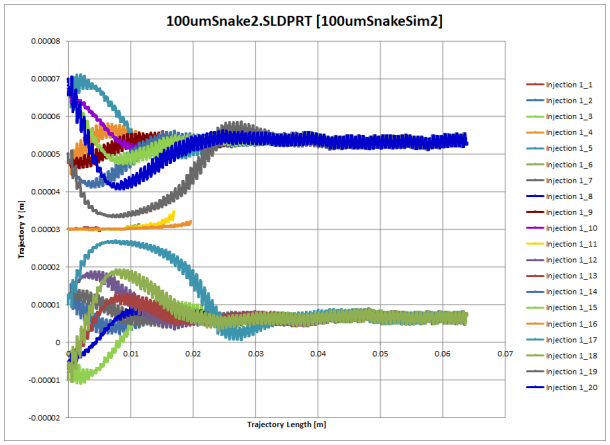

90 mBar

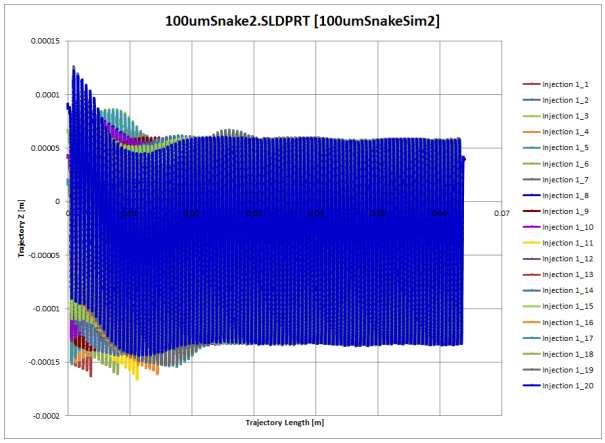

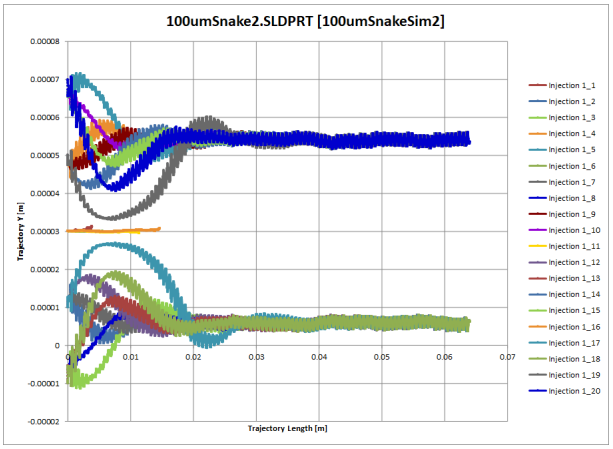

100 mBar

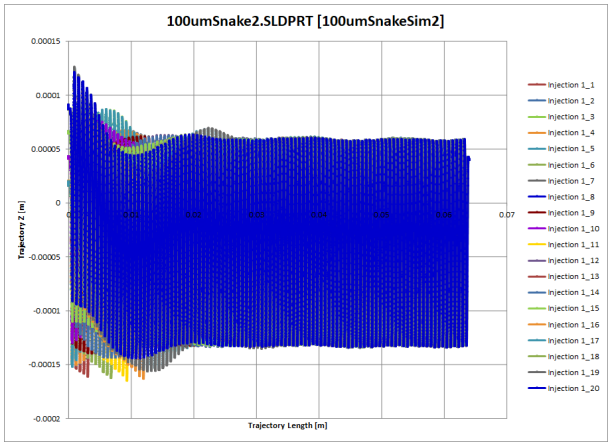

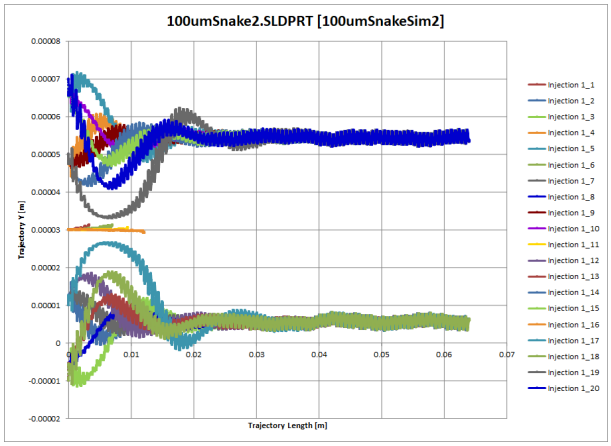

1000 mBar

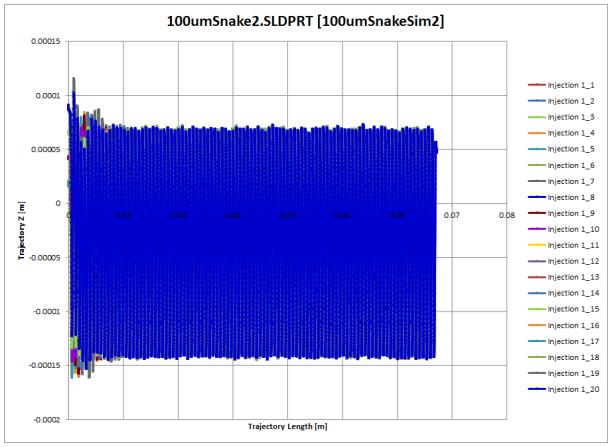

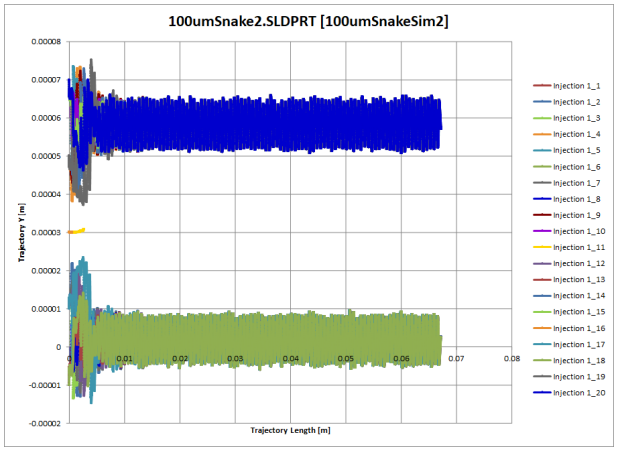

Appendix XI: 100um Particle Tracing Data

	Center (Average) Y	Center (Average) Z	St Dev Y	St Dev Z	Distance from Center		all numbers reported in meters unless otherwise noted
Channel Center	3.00E-05	5.34E-05	null	null	0.00E+00		
Initial	3.00E-05	5.34E-05	2.90E-05	2.87E-05	0.00E+00		
1 mBar	3.02E-05	6.50E-05	3.11E-06	2.14E-06	1.16E-05		
3 mBar	3.01E-05	6.34E-05	2.65E-06	2.28E-06	1.00E-05		
5 mBar	2.97E-05	6.15E-05	2.17E-06	2.01E-06	8.08E-06		
10 mBar	2.95E-05	5.69E-05	1.20E-06	9.72E-07	3.55E-06		
15 mBar	3.01E-05	5.05E-05	1.15E-06	5.98E-07	2.90E-06		
20 mBar	3.00E-05	4.72E-05	9.05E-07	3.77E-07	6.16E-06		
30 mBar	3.01E-05	4.16E-05	8.73E-07	1.55E-07	1.18E-05		

40 mBar	3.00E-05	3.89E-05	1.95E-06	5.34E-07	1.45E-05	Last Clear Centering	
50 mBar	2.94E-05	3.48E-05	6.43E-06	4.67E-07	1.86E-05		
60 mBar	2.82E-05	3.32E-05	1.64E-05	1.36E-06	2.03E-05		
70 mBar	2.99E-05	3.64E-05	2.21E-05	1.42E-07	1.70E-05	Clear Split in Stream	
80 mBar	3.00E-05	3.80E-05	2.37E-05	1.66E-07	1.54E-05		
90 mBar	2.98E-05	3.93E-05	2.44E-05	3.14E-07	1.41E-05		
100 mBar	2.99E-05	3.98E-05	2.46E-05	1.55E-08	1.36E-05		
1000 mBar	2.98E-05	4.67E-05	2.82E-05	1.89E-07	6.71E-06		
in um	**30 um in Y**	**50 um in Z**	**St Dev Y**	**St Dev Z**	**Distance from Center**		
Initial	30.00	53.39	29.02	28.68	0.00		
1 mBar	30.25	65.03	3.11	2.14	11.64		
3 mBar	30.07	63.41	2.65	2.28	10.02		
5 mBar	29.71	61.47	2.17	2.01	8.08		
10 mBar	29.45	56.90	1.20	0.97	3.55		
15 mBar	30.15	50.50	1.15	0.60	2.90	Closest to Center Point	
20 mBar	29.98	47.24	0.90	0.38	6.16		
30 mBar	30.09	41.56	0.87	0.16	11.83	Smallest St Dev both Y and Z	
40 mBar	30.04	38.91	1.95	0.53	14.48	Last Clear Centering	
50 mBar	29.44	34.80	6.43	0.47	18.60		
60 mBar	28.18	33.19	16.41	1.36	20.28		
70 mBar	29.90	36.36	22.15	0.14	17.04	Clear Split in Stream	
80 mBar	29.99	38.01	23.65	0.17	15.39		
90 mBar	29.84	39.31	24.44	0.31	14.08		
100 mBar	29.86	39.80	24.65	0.02	13.59		
1000 mBar	29.85	46.69	28.19	0.19	6.71		
Centered at 0							
Initial	0.00	-0.01					
1 mBar	0.25	11.63					
3 mBar	0.07	10.01					
5 mBar	-0.29	8.07					
10 mBar	-0.55	3.50					
15 mBar	0.15	-2.90		Closest to 0 in Z		Closer to Center Point	

20 mBar	-0.02	-6.16					
30 mBar	0.09	-11.84					
40 mBar	0.04	-14.49				Last Clear Centering	
50 mBar	-0.56	-18.60					
60 mBar	-1.82	-20.21					
70 mBar	-0.10	-17.04				Clear Split in Stream	
80 mBar	-0.01	-15.39					
90 mBar	-0.16	-14.09					
100 mBar	-0.14	-13.60					
1000 mBar	-0.15	-6.71					
Ranges	Range in Y (um)	Range in Z (um)					
1 mBar	13.48	7.38					
3 mBar	12.66	7.77					
5 mBar	10.27	6.72					
10 mBar	6.14	3.55					
15 mBar	6.50	2.10					
20 mBar	4.68	1.40					
30 mBar	3.16	0.42		Smallest combo, within single stream constraints			
40 mBar	7.46	1.70					
50 mBar	18.86	1.33					
60 mBar	36.45	3.30					
70 mBar	42.90	0.29					
80 mBar	45.81	0.34					
90 mBar	47.34	0.62					
100 mBar	47.75	0.05					
1000 mBar	54.60	0.37					

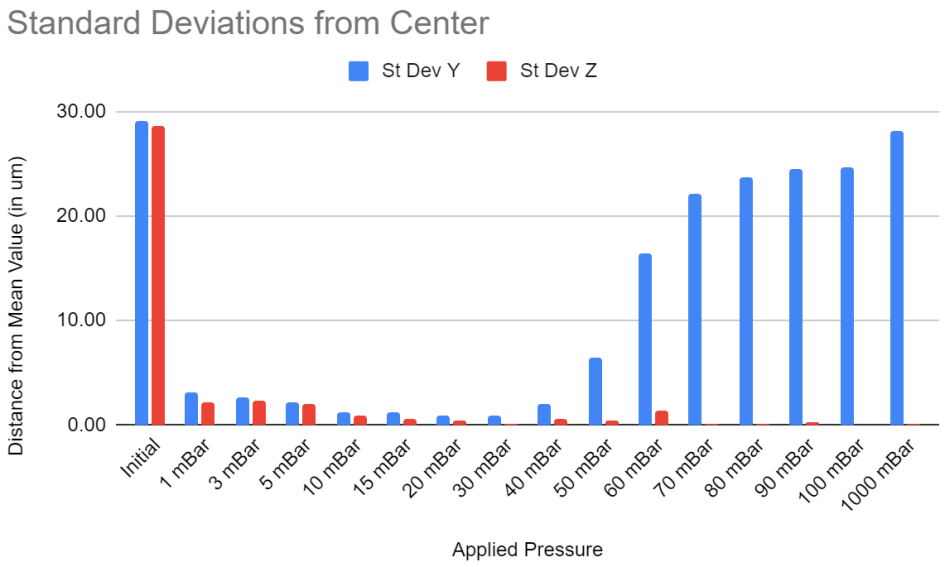
Standard Deviations from Center
St Dev Y
St Dev Z
30.00
20.00
10.00
0.00
Distance from Mean Value (in um)
Initial
1 mBar
3 mBar
5 mBar
10 mBar
15 mBar
20 mBar
30 mBar
40 mBar
50 mBar
60 mBar
70 mBar
80 mBar
90 mBar
100 mBar
1000 mBar
Applied Pressure

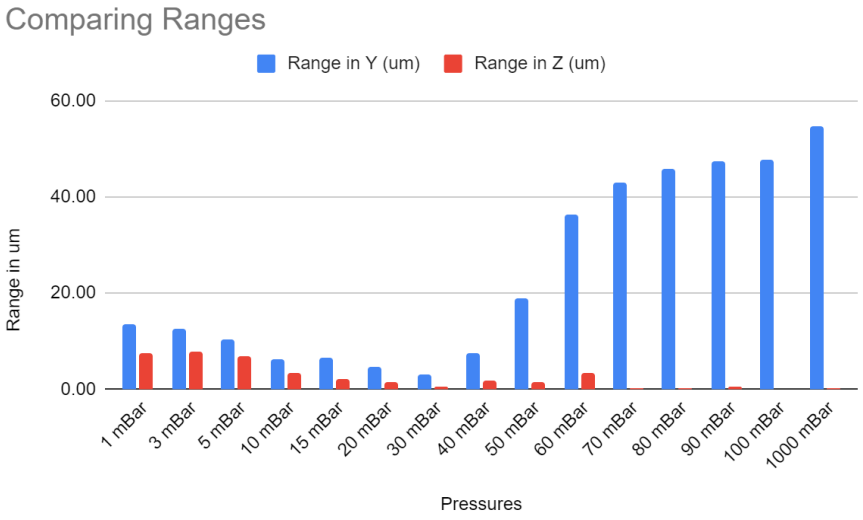
Comparing Ranges
Range in Y (um)
Range in Z (um)
60.00
40.00
20.00
0.00
Range in um
1 mBar
3 mBar
5 mBar
10 mBar
15 mBar
20 mBar
30 mBar
40 mBar
50 mBar
60 mBar
70 mBar
80 mBar
90 mBar
100 mBar
1000 mBar
Pressures

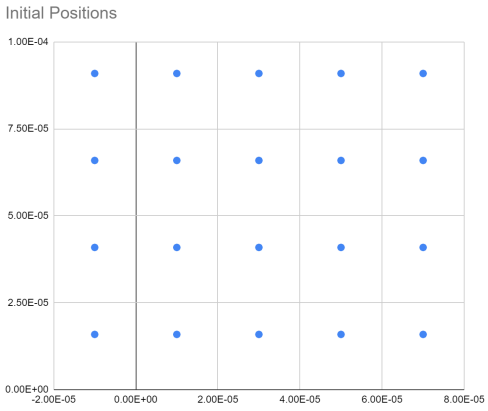
Initial Positions
1.00E-04
7.50E-05
5.00E-05
2.50E-05
0.00E+00
-2.00E-05
0.00E+00
2.00E-05
4.00E-05
6.00E-05
8.00E-05

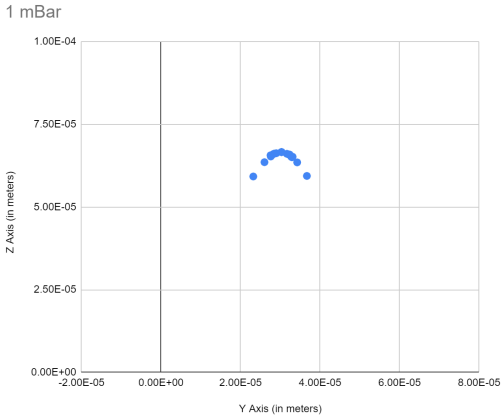
1 mBar
1.00E-04
7.50E-05
5.00E-05
2.50E-05
0.00E+00
Z Axis (in meters)
-2.00E-05
0.00E+00
2.00E-05
4.00E-05
6.00E-05
8.00E-05
Y Axis (in meters)

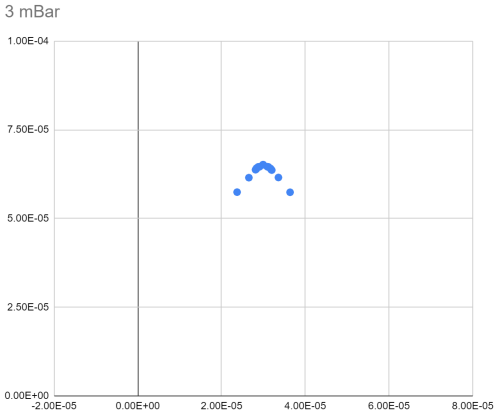
3 mBar
1.00E-04
7.50E-05
5.00E-05
2.50E-05
0.00E+00
-2.00E-05
0.00E+00
2.00E-05
4.00E-05
6.00E-05
8.00E-05

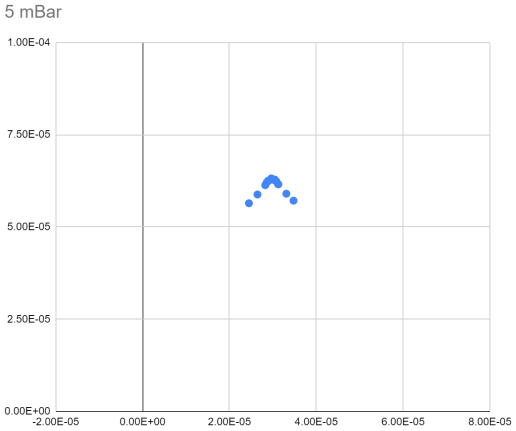
5 mBar
1.00E-04
7.50E-05
5.00E-05
2.50E-05
0.00E+00
-2.00E-05
0.00E+00
2.00E-05
4.00E-05
6.00E-05
8.00E-05

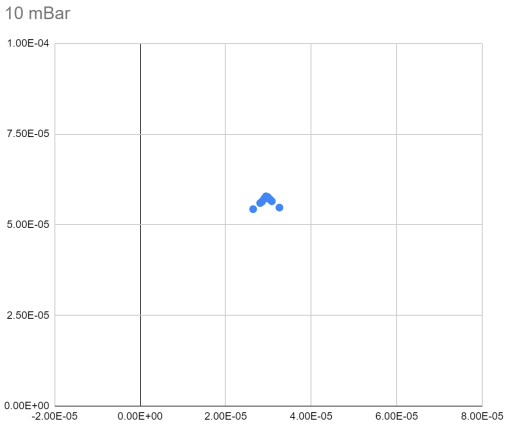
10 mBar
1.00E-04
7.50E-05
5.00E-05
2.50E-05
0.00E+00
-2.00E-05
0.00E+00
2.00E-05
4.00E-05
6.00E-05
8.00E-05

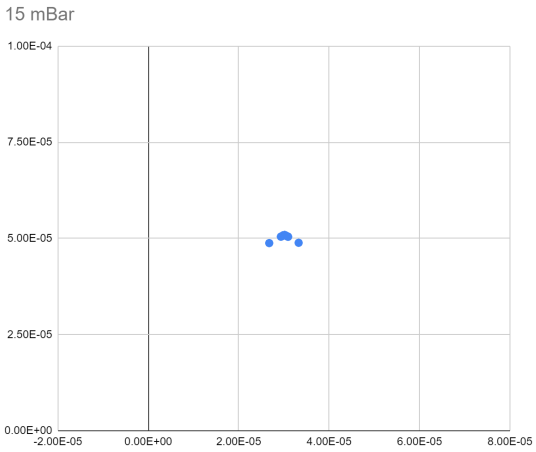
15 mBar
1.00E-04
7.50E-05
5.00E-05
2.50E-05
0.00E+00
-2.00E-05
0.00E+00
2.00E-05
4.00E-05
6.00E-05
8.00E-05

20 mBar

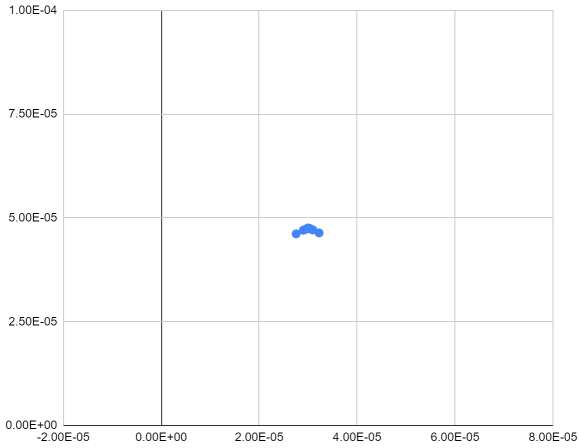

30 mBar

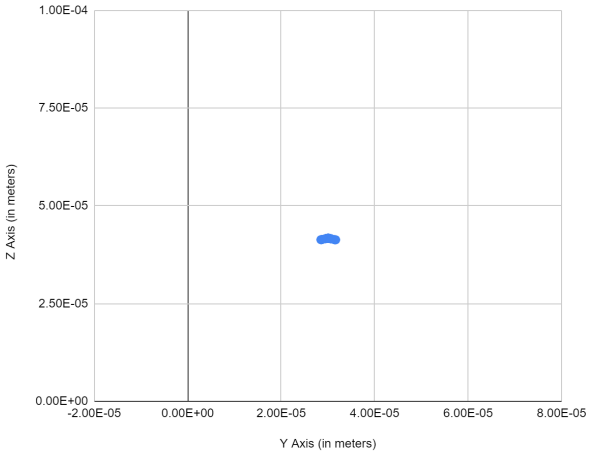

40 mBar

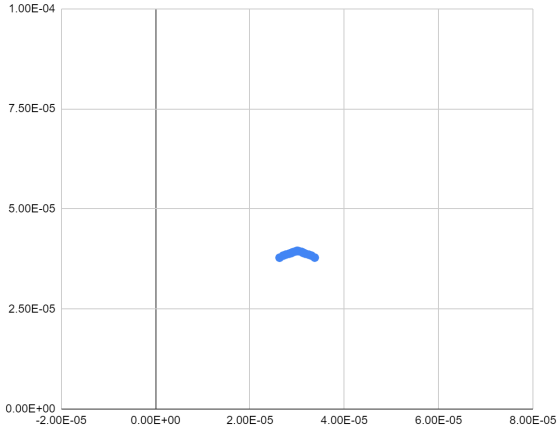

50 mBar

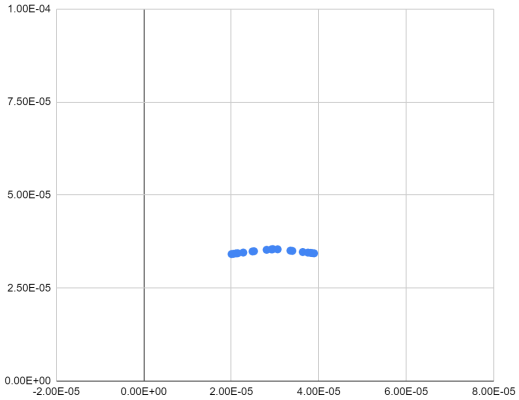

60 mBar

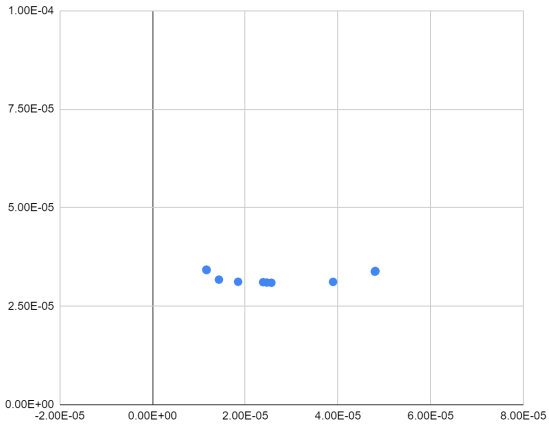

70 mBar

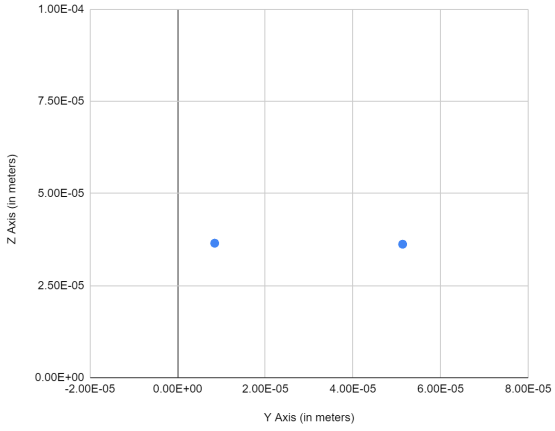

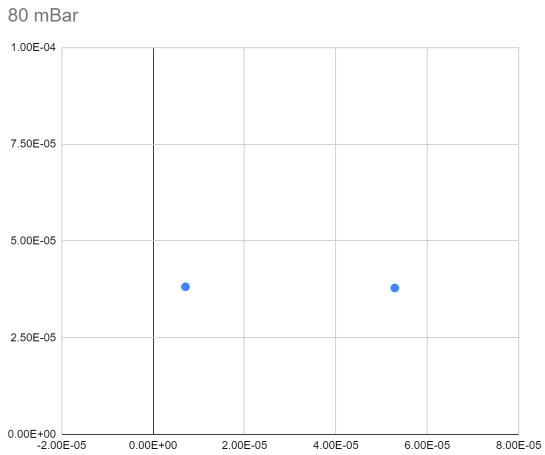
80 mBar
1.00E-04
7.50E-05
5.00E-05
2.50E-05
0.00E+00
-2.00E-05
0.00E+00
2.00E-05
4.00E-05
6.00E-05
8.00E-05

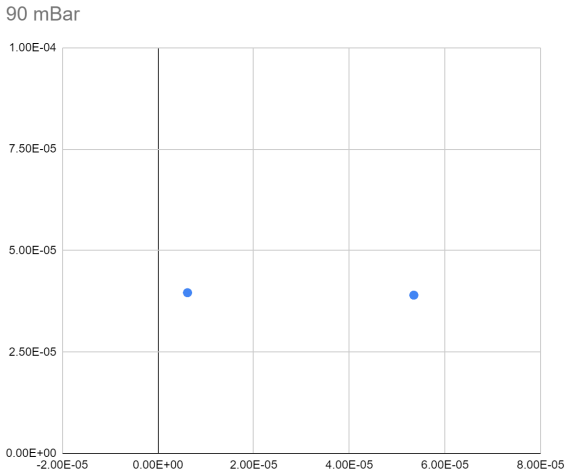
90 mBar
1.00E-04
7.50E-05
5.00E-05
2.50E-05
0.00E+00
-2.00E-05
0.00E+00
2.00E-05
4.00E-05
6.00E-05
8.00E-05

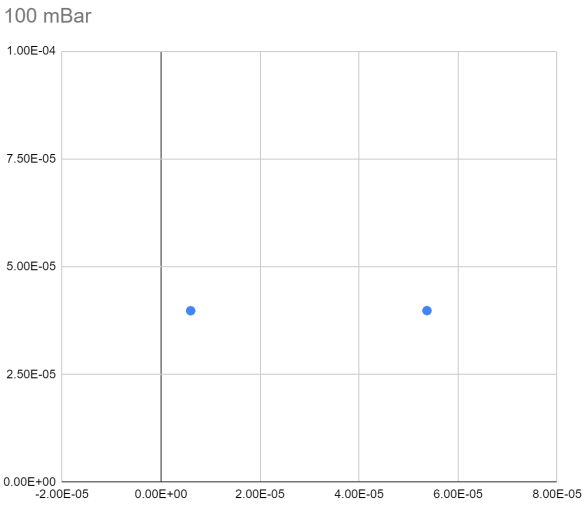
100 mBar
1.00E-04
7.50E-05
5.00E-05
2.50E-05
0.00E+00
-2.00E-05
0.00E+00
2.00E-05
4.00E-05
6.00E-05
8.00E-05

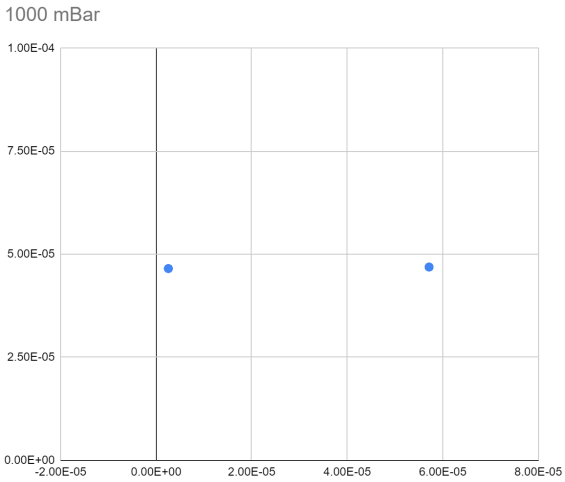
1000 mBar
1.00E-04
7.50E-05
5.00E-05
2.50E-05
0.00E+00
-2.00E-05
0.00E+00
2.00E-05
4.00E-05
6.00E-05
8.00E-05

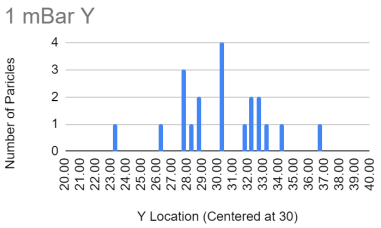
1 mBar Y
Number of Paricles
Y Location (Centered at 30)

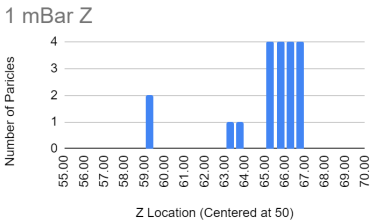
1 mBar Z
Number of Paricles
Z Location (Centered at 50)

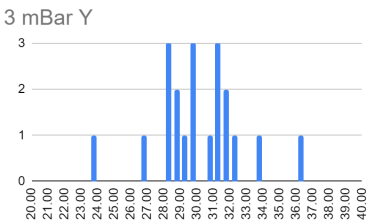
3 mBar Y

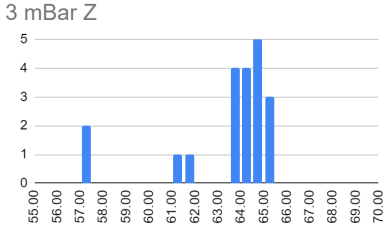
3 mBar Z

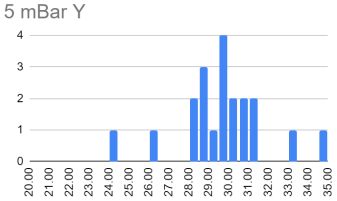
5 mBar Y

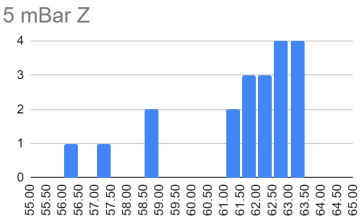
5 mBar Z

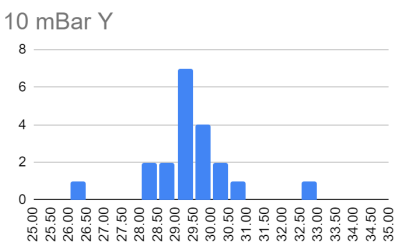
10 mBar Y

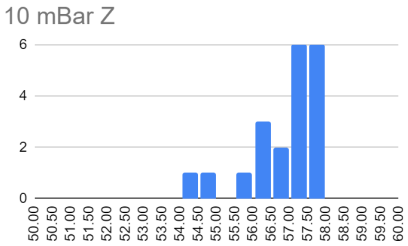
10 mBar Z

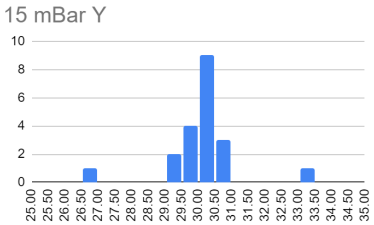
15 mBar Y

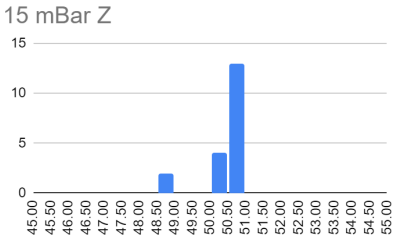
15 mBar Z

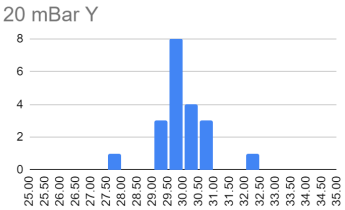
20 mBar Y

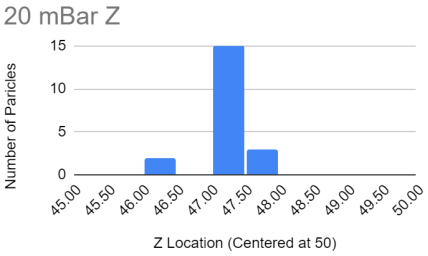
20 mBar Z
Number of Paricles
Z Location (Centered at 50)

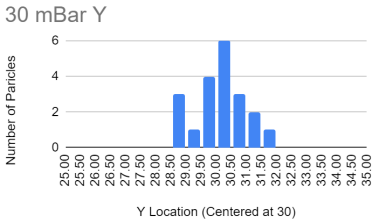
30 mBar Y
Number of Paricles
Y Location (Centered at 30)

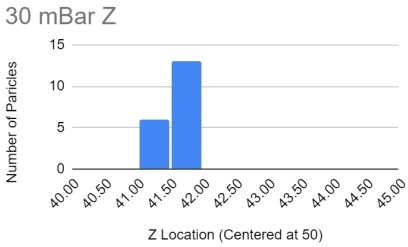
30 mBar Z
Number of Paricles
Z Location (Centered at 50)

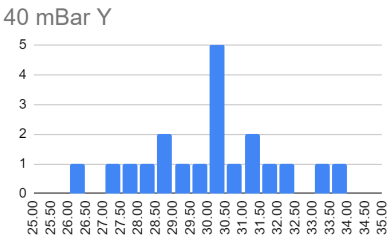
40 mBar Y

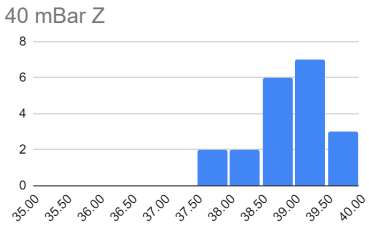
40 mBar Z

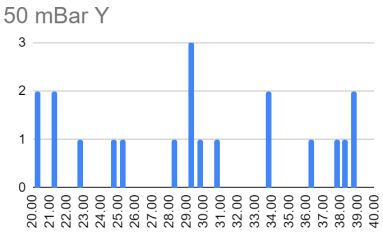
50 mBar Y

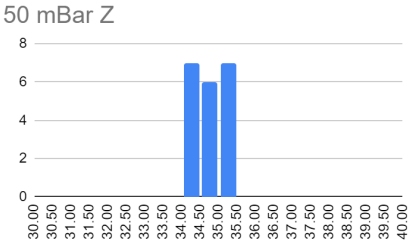
50 mBar Z

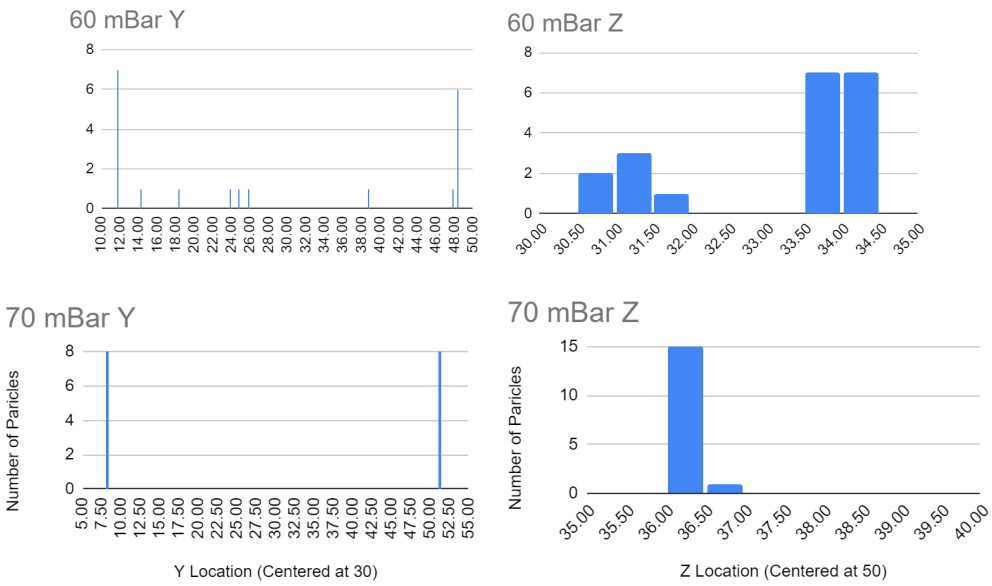

References

[1] J. Haron, "Flow Cytometry and Cell Sorting: A Practical Guide," *Mater. Methods*, Sep. 2020, Accessed: Oct. 07, 2020. [Online]. Available: /method/Flow-Cytometry-and-Cell-Sorting-A-Practical-Guide.html.

[2] P. P. A. Suthanthiraraj and S. W. Graves, "Fluidics," *Curr. Protoc. Cytom. Editor. Board J Paul Robinson Manag. Ed. Al*, vol. 0 1, p. Unit-1.2, Jul. 2013, doi: 10.1002/0471142956.cy0102s65.

[3] "Custom Quartz Flow Cell Manufacturing," *FireflySci Cuvette Shop*. https://www.fireflysci.com/custom-quartz-flow-cell-manufacturing (accessed Oct. 07, 2020).

[4] J. W. Lichtman and J.-A. Conchello, "Fluorescence microscopy," *Nat. Methods*, vol. 2, no. 12, Art. no. 12, Dec. 2005, doi: 10.1038/nmeth817.

[5] J. P. Golden, G. A. Justin, M. Nasir, and F. S. Ligler, "Hydrodynamic focusing – a versatile tool," *Anal. Bioanal. Chem.*, vol. 402, no. 1, pp. 325–335, Jan. 2012, doi: 10.1007/s00216-011-5415-3.

[6] "Plinko," *The Price Is Right Wiki*. https://priceisright.fandom.com/wiki/Plinko (accessed Oct. 07, 2020).

[7] J. C. Sturm, E. C. Cox, B. Comella, and R. H. Austin, "Ratchets in hydrodynamic flow: more than waterwheels," *Interface Focus*, vol. 4, no. 6, p. 20140054, Dec. 2014, doi: 10.1098/rsfs.2014.0054.

[8] A. Cossarizza *et al.*, "Guidelines for the use of flow cytometry and cell sorting in immunological studies," *Eur. J. Immunol.*, vol. 47, no. 10, pp. 1584–1797, 2017, doi: 10.1002/eji.201646632.

[9] D. D. Carlo, D. Irimia, R. G. Tompkins, and M. Toner, "Continuous inertial focusing, ordering, and separation of particles in microchannels," *Proc. Natl. Acad. Sci.*, vol. 104, no. 48, pp. 18892–18897, Nov. 2007, doi: 10.1073/pnas.0704958104.

[10] A. A. Nawaz *et al.*, "Intelligent image-based deformation-assisted cell sorting with molecular specificity," *Nat. Methods*, vol. 17, no. 6, Art. no. 6, Jun. 2020, doi: 10.1038/s41592-020-0831-y.

[11] "PDMS: a review on polydimethylsiloxane in microfluidics," *Elveflow*. https://www.elveflow.com/microfluidic-reviews/general-microfluidics/the-polydimethylsiloxane-pdms-and-microfluidics/ (accessed Oct. 07, 2020).